

2

DTIC FILE COPY

AD-A225 309

# NAVAL POSTGRADUATE SCHOOL Monterey, California



## THESIS

DTIC  
ELECTE  
AUG 17 1990  
S B D  
*Co*

CIRCUIT MODELS FOR INDUCTIVE STRIPS  
IN FIN-LINE  
by  
Georgios Karaminas  
December 1989  
Thesis Advisor Jeffrey. B. Knorr

Approved for public release; distribution is unlimited.

90 08 15 150

UNCLASSIFIED

SECURITY CLASSIFICATION OF THIS PAGE

REPORT DOCUMENTATION PAGE				Form Approved OMB No. 0704-0188	
1a REPORT SECURITY CLASSIFICATION <b>UNCLASSIFIED</b>			1b RESTRICTIVE MARKINGS		
2a. SECURITY CLASSIFICATION AUTHORITY			3 DISTRIBUTION/AVAILABILITY OF REPORT Approved for public release, distribution is unlimited		
2b. DECLASSIFICATION/DOWNGRADING SCHEDULE					
4. PERFORMING ORGANIZATION REPORT NUMBER(S)			5 MONITORING ORGANIZATION REPORT NUMBER(S)		
6a NAME OF PERFORMING ORGANIZATION Naval Postgraduate School		6b OFFICE SYMBOL (If applicable) 62	7a. NAME OF MONITORING ORGANIZATION Naval Postgraduate School		
6c. ADDRESS (City, State, and ZIP Code) Monterey, CA 93943-5000			7b. ADDRESS (City, State, and ZIP Code) Monterey, CA 93943-5000		
8a. NAME OF FUNDING/SPONSORING ORGANIZATION		8b. OFFICE SYMBOL (If applicable)	9 PROCUREMENT INSTRUMENT IDENTIFICATION NUMBER		
8c. ADDRESS (City, State, and ZIP Code)			10 SOURCE OF FUNDING NUMBERS		
		PROGRAM ELEMENT NO	PROJECT NO	TASK NO	WORK UNIT ACCESSION-NO.
11. TITLE (Include Security Classification): <b>CIRCUIT MODELS FOR INDUCTIVE STRIPS IN FIN-LINE</b>					
12. PERSONAL AUTHOR(S) Karaminas, Georgios					
13a. TYPE OF REPORT Master's Thesis		13b. TIME COVERED FROM _____ TO _____		14. DATE OF REPORT (Year, Month, Day) December 1989	15. PAGE COUNT 109
16 SUPPLEMENTARY NOTATION The views expressed in this thesis are those of the author and do not reflect the official policy or position of the Department of Defense or the U.S. Government.					
17 COSATI CODES			18 SUBJECT TERMS (Continue on reverse if necessary and identify by block number)		
FIELD	GROUP	SUB-GROUP	fin-line, finline, finline model, fin-line model		
19 ABSTRACT (Continue on reverse if necessary and identify by block number) This thesis describes a C.A.D compatible circuit model for an inductive strip centered in WR(90) fin-line with $W/b < 1$ , $E_r = 1$ . The circuit model is shown to predict strip scattering coefficients which agree closely with those computed numerically using the spectral domain method.					
20 DISTRIBUTION/AVAILABILITY OF ABSTRACT <input checked="" type="checkbox"/> UNCLASSIFIED/UNLIMITED <input type="checkbox"/> SAME AS RPT <input type="checkbox"/> DTIC USERS			21 ABSTRACT SECURITY CLASSIFICATION Unclassified		
22a. NAME OF RESPONSIBLE INDIVIDUAL Jeffrey B. Knorr			22b TELEPHONE (Include Area Code) (408)646-2815		22c OFFICE SYMBOL 62Ko

DD Form 1473, JUN 86

Previous editions are obsolete

SECURITY CLASSIFICATION OF THIS PAGE

S/N 0102-LF-014-6603

UNCLASSIFIED

Approved for public release; distribution is unlimited.

Circuit Models for Inductive Strips in Fin-Line

by

Georgios Karaminas  
Lieutenant Hellenic Navy  
B. S., Hellenic Naval Academy, 1979

Submitted in partial fulfillment of the  
requirements for the degree of

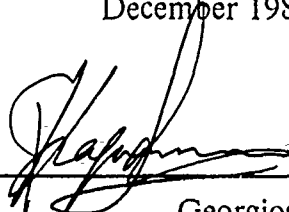
MASTER OF SCIENCE IN ELECTRICAL ENGINEERING

from the

NAVAL POSTGRADUATE SCHOOL

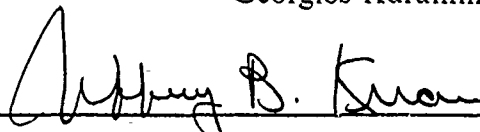
December 1989

Author:

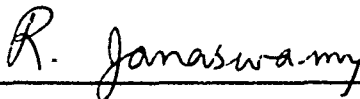


Georgios Karaminas

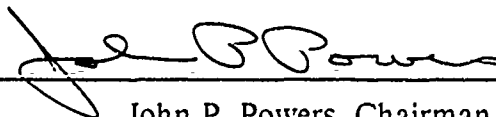
Approved by:



Jeffrey B. Knorr, Thesis Advisor



R. Janaswamy, Second Reader



John P. Powers, Chairman,  
Department of Electrical and Computer Engineering

2

## ABSTRACT

This thesis describes a CAD-compatible circuit model for an inductive strip centered in WR(90) fin-line with  $W/b < 1$ ,  $E_r = 1$ . The circuit model is shown to predict strip scattering coefficients which agree closely with those computed numerically using the spectral domain method.

RHY

<b>Accession For</b>	
NTIS GRA&I	<input checked="" type="checkbox"/>
DTIC TAB	<input type="checkbox"/>
Unannounced	<input type="checkbox"/>
Justification _____	
By _____	
Distribution/	
<b>Availability Codes</b>	
Dist	Avail and/or Special
A-1	



## TABLE OF CONTENTS

I. INTRODUCTION TO FIN-LINE .....	1
II. MODELING THE WR(90) FIN-LINE .....	5
III. MODELING AN INDUCTIVE STRIP IN HOMOGENEOUS FIN-LINE .....	12
IV. CONCLUSIONS AND RECOMMENDATIONS .....	29
A. CONCLUSIONS .....	29
B. RECOMMENDATIONS .....	30
APPENDIX A. TABLES .....	31
APPENDIX B. SUPPORTIVE FIGURES .....	47
LIST OF REFERENCES .....	93
INITIAL DISTRIBUTION LIST .....	94

## LIST OF TABLES

Table 1.	Numerical values of $\frac{\lambda'}{\lambda}$ and $Z_{0v}$ for $W/b=0.5$ . . . . .	6
Table 2.	Calculated values of cutoff wavelength and characteristic impedance vs.. $W/b$ for WR(90) fin-line. . . . .	6
Table 3.	Calculated values of $a_{eq}/a$ and $b_{eq}/b$ vs. $W/b$ for WR(90) fin-line. . . . .	8
Table 4.	Computed scattering coefficients for WR(90) fin-line for $W/b=0.5$ and $T=20, 50, 100, 200,$ and $500$ mils ( $D=10$ mils). . . . .	13
Table 5.	TOUCHSTONE data file of scattering coefficients for $W/b=0.5$ $T=100$ mils. . . . .	13
Table 6.	Predicted values of $L$ vs. $W/b$ for WR(90) fin-line and strip length $T$ using the polynomial form. . . . .	16
Table 7.	Predicted values of $L$ vs. $W/b$ for WR(90) fin-line and strip length $T$ using the exponential form. . . . .	18
Table 8.	Computed scattering coefficients for WR(90) fin-line for $W/b=0.25$ and $T=20, 50, 100, 200,$ and $500$ mils ( $D=10$ mils). . . . .	31
Table 9.	Computed scattering coefficients for WR(90) fin-line for $W/b=0.2$ and $T=20, 50, 100, 200,$ and $500$ mils ( $D=10$ mils). . . . .	32
Table 10.	Touchstone data file containing the computed scattering coefficients of an inductive strip of length $T=20$ mils centered in WR(90) fin-line, $W/b=0.5$ . . . . .	33
Table 11.	Touchstone data file containing the computed scattering coefficients of an inductive strip of length $T=50$ mils centered in WR(90) fin-line, $W/b=0.5$ . . . . .	34
Table 12.	Touchstone data file containing the computed scattering coefficients of an inductive strip of length $T=200$ mils centered in WR(90) fin-line, $W/b=0.5$ . . . . .	35
Table 13.	Touchstone data file containing the computed scattering coefficients of an inductive strip of length $T=500$ mils centered in WR(90) fin-line, $W/b=0.5$ . . . . .	36

Table 14. Touchstone data file containing the computed scattering coefficients of an inductive strip of length $T = 20$ mils centered in WR(90) fin-line, $W/b = 0.25$ . . . . .	37
Table 15. Touchstone data file containing the computed scattering coefficients of an inductive strip of length $T = 50$ mils centered in WR(90) fin-line, $W/b = 0.25$ . . . . .	38
Table 16. Touchstone data file containing the computed scattering coefficients of an inductive strip of length $T = 100$ mils centered in WR(90) fin-line, $W/b = 0.25$ . . . . .	39
Table 17. Touchstone data file containing the computed scattering coefficients of an inductive strip of length $T = 200$ mils centered in WR(90) fin-line, $W/b = 0.25$ . . . . .	40
Table 18. Touchstone data file containing the computed scattering coefficients of an inductive strip of length $T = 500$ mils centered in WR(90) fin-line, $W/b = 0.25$ . . . . .	41
Table 19. Touchstone data file containing the computed scattering coefficients of an inductive strip of length $T = 20$ mils centered in WR(90) fin-line, $W/b = 0.2$ . . . . .	42
Table 20. Touchstone data file containing the computed scattering coefficients of an inductive strip of length $T = 50$ mils centered in WR(90) fin-line, $W/b = 0.2$ . . . . .	43
Table 21. Touchstone data file containing the computed scattering coefficients of an inductive strip of length $T = 100$ mils centered in WR(90) fin-line, $W/b = 0.2$ . . . . .	44
Table 22. Touchstone data file containing the computed scattering coefficients of an inductive strip of length $T = 200$ mils centered in WR(90) fin-line, $W/b = 0.2$ . . . . .	45
Table 23. Touchstone data file containing the computed scattering coefficients of an inductive strip of length $T = 500$ mils centered in WR(90) fin-line, $W/b = 0.2$ . . . . .	46

## LIST OF FIGURES

Figure 1. Cross-sectional view of a fin-line. ....	2
Figure 2. View of a fin-line strip of axial length T centered in a fin-line cavity. ..	2
Figure 3. Three typical fin-line structures. ....	3
Figure 4. Homogeneous fin-line and equivalent rectangular waveguide structures. ....	6
Figure 5. Plot of $a_{eq}/a$ vs. $W/b$ for a WR(90) fin-line. ....	9
Figure 6. Plot of $b_{eq}/b$ vs. $W/b$ for a WR(90) fin-line. ....	10
Figure 7. $ S_{11} $ vs. frequency for inductive strips centered in WR(90) fin-line. $W/b=0.5, E_{r2} = 1$ . ....	14
Figure 8. $\theta_{11}$ vs. frequency for inductive strips centered in WR(90) fin-line. $W/b=0.5, E_{r2} = 1$ . ....	15
Figure 9. Circuit model of an inductive strip in fin-line. ....	16
Figure 10. TOUCHSTONE circuit file computing the scattering coefficients of the circuit model (part 1). ....	17
Figure 11. TOUCHSTONE circuit file computing the scattering coefficients of the circuit model (part 2). ....	18
Figure 12. Computed and predicted values of $ S_{11} $ vs. frequency for a T=100 mils inductive strip centered in WR(90) fin-line $W/b=0.5, E_{r2} = 1$ Model inductance L=8.2 nH. ....	19
Figure 13. Computed and predicted values of $\theta_{11}$ vs. frequency for a T=100 mil inductive strip centered in WR(90) fin-line $W/b=0.5, E_{r2} = 1$ Model inductance L=8.2 nH. ....	20
Figure 14. Smith chart plot of computed and predicted values of $S_{11}$ and $S_{21}$ for a T=100 mil inductive strip centered in WR(90) fin-line, $W/b=0.5, E_{r2} = 1$ Model inductance L=8.2 nH. ....	21
Figure 15. Plot of the model inductance L as an exponential function of the strip length T, for $W/b = 1.0, 0.5, 0.25, 0.2$ . ....	22

Figure 16. Plots of the model inductance $L$ as a polynomial function of the strip length $T$ , for $W/b = 1.0, 0.5, 0.25, 0.2$ . .....	27
Figure 17. Difference between the exponential and polynomial plots of the model inductance $L$ , for $W/b = 0.5, 0.25, 0.2$ . .....	28
Figure 18. $ S_{11} $ vs. frequency for inductive strips centered in WR(90) fin-line. $W/b = 0.25, E_{r2} = 1$ . .....	47
Figure 19. $\theta_{11}$ vs. frequency for inductive strips centered in WR(90) fin-line. $W/b = 0.25, E_{r2} = 1$ . .....	48
Figure 20. $ S_{11} $ vs. frequency for inductive strips centered in WR(90) fin-line. $W/b = 0.2, E_{r2} = 1$ . .....	49
Figure 21. $\theta_{11}$ vs. frequency for inductive strips centered in WR(90) fin-line. $W/b = 0.2, E_{r2} = 1$ . .....	50
Figure 22. Computed and predicted values of $ S_{11} $ vs. frequency for a $T = 20$ mils inductive strip centered in WR(90) fin-line, $W/b = 0.5, E_{r2} = 1$ . Model inductance $L = 10.7$ nH. ....	51
Figure 23. Computed and predicted values of $\theta_{11}$ vs. frequency for a $T = 20$ mils inductive strip centered in WR(90) fin-line, $W/b = 0.5, E_{r2} = 1$ . Model inductance $L = 10.7$ nH. ....	52
Figure 24. Smith chart plot of computed and predicted values of $S_{11}$ and $S_{21}$ for a $T = 20$ mils inductive strip centered in WR(90) fin-line, $W/b = 0.5, E_{r2} = 1$ . Model inductance $L = 10.7$ nH. ....	53
Figure 25. Computed and predicted values of $ S_{11} $ vs. frequency for a $T = 50$ mils inductive strip centered in WR(90) fin-line, $W/b = 0.5, E_{r2} = 1$ . Model inductance $L = 9.35$ nH. ....	54
Figure 26. Computed and predicted values of $\theta_{11}$ vs. frequency for a $T = 50$ mils inductive strip centered in WR(90) fin-line, $W/b = 0.5, E_{r2} = 1$ . Model inductance $L = 9.35$ nH. ....	55
Figure 27. Smith chart plot of computed and predicted values of $S_{11}$ and $S_{21}$ for a $T = 50$ mils inductive strip centered in WR(90) fin-line, $W/b = 0.5, E_{r2} = 1$ . Model inductance $L = 9.35$ nH. ....	56

Figure 28. Computed and predicted values of $ S_{11} $ vs. frequency for a $T=200$ mils inductive strip centered in WR(90) fin-line, $W/b=0.5$ , $E_{r2}=1$ . Model inductance $L=7.10$ nH. ....	57
Figure 29. Computed and predicted values of $\theta_{11}$ vs. frequency for a $T=200$ mils inductive strip centered in WR(90) fin-line, $W/b=0.5$ , $E_{r2}=1$ . Model inductance $L=7.10$ nH. ....	58
Figure 30. Smith chart plot of computed and predicted values of $S_{11}$ and $S_{21}$ for a $T=200$ mils inductive strip centered in WR(90) fin-line, $W/b=0.5$ , $E_{r2}=1$ . Model inductance $L=8.20$ nH. ....	59
Figure 31. Computed and predicted values of $ S_{11} $ vs. frequency for a $T=500$ mils inductive strip centered in WR(90) fin-line, $W/b=0.5$ , $E_{r2}=1$ . Model inductance $L=5.90$ nH. ....	60
Figure 32. Computed and predicted values of $ S_{11} $ vs. frequency for a $T=500$ mils inductive strip centered in WR(90) fin-line, $W/b=0.5$ , $E_{r2}=1$ . Model inductance $L=5.90$ nH. ....	61
Figure 33. Smith chart plot of computed and predicted values of $S_{11}$ and $S_{21}$ for a $T=500$ mils inductive strip centered in WR(90) fin-line, $W/b=0.5$ , $E_{r2}=1$ . Model inductance $L=5.90$ nH. ....	62
Figure 34. Computed and predicted values of $ S_{11} $ vs. frequency for a $T=20$ mils inductive strip centered in WR(90) fin-line, $W/b=0.25$ , $E_{r2}=1$ . Model inductance $L=6.60$ nH. ....	63
Figure 35. Computed and predicted values of $\theta_{11}$ vs. frequency for a $T=20$ mils inductive strip centered in WR(90) fin-line, $W/b=0.25$ , $E_{r2}=1$ . Model inductance $L=6.60$ nH. ....	64
Figure 36. Smith chart plot of computed and predicted values of $S_{11}$ and $S_{21}$ for a $T=20$ mils inductive strip centered in WR(90) fin-line, $W/b=0.25$ , $E_{r2}=1$ . Model inductance $L=6.60$ nH. ....	65
Figure 37. Computed and predicted values of $ S_{11} $ vs. frequency for a $T=50$ mils inductive strip centered in WR(90) fin-line, $W/b=0.25$ , $E_{r2}=1$ . Model inductance $L=5.65$ nH. ....	66

Figure 38. Computed and predicted values of $\theta_{11}$ vs. frequency for a $T = 50$ mils inductive strip centered in WR(90) fin-line, $W/b = 0.25$ , $E_{r2} = 1$ . Model inductance $L = 5.65$ nH. ....	67
Figure 39. Smith chart plot of computed and predicted values of $S_{11}$ and $S_{21}$ for a $T = 50$ mils inductive strip centered in WR(90) fin-line, $W/b = 0.25$ , $E_{r2} = 1$ . Model inductance $L = 5.65$ nH. ....	68
Figure 40. Computed and predicted values of $ S_{11} $ vs. frequency for a $T = 100$ mils inductive strip centered in WR(90) fin-line, $W/b = 0.25$ , $E_{r2} = 1$ . Model inductance $L = 5.005$ nH. ....	69
Figure 41. Computed and predicted values of $\theta_{11}$ vs. frequency for a $T = 100$ mils inductive strip centered in WR(90) fin-line, $W/b = 0.25$ , $E_{r2} = 1$ . Model inductance $L = 5.005$ nH. ....	70
Figure 42. Smith chart plot of computed and predicted values of $S_{11}$ and $S_{21}$ for a $T = 100$ mils inductive strip centered in WR(90) fin-line, $W/b = 0.25$ , $E_{r2} = 1$ . Model inductance $L = 5.005$ nH. ....	71
Figure 43. Computed and predicted values of $ S_{11} $ vs. frequency for a $T = 200$ mils inductive strip centered in WR(90) fin-line, $W/b = 0.25$ , $E_{r2} = 1$ . Model inductance $L = 4.20$ nH. ....	72
Figure 44. Computed and predicted values of $\theta_{11}$ vs. frequency for a $T = 200$ mils inductive strip centered in WR(90) fin-line, $W/b = 0.25$ , $E_{r2} = 1$ . Model inductance $L = 4.20$ nH. ....	73
Figure 45. Smith chart plot of computed and predicted values of $S_{11}$ and $S_{21}$ for a $T = 200$ mils inductive strip centered in WR(90) fin-line, $W/b = 0.25$ , $E_{r2} = 1$ . Model inductance $L = 4.20$ nH. ....	74
Figure 46. Computed and predicted values of $ S_{11} $ vs. frequency for a $T = 500$ mils inductive strip centered in WR(90) fin-line, $W/b = 0.25$ , $E_{r2} = 1$ . Model inductance $L = 3.82$ nH. ....	75
Figure 47. Computed and predicted values of $\theta_{11}$ vs. frequency for a $T = 500$ mils inductive strip centered in WR(90) fin-line, $W/b = 0.25$ , $E_{r2} = 1$ . Model inductance $L = 3.82$ nH. ....	76

Figure 48. Smith chart plot of computed and predicted values of $S_{11}$ and $S_{21}$ for a $T = 500$ mils inductive strip centered in WR(90) fin-line, $W/b = 0.25$ , $E_{r2} = 1$ Model inductance $L = 3.82$ nH. ....	77
Figure 49. Computed and predicted values of $ S_{11} $ vs. frequency for a $T = 20$ mils inductive strip centered in WR(90) fin-line, $W/b = 0.2$ , $E_{r2} = 1$ . Model inductance $L = 4.89$ nH. ....	78
Figure 50. Computed and predicted values of $\theta_{11}$ vs. frequency for a $T = 20$ mils inductive strip centered in WR(90) fin-line, $W/b = 0.2$ , $E_{r2} = 1$ . Model inductance $L = 4.89$ nH. ....	79
Figure 51. Smith chart plot of computed and predicted values of $S_{11}$ and $S_{21}$ for a $T = 20$ mils inductive strip centered in WR(90) fin-line, $W/b = 0.2$ , $E_{r2} = 1$ . Model inductance $L = 4.89$ nH. ....	80
Figure 52. Computed and predicted values of $ S_{11} $ vs. frequency for a $T = 50$ mils inductive strip centered in WR(90) fin-line, $W/b = 0.2$ , $E_{r2} = 1$ . Model inductance $L = 4.18$ nH. ....	81
Figure 53. Computed and predicted values of $\theta_{11}$ vs. frequency for a $T = 50$ mils inductive strip centered in WR(90) fin-line, $W/b = 0.2$ , $E_{r2} = 1$ . Model inductance $L = 4.18$ nH. ....	82
Figure 54. Smith chart plot of computed and predicted values of $S_{11}$ and $S_{21}$ for a $T = 50$ mils inductive strip centered in WR(90) fin-line, $W/b = 0.2$ , $E_{r2} = 1$ . Model inductance $L = 4.18$ nH. ....	83
Figure 55. Computed and predicted values of $ S_{11} $ vs. frequency for a $T = 100$ mils inductive strip centered in WR(90) fin-line, $W/b = 0.2$ , $E_{r2} = 1$ . Model inductance $L = 3.55$ nH. ....	84
Figure 56. Computed and predicted values of $\theta_{11}$ vs. frequency for a $T = 100$ mils inductive strip centered in WR(90) fin-line, $W/b = 0.2$ , $E_{r2} = 1$ . Model inductance $L = 3.55$ nH. ....	85
Figure 57. Smith chart plot of computed and predicted values of $S_{11}$ and $S_{21}$ for a $T = 100$ mils inductive strip centered in WR(90) fin-line, $W/b = 0.2$ , $E_{r2} = 1$ . Model inductance $L = 3.55$ nH. ....	86

Figure 58. Computed and predicted values of  $|S_{11}|$  vs. frequency for a  $T=200$  mils inductive strip centered in WR(90) fin-line,  $W/b=0.2$ ,  $E_{r2} = 1$ . Model inductance  $L = 3.06$  nH. .... 87

Figure 59. Computed and predicted values of  $\theta_{11}$  vs. frequency for a  $T=200$  mils inductive strip centered in WR(90) fin-line,  $W/b=0.2$ ,  $E_{r2} = 1$ . Model inductance  $L = 3.06$  nH. .... 88

Figure 60. Smith chart plot of computed and predicted values of  $S_{11}$  and  $S_{21}$  for a  $T=200$  mils inductive strip centered in WR(90) fin-line,  $W/b=0.2$ ,  $E_{r2} = 1$ . Model inductance  $L = 3.06$  nH. .... 89

Figure 61. Computed and predicted values of  $|S_{11}|$  vs. frequency for a  $T=500$  mils inductive strip centered in WR(90) fin-line,  $W/b=0.2$ ,  $E_{r2} = 1$ . Model inductance  $L = 2.70$  nH. .... 90

Figure 62. Computed and predicted values of  $\theta_{11}$  vs. frequency for a  $T=500$  mils inductive strip centered in WR(90) fin-line,  $W/b=0.2$ ,  $E_{r2} = 1$ . Model inductance  $L = 2.70$  nH. .... 91

Figure 63. Smith chart plot of Computed and predicted values of  $S_{11}$  and  $S_{21}$  for a  $T=500$  mils inductive strip centered in WR(90) fin-line,  $W/b=0.2$ ,  $E_{r2} = 1$ . Model inductance  $L = 2.70$  nH. .... 92

## ACKNOWLEDGEMENTS

I would like to thank Prof. Jeffery B. Knorr for his continued support, guidance and most of all faith. I would also like to thank Mrs. Janeen Groshmeier for her counsel and assistance. Most importantly, I would like to thank my wife, Xanthippi, for her assistance in preparing the figures and graphs. Her continued emotional support has made the completion of this research possible.

## I. INTRODUCTION TO FIN-LINE

The use of fin-line as a transmission structure for millimeter-wave integrated circuits was first proposed by Meier in 1974 [Ref. 1]. The advantages of this structure are low-attenuation, single mode operation, containment of spurious emissions, ease of production, and compatibility with integrated circuit technology. Fin-line has become established as a viable transmission structure, and, therefore, studies contributing to its effective utilization are of widespread interest.

Knorr and Shayda have applied the spectral-domain method to determine the transmission characteristics of fin-line [Ref. 2: pp. 737-738] and Knorr [Ref. 3 pp. 1200-1201] has used the method to investigate the end effect in a shorted fin-line. Lastly, Knorr and Deal [Ref. 5, 6] have used the spectral domain method to compute the scattering coefficients of an inductive strip in fin-line. These studies addressed the proper choice of basis functions and accurately determined the fin-line guide wavelength and characteristic impedance as well as the equivalent reactance of a shorting septum, and the scattering coefficients of an inductive strip.

One discontinuity of considerable practical importance is the inductive strip in fin-line. It is used to construct simple resonators as well as more complicated multi-resonator filters. The geometry for a fin-line is illustrated in Figure 1 on page 2 and a cross-sectional view of the fin-line in which the strip resides is shown in Figure 2 on page 2. Figure 3 on page 3 shows cross-sectional views of three fin-line configurations [Ref. 4]. In the configuration of Figure 3b, the fins are printed on opposite sides of a single dielectric substrate. Since the fins are directly grounded to the metal waveguide walls, this configuration is applicable only to passive devices. In the configuration of Figure 3c, however, the fins are printed on the mating surfaces of the two dielectric substrates. Since the fins are insulated from the waveguide at dc, bias may be introduced for active components.

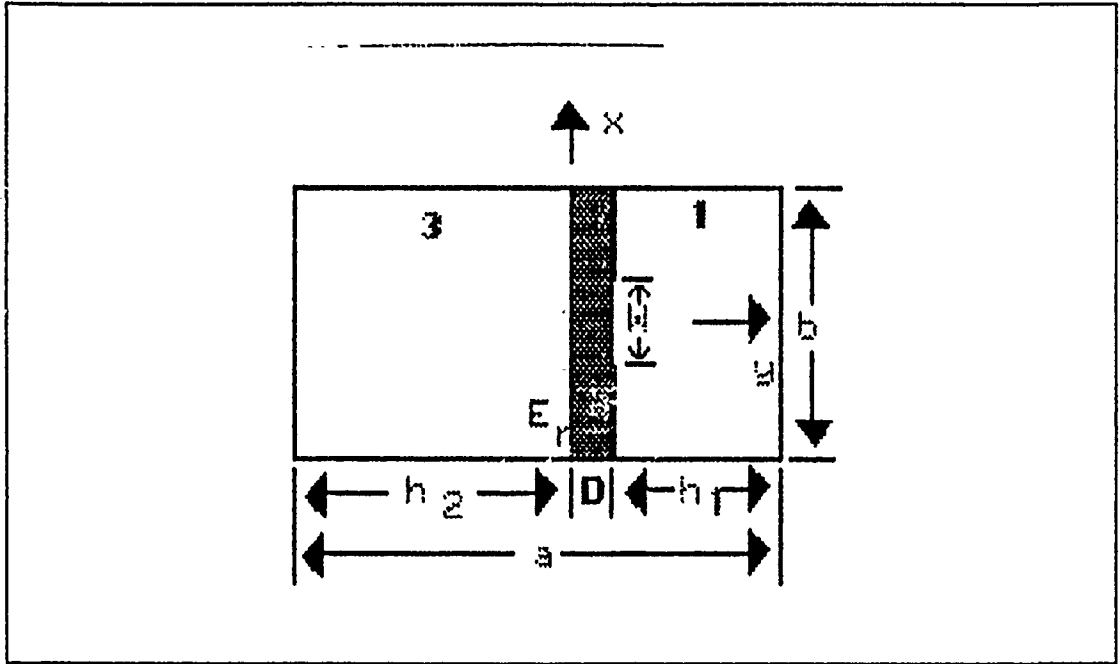


Figure 1. Cross-sectional view of a fin-line.

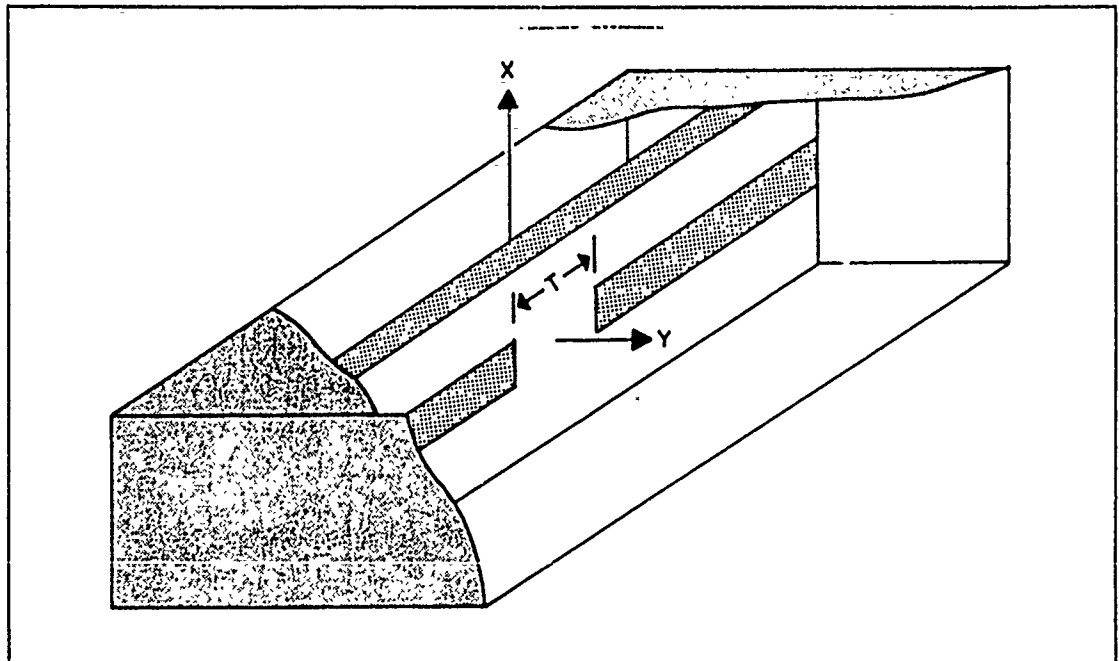


Figure 2. View of a fin-line strip of axial length  $T$  centered in a fin-line cavity.

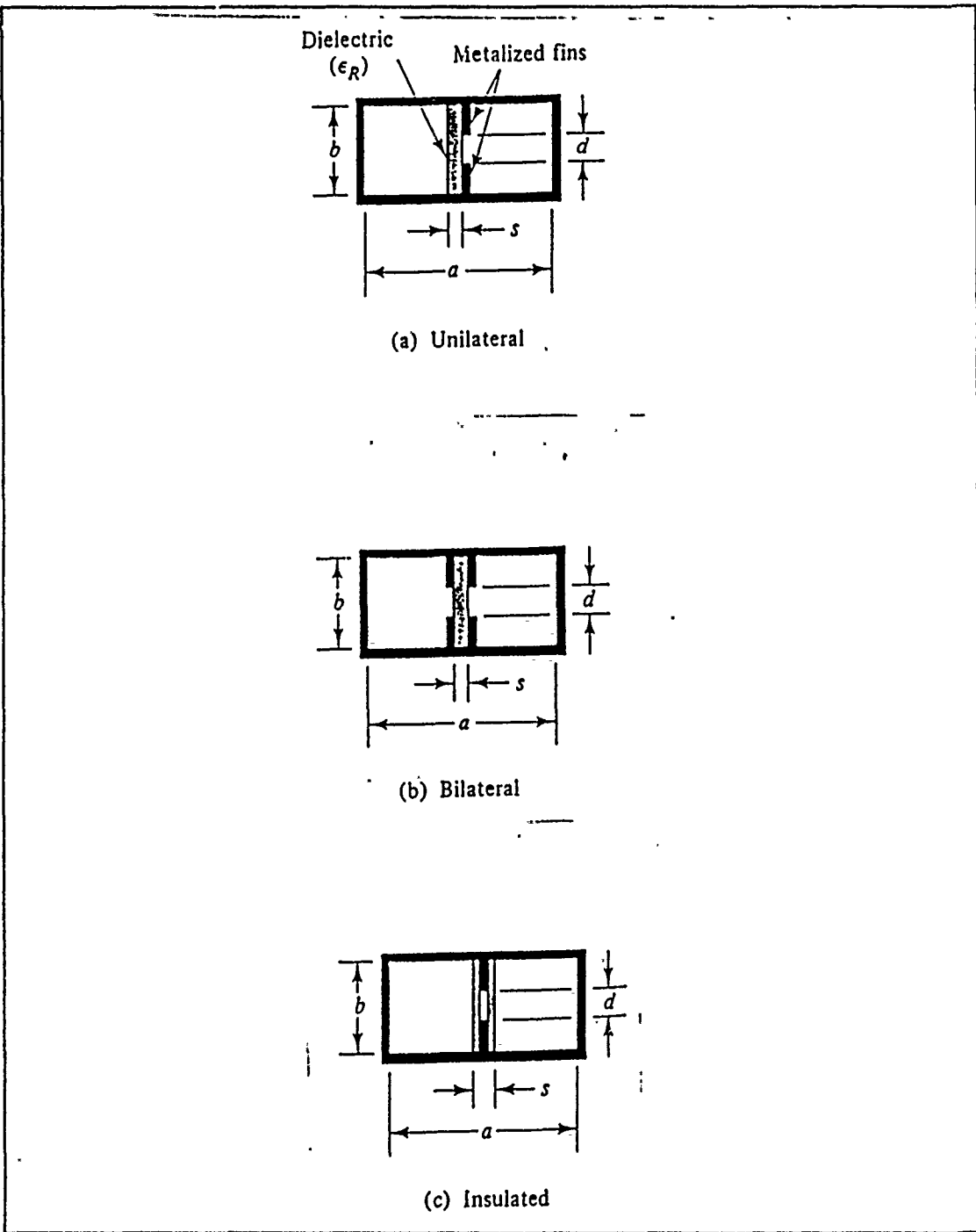


Figure 3. Three typical fin-line structures.

The electric field in the plane containing the fins is predominantly in the  $x$ -direction. A wave incident on the strip induces a current on the strip and the associated stored magnetic energy of the evanescent field gives the strip its inductive property. If the strip is very long, the field decays with distance and the strip behaves like a shorting septum [Ref. 3: pp. 1196]. If the strip is sufficiently short, the incident wave is partially backscattered and partially forward scattered. The scattering coefficients  $S_{11}$  and  $S_{21}$  are functions of the strip width, fin separation, dielectric constant, shield size, and strip length.

The purpose of this thesis is to develop a circuit model for the inductive strip in homogeneous ( $E_r = 1$ ) unilateral fin-line. The model will be developed by matching model data to numerical data derived from the spectral domain technique for different values of  $W/b$  and  $T/D$ .

This model can be used to design millimeter wave filters. Thus, a good check on the accuracy and utility of the model could be obtained by using the model to design some filters and then comparing the measured and predicted performance of the filters.

## II. MODELING THE WR(90) FIN-LINE

The integrated fin-line structure can be viewed as a slotline with a shield, a ridged waveguide with dielectric, or a slab-loaded waveguide with fins. For thin slabs with low values of  $E_r$ , the fin-line structure is essentially the same as a narrow-width ridged waveguide. In practice, when fin-lines are constructed, the dielectric material is often allowed to pass through the broad wall of the shield [Ref. 2: pp. 737]. An additional dielectric spacer may be used to provide complete dc isolation of a fin from the shield. This allows biasing of solid-state devices mounted between the fins [Ref. 2: pp. 737]. The integrated fin-line is often utilized as a medium for constructing millimeter wave circuits. In this chapter we model the fin-line using spectral domain data, for wavelength and characteristic impedance.

For homogeneous fin-line the wavelength and characteristic impedance are given exactly by the relations 1(a):

$$\frac{\lambda'}{\lambda} = \frac{1}{\sqrt{1 - \left(\frac{\lambda}{\lambda_c}\right)^2}} \quad Z_{0v} = \frac{Z_{0v\infty}}{\sqrt{1 - \left(\frac{\lambda}{\lambda_c}\right)^2}} \quad (1a)$$

$$Z_{0v} = \left(2 \frac{b_{eq}}{a_{eq}}\right) \eta_0 \left(\frac{\lambda'}{\lambda}\right) \quad \frac{\lambda'}{\lambda} = \frac{1}{\sqrt{1 - \left(\frac{\lambda}{2a_{eq}}\right)^2}} \quad (1b)$$

where  $\lambda_c$  and  $Z_{0v\infty}$  are the cutoff wavelength and high-frequency limit impedance of the fin-line.

Figure 4 on page 6 shows a homogeneous fin-line structure as well as an equivalent rectangular waveguide structure. Since the homogeneous rectangular waveguide is governed by the same equations 1(a) for the cutoff wavelength and characteristic impedance, we can construct a waveguide with dimensions  $a_{eq}$  and

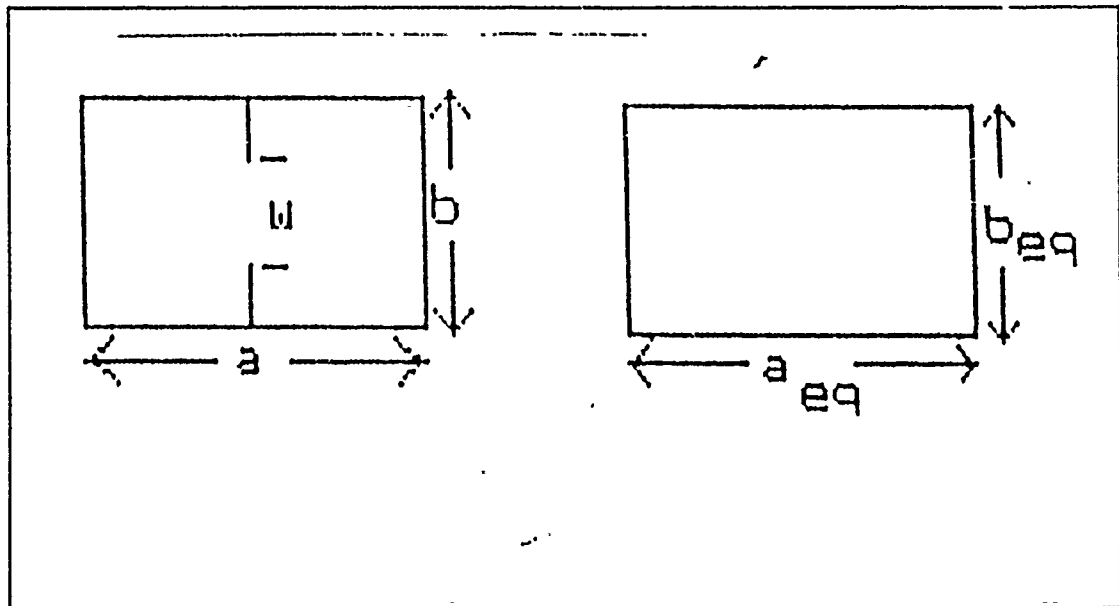


Figure 4. Homogeneous fin-line and equivalent rectangular waveguide structures.

$b_{eq}$  which will have the same cutoff wavelength and impedance as expressed in equations 1(b). The choice of WR(90) fin-line was made because some experimental data existed for strips in homogeneous fin-line with  $W/b < 1$  in the frequency range of 8.0-12.0 GHz.

In equation (1), the values of  $\frac{\lambda'}{\lambda}$  and  $Z_{0v}$  for each particular frequency and for various values of  $W/b$  were determined by using the spectral domain technique for WR(90) fin-line.

Table 1 on page 7 shows the computed values of  $\frac{\lambda'}{\lambda}$  and  $Z_{0v}$  for  $W/b = 0.5$ . Similar results for  $W/b = 1.0, 0.25, 0.2, 0.1, 0.05, 0.02, 0.01$  are tabulated in Table 8 in Appendix A. Then, by using equation (1), the values of  $\lambda_c$  and  $Z_{0v\infty}$  for each frequency were calculated as shown in Table 2 on page 7. This table gives the values of  $\lambda_c$  and  $Z_{0v\infty}$  for the frequency interval 8.0-12.0 GHz.

In order to find the values of  $a_{eq}/a$  and  $b_{eq}/b$  to design our model we use the equations:

Table 1. Numerical values of  $\frac{\lambda'}{\lambda}$  and  $Z_{ov}$  for  $W/b=0.5$ .

Frequency	$\frac{\lambda'}{\lambda}$	$Z_{ov}$	W/b
8.0000	1.4665	424.2608	0.5
8.5000	1.3787	398.8695	0.5
9.0000	1.3165	380.7870	0.5
9.5000	1.2683	367.2257	0.5
10.0000	1.2344	356.7146	0.5
10.5000	1.2032	348.5253	0.5
11.0000	1.1806	341.7068	0.5
11.5000	1.1608	336.2265	0.5
12.0000	1.1466	331.0608	0.5

Table 2. Calculated values of cutoff wavelength and characteristic impedance vs. W/b for WR(90) fin-line.

W/b	$\lambda_c$	$Z_{ov}$
1.0	1.8	334.80
0.5	2.02	289.32
0.25	2.32	230.89
0.2	2.42	215.04
0.1	2.71	175.65
0.05	2.98	147.43
0.02	3.30	121.41
0.01	3.42	108.72

$$\frac{a_{eq}}{a} = \frac{\lambda_c}{2a} \quad (2a)$$

$$\frac{b_{eq}}{b} = \left( \frac{Z_{0v\infty}}{\eta_0} \right) \left( \frac{a_{eq}}{a} \right) \left( \frac{a}{2b} \right) \quad (2b)$$

where:  $\eta_0 = 120\pi$   
 $a = 900$  mils  
 $b = 400$  mils.

Equations 2(a) and 2(b) are general equations for any value of a and b, which have been derived by Knorr, so we can use them for the particular case where the relationship between the fin-line shield dimensions is  $b/a = 4/9$ .

**Table 3.** Calculated values of  $a_{eq}/a$  and  $b_{eq}/b$  vs.  $W/b$  for WR(90) fin-line.

$W/b$	$a_{eq}/a$	$b_{eq}/b$
1.00	1.00	1.0000
0.5	1.12	0.9687
0.25	1.29	0.8888
0.2	1.34	0.8624
0.1	1.50	0.7892
0.05	1.65	0.7285
0.02	1.85	0.6623
0.01	1.90	0.6164

The computed values are tabulated in Table 3. Figure 5 on page 9 and Figure 6 on page 10 show the plots of  $a_{eq}/a$  and  $b_{eq}/b$  vs.  $W/b$  respectively, where by using a best fit curve program we determined the following polynomials of 5th degree.

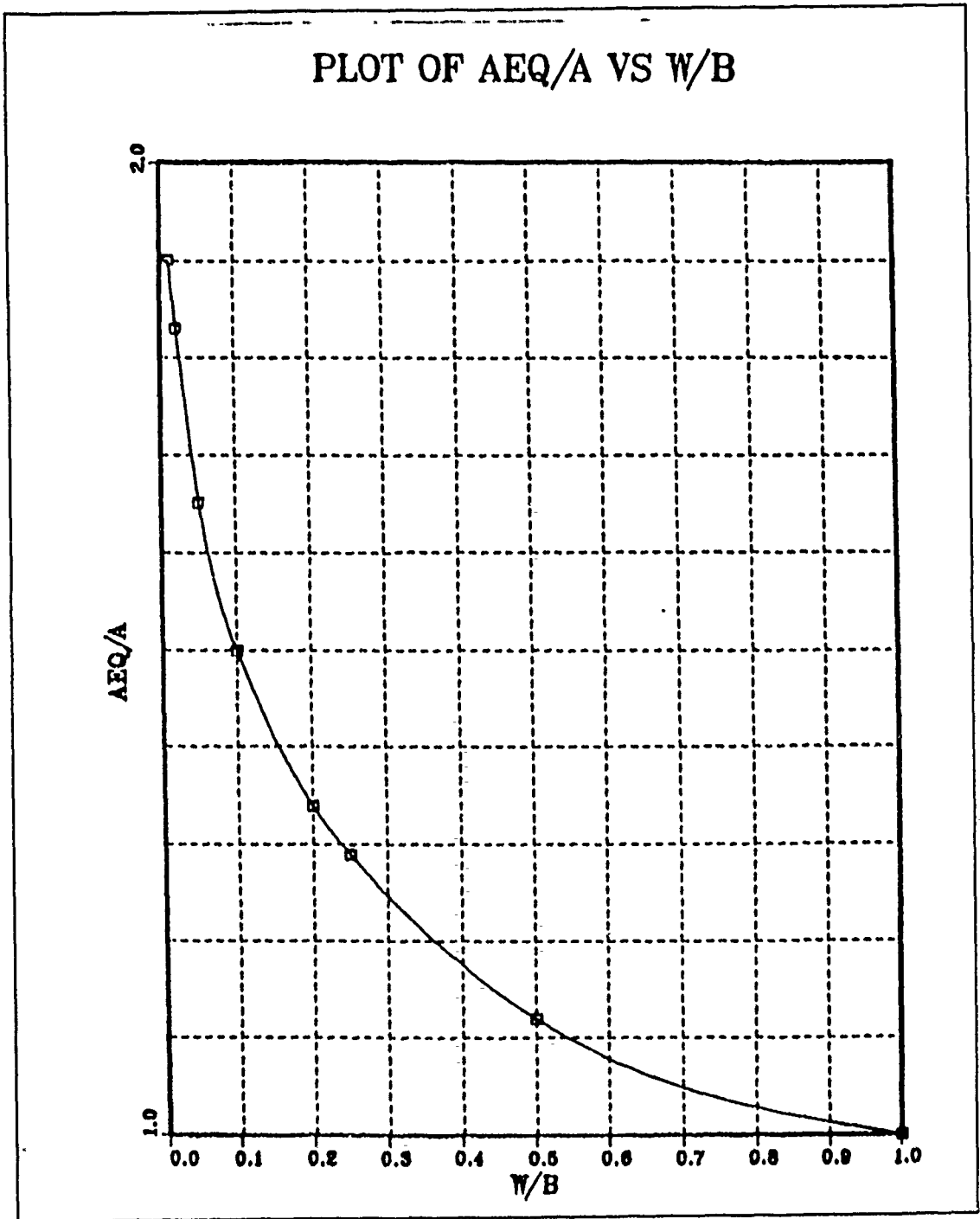


Figure 5. Plot of  $a_{eq}/a$  vs.  $W/b$  for a WR(90) fin-line.

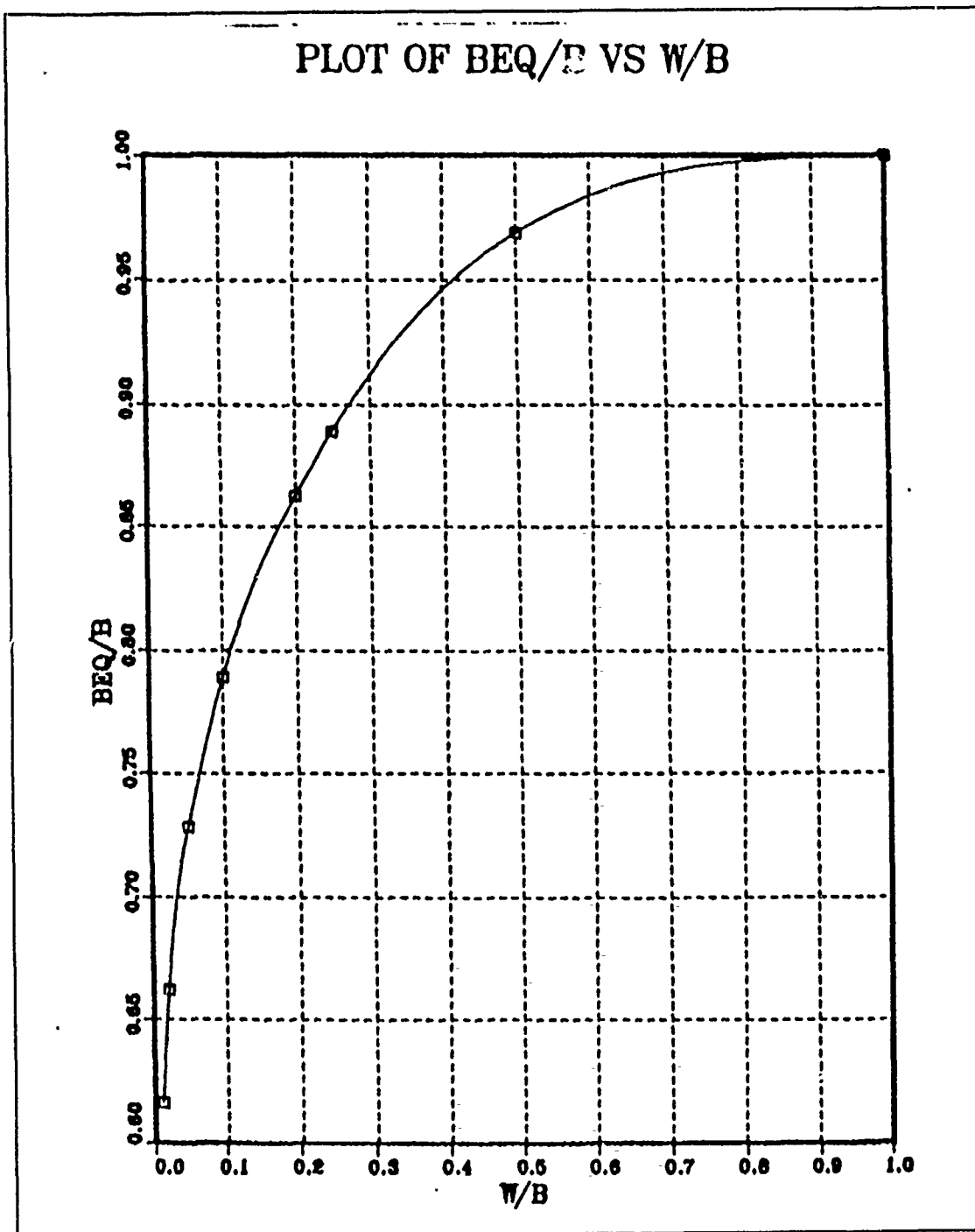


Figure 6. Plot of  $b_{e1}/b$  vs.  $W/b$  for a WR(90) fin-line.

$$\frac{a_{eq}}{a} = -247.3607\left(\frac{W}{b}\right)^5 + 471.5724\left(\frac{W}{b}\right)^4 - 289.3820\left(\frac{W}{b}\right)^3 + 74.0446\left(\frac{W}{b}\right)^2 - 9.8651\left(\frac{W}{b}\right) + 1.9909 \quad (3)$$

$$\frac{b_{eq}}{i} = 160.6892\left(\frac{W}{b}\right)^5 - 300.4026\left(\frac{W}{b}\right)^4 + 176.6337\left(\frac{W}{b}\right)^3 - 41.2604\left(\frac{W}{b}\right)^2 + 4.7638\left(\frac{W}{b}\right) + 0.5763 \quad (4)$$

These polynomials will be used to design the model of the fin-line structure.

### III. MODELING AN INDUCTIVE STRIP IN HOMOGENEOUS FIN-LINE

The inductive strip in fin-line is used to construct simple resonators as well as more complicated multi-resonator filters. The geometry for an inductive strip is illustrated in Figure 2, Chapter 1.

The scattering coefficients  $S_{11}$  and  $S_{21}$  are functions of strip width, fin separation, dielectric constant, and strip length. The inductive strip is lossless, reciprocal, and symmetric, so its scattering matrix is unitary with  $S_{11} = S_{22}$  and  $S_{12} = S_{21}$ . The unitary property leads to:

$$|S_{21}| = [1 - |S_{11}|^2]^{\frac{1}{2}} \quad (5)$$

$$\vartheta_{12} = \vartheta_{11} \pm \frac{\pi}{2} \quad (6)$$

where, in (6), the minus (-) sign is chosen because the strip is inductive. [Ref. 5: pp. 1013]

Theoretically, the problem can be solved by applying the spectral-domain method to fin-line resonators which are end-coupled by a thin, lossless strip. This permits the scattering matrix of the strip to be computed as reported by Knorr and Deal [Ref. 5: pp. 1011].

Some experimental measurements have been made to validate the numerical data generated using the code written by Deal [Ref. 6]. To ease measurement difficulties, all measurements were made using X-band test structures. Shield size was 0.4x0.9 in WR(90) fin-line and the fins were centered in the shield. With no dielectric, it is easy to establish the reference planes required for the measurement. Figure 7 on page 14 and Figure 8 on page 15 show  $|S_{11}|$  and  $\angle S_{11}$  for different strip lengths in fin-line with  $W/b = 0.5$ . Curves are presented for  $T = 20$ ,

50, 100, 200, and 500 mils. Similar data for  $W/b=0.25$  and  $W/b=0.2$  are shown in Figures 18-19 and Figures 20-21 respectively, in Appendix B.

The ultimate goal is to design a model of an inductive strip in a fin-line. Typically, fin-line has a dielectric substrate with a dielectric constant  $> 1$ , but this increases the complexity of the problem, so the first step is to work with homogeneous ( $E_r = 1$ ) fin-line.

Figure 9 on page 16 shows the circuit model of the inductive strip in fin-line, where  $T$  is the strip length and  $L$  is the inductance. As described in [Ref. 7.], the dimensions of the waveguide will be  $a_{eq}/2$  and  $b_{eq}$  which are evaluated by using the computed values of  $\lambda_c$  and  $Z_{0v\infty}$  from Table 3 on page 8 for each different value of  $W/b$ . The computed values of  $a_{eq}$  and  $b_{eq}$  will be used with the existing numerical and experimental data for strips in WR(90) fin-line with  $W/b < 1$  to build a circuit model for the strips.

The computed scattering coefficients from the Tables 4, 8 and 9 were used to create a data file for  $W/b=0.5, 0.25, 0.2$  and for  $T=20, 50, 100, 200,$  and  $500$  mils respectively as shown in Table 5 and Tables 10-23 in Appendix A. A TOUCHSTONE circuit file then was created to compute the scattering coefficients of the circuit model as shown in Figure 10 on page 17 and Figure 11 on page 18.

Table 5. TOUCHSTONE data file of scattering coefficients for  $W/b=0.5$   $T=100$  mils.

1 SCATTERING PARAMETERS:									
1	FREQ	/S11/	<S11	/S21/	<S21	/S12/	<S12	/S22/	<S22
8.0	.9649	153.6750	.2627	63.6750	.2627	63.6750	.9649	153.6750	
9.5	.9517	149.4281	.3069	59.4281	.3069	59.3069	.9517	149.4281	
9.0	.9367	145.2937	.3500	55.2937	.3500	55.2937	.9367	145.2937	
9.5	.9193	141.5109	.3935	51.5109	.3935	51.5109	.9193	141.5109	
10.0	.9002	136.8422	.4355	46.8422	.4355	46.8422	.9002	136.8422	
10.5	.8776	133.3406	.4794	43.3406	.4794	43.3406	.8776	133.3406	
11.0	.8539	129.0234	.5204	39.0234	.5204	39.0234	.8539	129.0234	
11.5	.8269	125.9875	.5623	35.9875	.5623	35.9875	.8269	125.9875	
12.0	.7975	120.1500	.6034	30.1500	.6034	30.1500	.7975	120.1500	

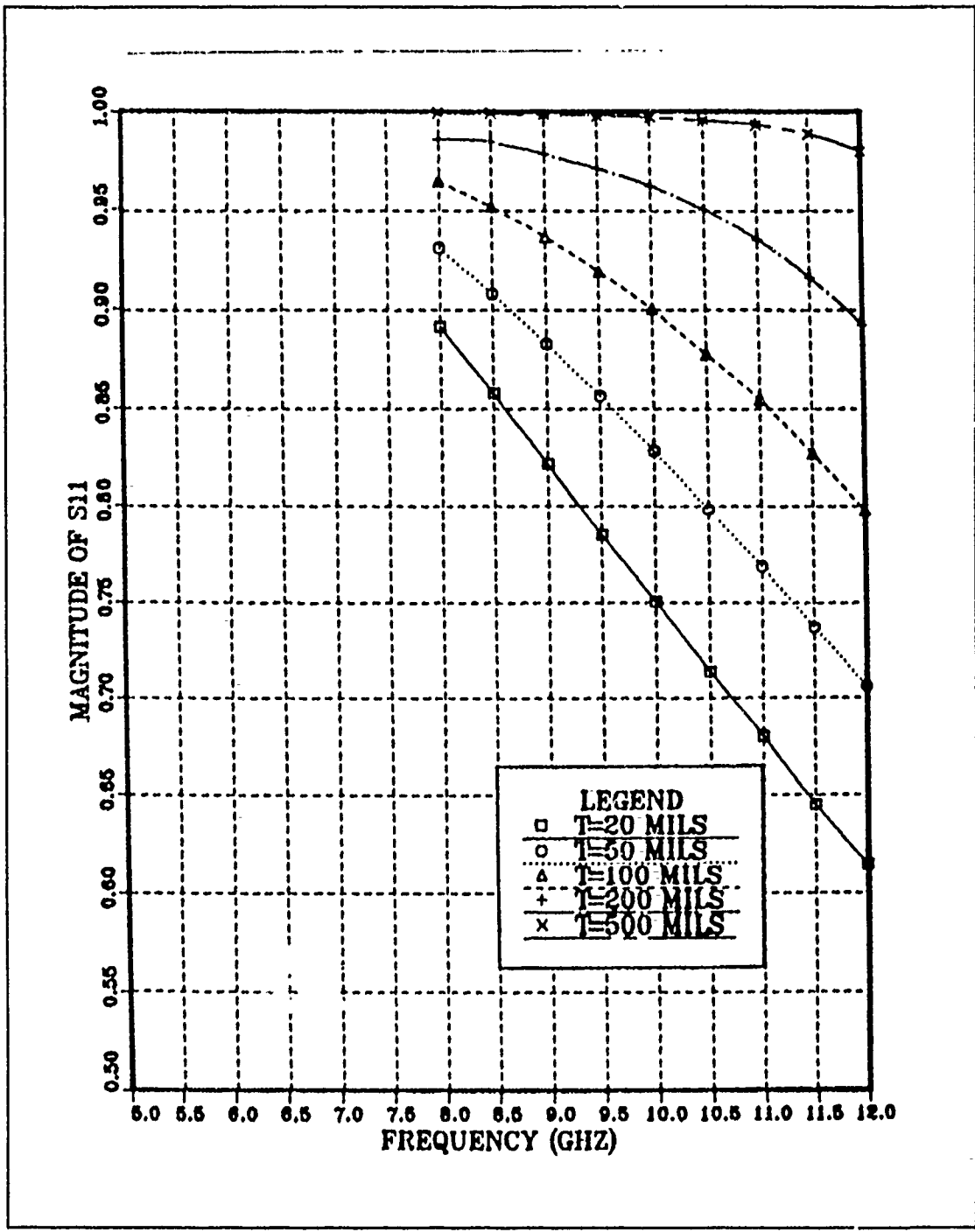


Figure 7.  $|S_{11}|$  vs. frequency for inductive strips centered in WR(90) fin-line.  
 $W/b=0.5, E_{r2} = 1.$

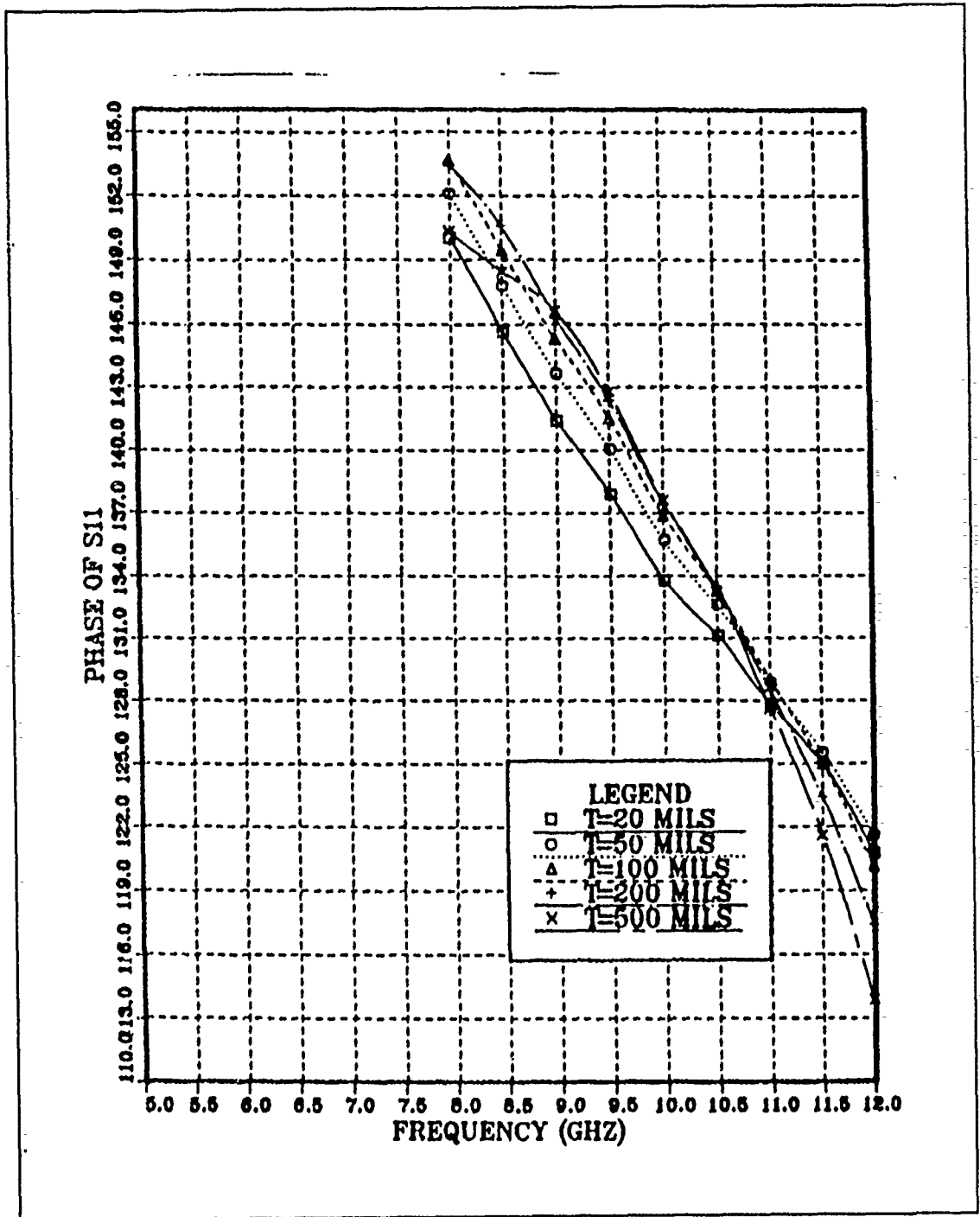


Figure 8.  $\theta_{11}$  vs. frequency for inductive strips centered in WR(90) fin-line.  
 $W/b = 0.5$ ,  $E_r = 1$ .

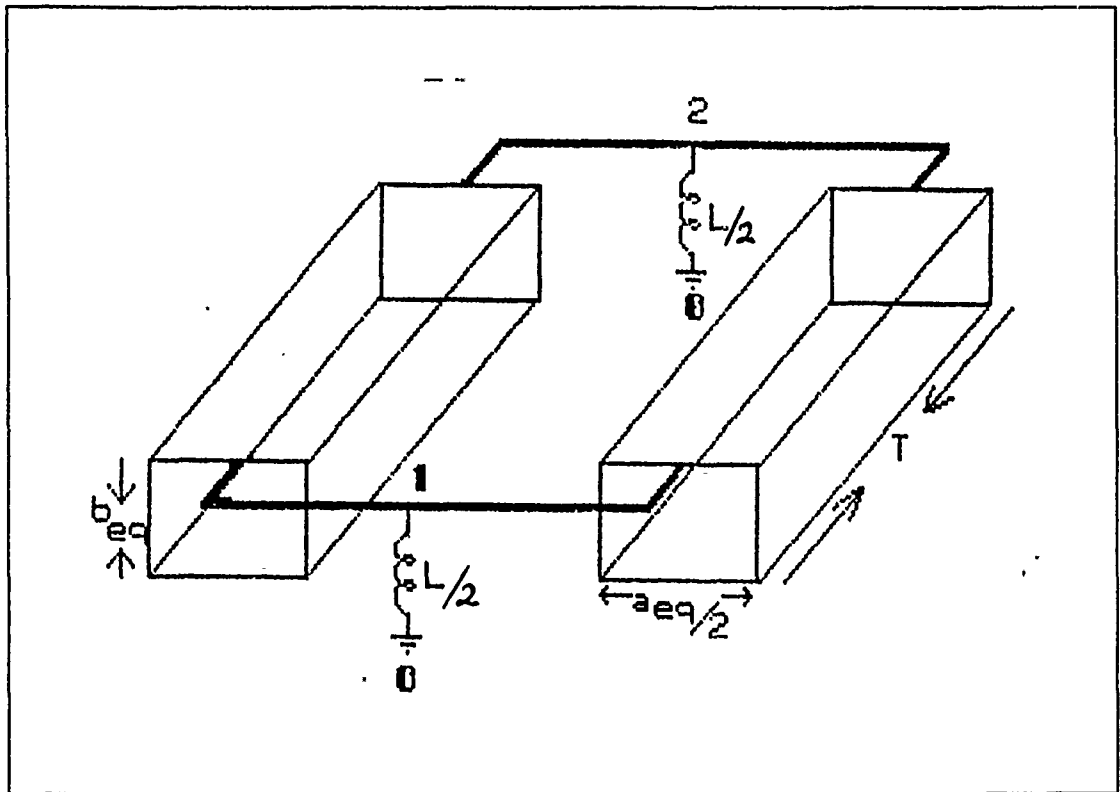


Figure 9. Circuit model of an inductive strip in fin-line.

Our goal is to match the scattering characteristics of the strip model to the computed scattering coefficients. By changing the value of the inductance  $L$ , we can find the value for which we obtain the best fit to the computed data.

The comparisons between the computed scattering coefficients and those predicted by the model for the case of  $W/b=0.5$  and  $T=100$  mils are illustrated in Figure 12 on page 19 and Figure 13 on page 20 which show the magnitude and phase curves respectively. These curves were made by using the TOUCHSTONE Microwave Circuit Simulator marketed by EEsos, Inc., Westlake Village, CA. By observing the phase curve in Figure 12 we can see that the error is about 3-4 % for the choice  $L=8.2$  nH.

Figure 14 on page 21 shows a Smith chart plot of calculated scattering coefficients  $S_{11}$  and  $S_{12}$  and those predicted by the model for the particular case of  $W/b=0.5$  and  $T=100$  mils.

```

CIRCUIT : MODEL OF 0.100 IN, INDUCTIVE STRIP OF J1(90)
          FINLINE. W/b = 0.5, STRIP CENTERED.

DIM
  FREQ  GHz
  RES   OH
  IND   NH
  CAP   pf
  LNG   MIL
  TIME  PS
  COND  /OH
  ANG   DEG

VAR
  a = 900
  b = 400
  W = 80
  T = 100
  L = 8.20

EQN
  X3 = T/2
  X1a1 = (-247.3607*(W/b)**5)
  X1a2 = (471.5724*(W/b)**4)
  X1a3 = (-299.3820*(W/b)**3)
  X1a4 = (74.0446*(W/b)**2)
  X1a5 = (-9.8651*(W/b))+1.9909
  Aeq = (X1a1+X1a2+X1a3+X1a4+X1a5)*a

  X1b1 = (160.6892*(W/b)**5)
  X1b2 = (-300.4026*(W/b)**4)
  X1b3 = (176.6337*(W/b)**3)
  X1b4 = (-41.2604*(W/b)**2)
  X1b5 = (4.7638*(W/b))+0.5763
  Beq = (X1b1+X1b2+X1b3+X1b4+X1b5)*b

  X1 = Aeq/2

```

Figure 10. TOUCHSTONE circuit file computing the scattering coefficients of the circuit model (part 1).

Similar plots can be obtained for  $W/b=0.5, 0.25, 0.2,$  and  $T=20, 50, 100, 200$  and  $500$  mils in magnitude, phase, and on the Smith chart. These plots are illustrated in Figures 22-63 respectively and were obtained by using the corresponding optimum value of  $L$  for each case. Table 6 on page 23 shows all the predicted values of  $L$  for each particular case, along with those values of  $L$  for

```

CKT
IND .1 0 L*L
RUG 1 2 A ^ X1 B ^ Beq L ^ X3 ER = 1 RHO = 1
DEF2P 1 2 A

A 1 2
A 1 2
A 3 2
A 3 2
DEF2P 1 3 STRIPMOD

S2PA 1 2 0 T90wbS10.s2p
DEF2P 1 2 T90wbS10

RUGT 1 A ^ Aeq D ^ Deq ER = 1 RHO = 1
DEFIP 1 WEDGE

TERM
STRIPMOD WEDGE WEDGE

OUT
T90wbS10 S11 SC2
| T90wbS10 S21 SC2
| T90wbS10 MAG(S11) GR1
| T90wbS10 ANG(S11) GR2
| STRIPMOD S11 SC2
| STRIPMOD S21 SC2
| STRIPMOD MAG(S11) GR1
| STRIPMOD ANG(S11) GR2

FREQ
SWEEP 0.0 12. 0.5

GRID
RANGE 8.0 12. 1.0
GR1 0.0 1. 0.1
GR2 30 100 5.0

```

Figure 11. TOUCHSTONE circuit file computing the scattering coefficients of the circuit model (part 2).

$W/b = 1.0$  as determined by Knorr [Ref. 7: pp. 13]. The table shows that as strip length increases from  $T = 20$  to 500 mils, the value of  $L$  decreases. As  $W/b$  decreases for each particular value of  $T$ , then again the inductance decreases.

Having obtained the inductance for the various strip lengths ( $T = 20, 50, 100, 200, 500$  mils) and for various values of  $W/b$  modeled previously, it is a simple matter to explore the possibility that the curve  $L(T)$  can be approximated by

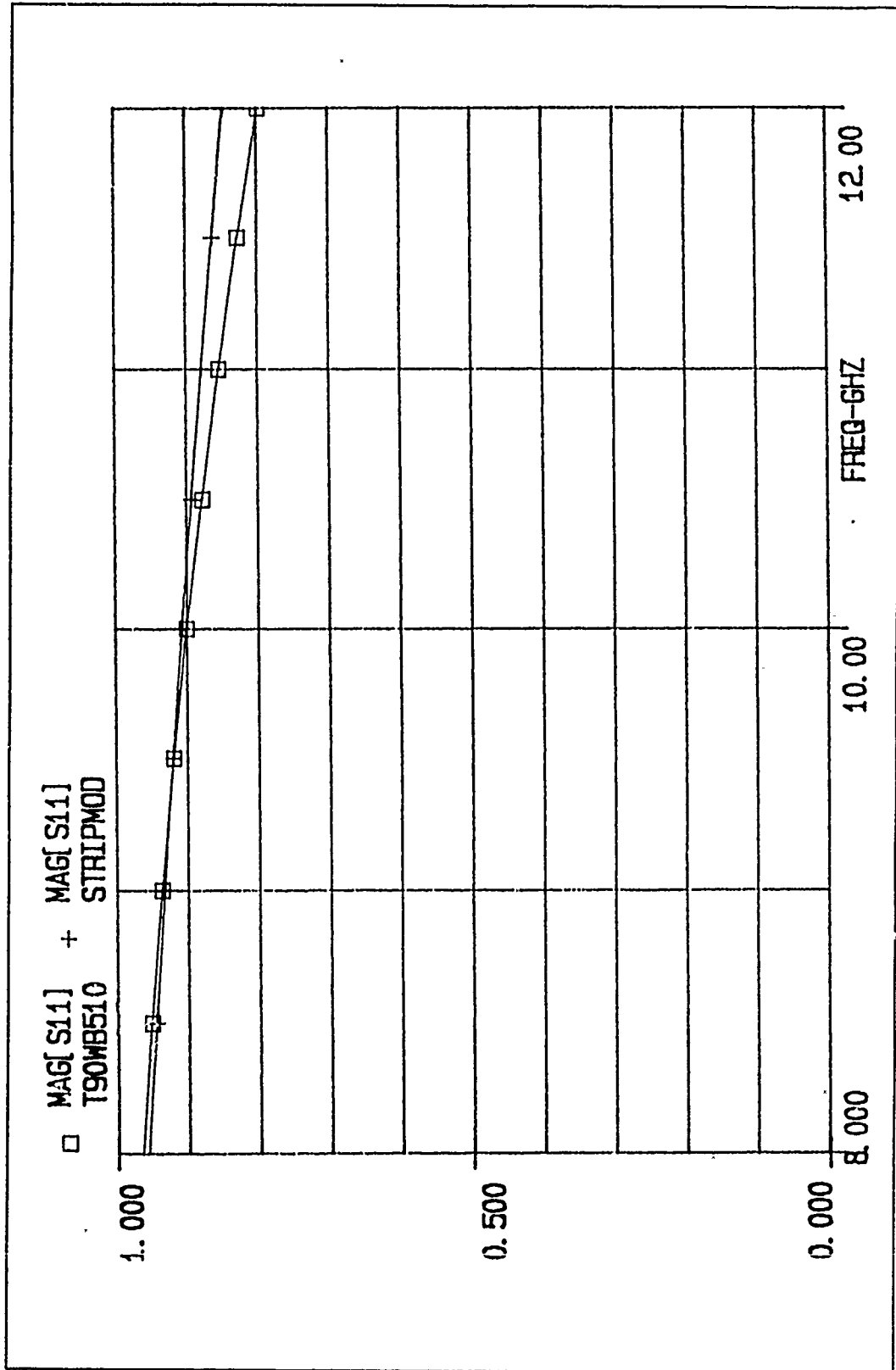


Figure 12. Computed and predicted values of  $|S_{11}|$  vs. frequency for a  $T = 100$  mils inductive strip centered in WR(90) waveguide  $W/b = 0.5$ ,  $E_{r2} = 1$ . Model inductance  $L_{eff} = 8.2$  nH.

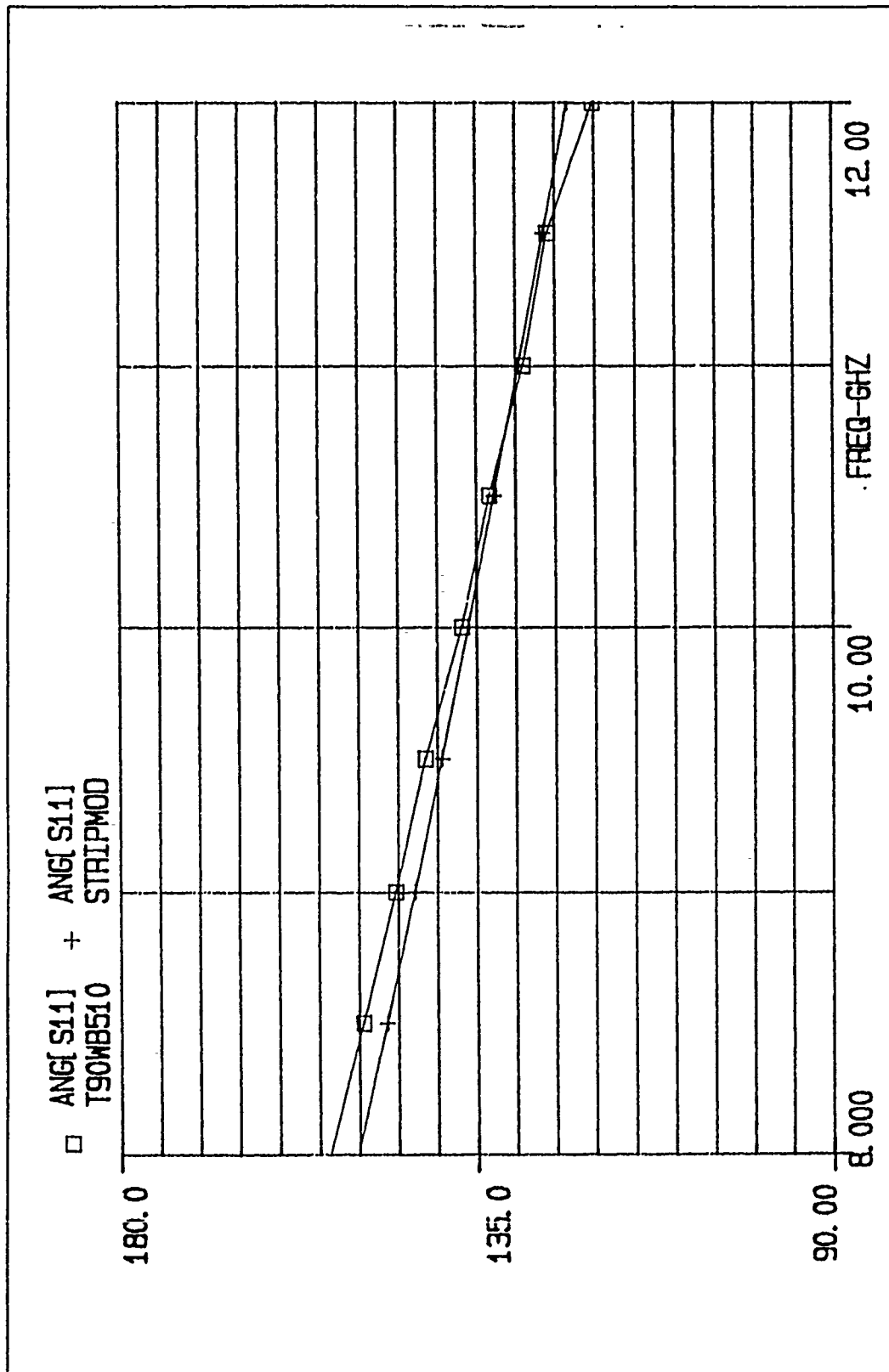


Figure 13. Computed and predicted values of  $\theta_{11}$  vs. frequency for a  $T = 100$  mils inductive strip centered in WR(90) waveguide  $W/b = 0.5$ ,  $E_{r2} = 1$ . Model inductance  $L = 8.2$  nH.

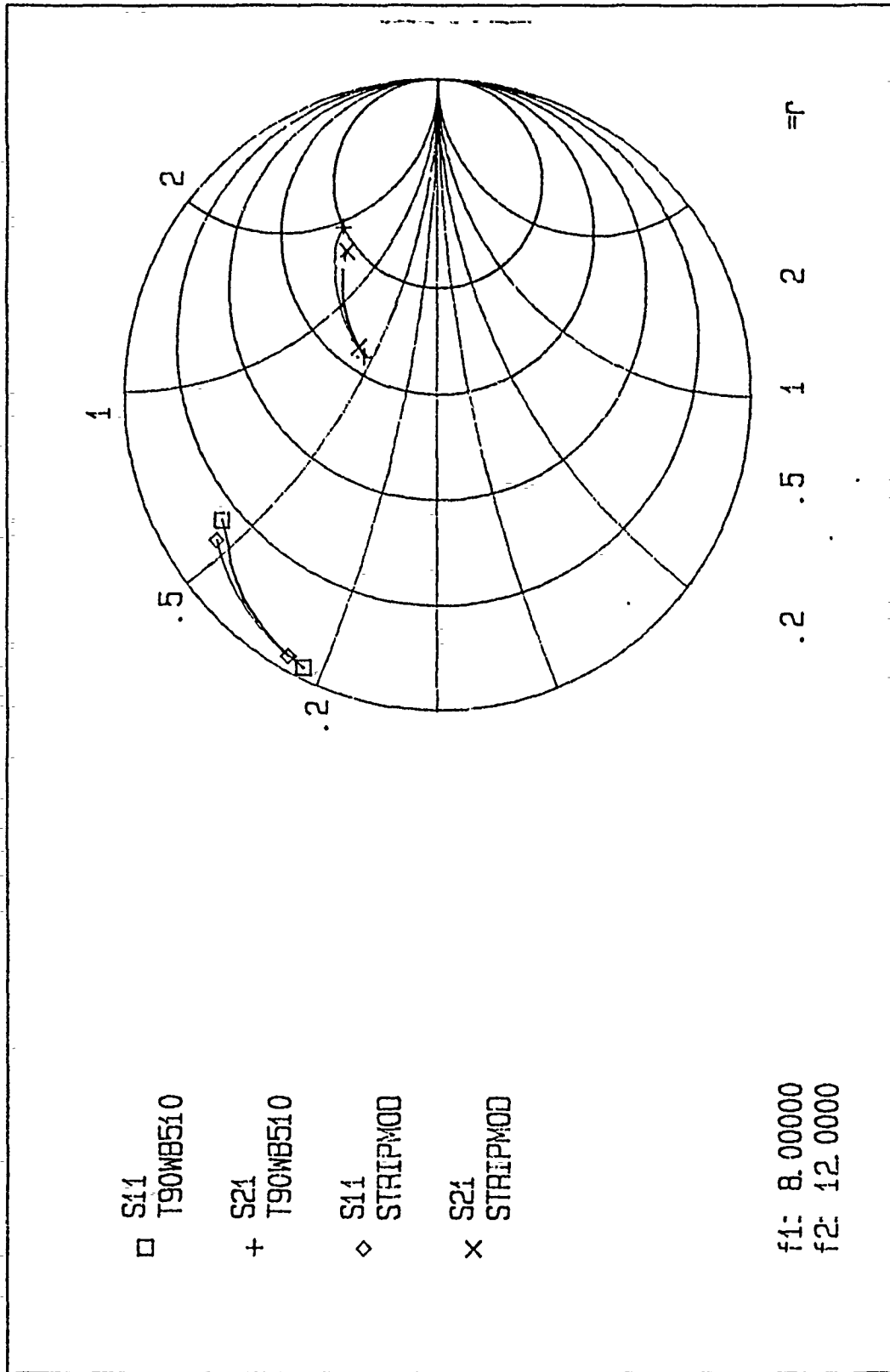


Figure 14. Smith chart plot of computed and predicted values of  $S_{11}$  and  $S_{21}$  for a  $T = 100$  mil inductive strip centered in WR(90) waveguide,  $W/b = 0.5$ ,  $E_2 = 1$ . Model inductance  $L = 8.2$  nH.

Table 4. Computed scattering coefficients for WR(90) fin-line for  $W/b=0.5$  and  $T=20, 50, 100, 200,$  and  $500$  mils ( $D=10$  mils).

FREQUENCY	S11 Mag.	S11 Phase	S12 Mag.	S12 Phase	T OVER D
8.0000	0.8918	150.0188	0.4525	60.0187	2.0000
8.5000	0.8576	145.6312	0.5143	55.6312	2.0000
9.0000	0.8217	141.4125	0.5700	51.4125	2.0000
9.5000	0.7852	137.8969	0.6193	47.8969	2.0000
10.0000	0.7508	133.8047	0.6606	43.8047	2.0000
10.5000	0.7140	131.1328	0.7001	41.1328	2.0000
11.0000	0.6799	127.8141	0.7333	37.8141	2.0000
11.5000	0.6451	124.9875	0.7641	34.9875	2.0000
12.0000	0.6150	120.8100	0.7940	30.8100	2.0000
FREQUENCY	S11 Mag.	S11 Phase	S12 Mag.	S12 Phase	T OVER D
8.0000	0.9312	152.0859	0.3645	62.0859	5.0000
8.5000	0.9079	147.7547	0.4191	57.7547	5.0000
9.0000	0.8832	143.6344	0.4690	53.6344	5.0000
9.5000	0.8560	140.0484	0.5170	50.0484	5.0000
10.0000	0.8283	135.6750	0.5603	45.6750	5.0000
10.5000	0.7981	132.6094	0.6026	42.6094	5.0000
11.0000	0.7685	128.8687	0.6399	38.8687	5.0000
11.5000	0.7371	125.5500	0.6757	35.5500	5.0000
12.0000	0.7062	121.6406	0.7080	31.6406	5.0000
FREQUENCY	S11 Mag.	S11 Phase	S12 Mag.	S12 Phase	T OVER D
8.0000	0.9649	153.6750	0.2627	63.6750	10.0000
8.5000	0.9517	149.4281	0.3069	59.4281	10.0000
9.0000	0.9367	145.2937	0.3500	55.2937	10.0000
9.5000	0.9193	141.5109	0.3935	51.5109	10.0000
10.0000	0.9002	136.8422	0.4355	46.8422	10.0000
10.5000	0.8776	133.3406	0.4794	43.3406	10.0000
11.0000	0.8539	129.0234	0.5204	39.0234	10.0000
11.5000	0.8269	124.9875	0.5623	34.9875	10.0000
12.0000	0.7975	120.1500	0.6034	30.1500	10.0000
FREQUENCY	S11 Mag.	S11 Phase	S12 Mag.	S12 Phase	T OVER D
8.0000	0.9862	153.4641	0.1656	63.4641	20.0000
8.5000	0.9848	150.5531	0.1736	60.5531	20.0000
9.0000	0.9789	146.3062	0.2045	56.3062	20.0000
9.5000	0.9714	142.3406	0.2375	52.3062	20.0000
10.0000	0.9625	137.4609	0.2714	47.4609	20.0000
10.5000	0.9501	133.4250	0.3120	43.4250	20.0000
11.0000	0.9355	128.4750	0.3532	38.4750	20.0000
11.5000	0.9161	123.4125	0.4010	33.4125	20.0000
12.0000	0.8928	117.4078	0.4505	27.4078	20.0000
FREQUENCY	S11 Mag.	S11 Phase	S12 Mag.	S12 Phase	T OVER D
8.0000	0.9999	150.3000	0.0255	60.3000	50.0000
8.5000	0.9995	148.4437	0.0355	58.4437	50.0000
9.0000	0.9989	146.5875	0.0464	56.5875	50.0000
9.5000	0.9984	142.7625	0.0557	52.7625	50.0000
10.0000	0.9975	137.5875	0.0709	47.5875	50.0000
10.5000	0.9960	133.3125	0.0895	43.3125	50.0000
11.0000	0.9934	127.6172	0.1151	37.6172	50.0000
11.5000	0.9887	121.6266	0.1501	31.6266	50.0000
12.0000	0.9802	113.8641	0.1980	23.9641	50.0000

**Table 6. Predicted values of L vs. W/b for WR(90) fin-line and strip length T using the polynomial form.**

W/b	T = 20 mils	T = 50 mils	T = 100mils	T = 200 mils	T = 500 mils
1.00	27.00	23.00	20.000	17.00	16.00
0.5	10.70	9.30	8.200	7.20	5.90
0.25	6.60	5.65	5.005	4.20	3.82
0.2	4.89	4.18	3.550	3.06	2.70

some simple analytical expression. A good fit to these data is the polynomial form of 5th degree, which can be found using a best fit curve program:

a) for W/b = 1.0:

$$L = 0.0003\left(\frac{T}{D}\right)^5 - 0.0270\left(\frac{T}{D}\right)^4 + 0.6999\left(\frac{T}{D}\right)^3 - 6.8761\left(\frac{T}{D}\right)^2 + 24.6634\left(\frac{T}{D}\right)$$

b) for W/b = 0.5:

$$L = 0.0001\left(\frac{T}{D}\right)^5 - 0.0105\left(\frac{T}{D}\right)^4 + 0.2729\left(\frac{T}{D}\right)^3 - 2.6880\left(\frac{T}{D}\right)^2 + 9.7166\left(\frac{T}{D}\right)$$

c) for W/b = 0.25:

$$L = 0.0001\left(\frac{T}{D}\right)^5 - 0.0066\left(\frac{T}{D}\right)^4 + 0.1711\left(\frac{T}{D}\right)^3 - 1.6789\left(\frac{T}{D}\right)^2 + 6.0250\left(\frac{T}{D}\right)$$

d) for W/b = 0.2:

$$L = 0.0001\left(\frac{T}{D}\right)^5 - 0.0048\left(\frac{T}{D}\right)^4 + 0.1256\left(\frac{T}{D}\right)^3 - 1.2381\left(\frac{T}{D}\right)^2 + 4.4567\left(\frac{T}{D}\right)$$

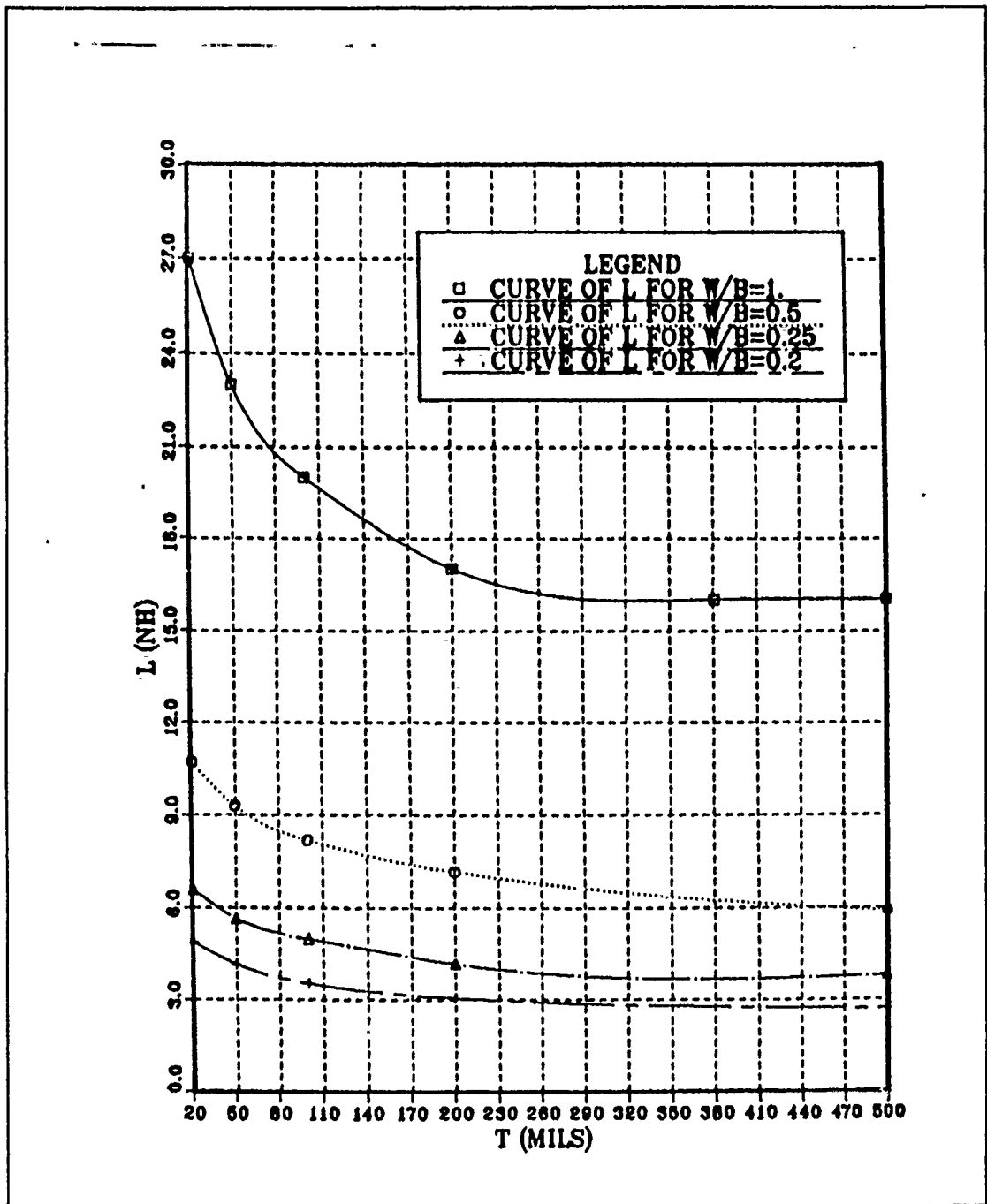


Figure 15. Plots of the model inductance  $L$  as a polynomial function of the strip length  $T$ , for  $W/b = 1.0, 0.5, 0.25, 0.2$ .

Figure 15 on page 24 shows the graphs of the model inductance L as a function of T.

Another possible form which can fit these data is an exponential curve which has the following form for each value of W/b:

a) For  $W/b=1.0$ :  $L = 16 + 14.4 * \exp(-T/75)$  nH

b) for  $W/b=0.5$ :  $L = 5.9 + 5.769 * \exp(-T/108.738)$  nH

c) for  $W/b=0.25$ :  $L = 3.82 + 3.44 * \exp(-T/93.8187)$  nH

d) for  $W/b=0.2$ :  $L = 2.7 + 2.7746 * \exp(-T/84.529)$  nH

where strip length T is in mils.

We can see that as W/b decreases the value of the inductance decreases. This reflects the fact that as the space between the fins decreases, a strip of fixed length will reflect a higher fraction of the incident power. Table 7 shows the calculated values of L using these exponential formulas for each value of T. Figure 16 on page 26 shows the graphs of the model inductance L, as a function of the strip length T, for W/b = 1.0, 0.5, 0.25, 0.2. The values listed on Table 7 are circled on the graphs.

**Table 7. Predicted values of L vs. W/b for WR(90) fin-line and strip length T using the exponential form.**

W/b	T = 20 mils	T = 50 mils	T = 100mils	T = 200 mils	T = 500 mils
1.00	27.000	23.000	20.0000	17.000	16.000
0.5	10.699	9.540	8.1900	6.816	5.958
0.25	6.599	5.839	5.0049	4.228	3.836
0.2	4.889	4.235	3.5499	2.960	2.707

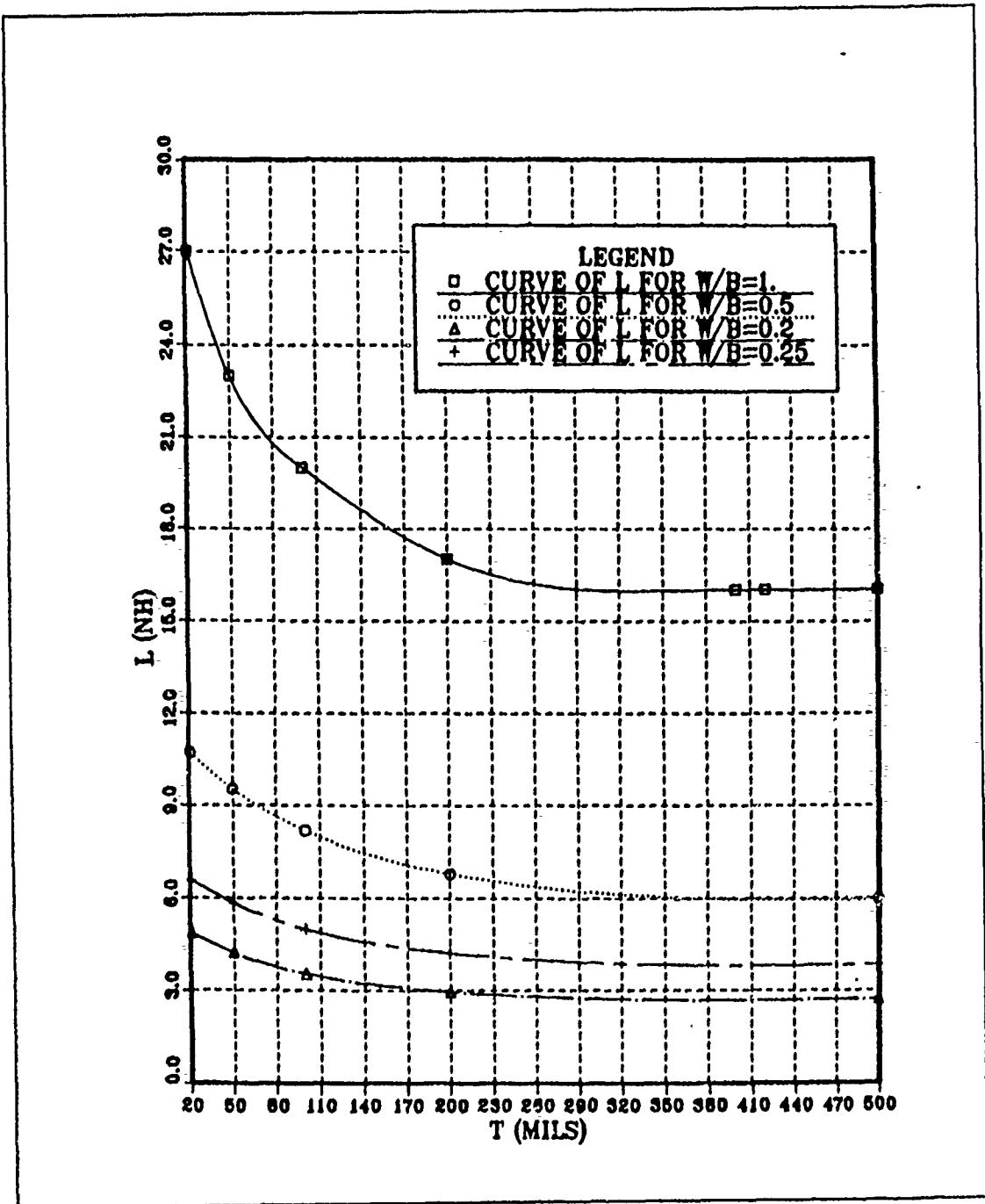


Figure 16. Plot of the model inductance  $L$  as an exponential function of the strip length  $T$ , for  $W/b = 1.0, 0.5, 0.25, 0.2$ .

Comparing the values of  $L$  between Table 6 on page 23 and Table 7, we see that there is a slight difference between them. Figure 17 on page 27 shows the difference between the exponential and polynomial form for each value of  $W, b$ .

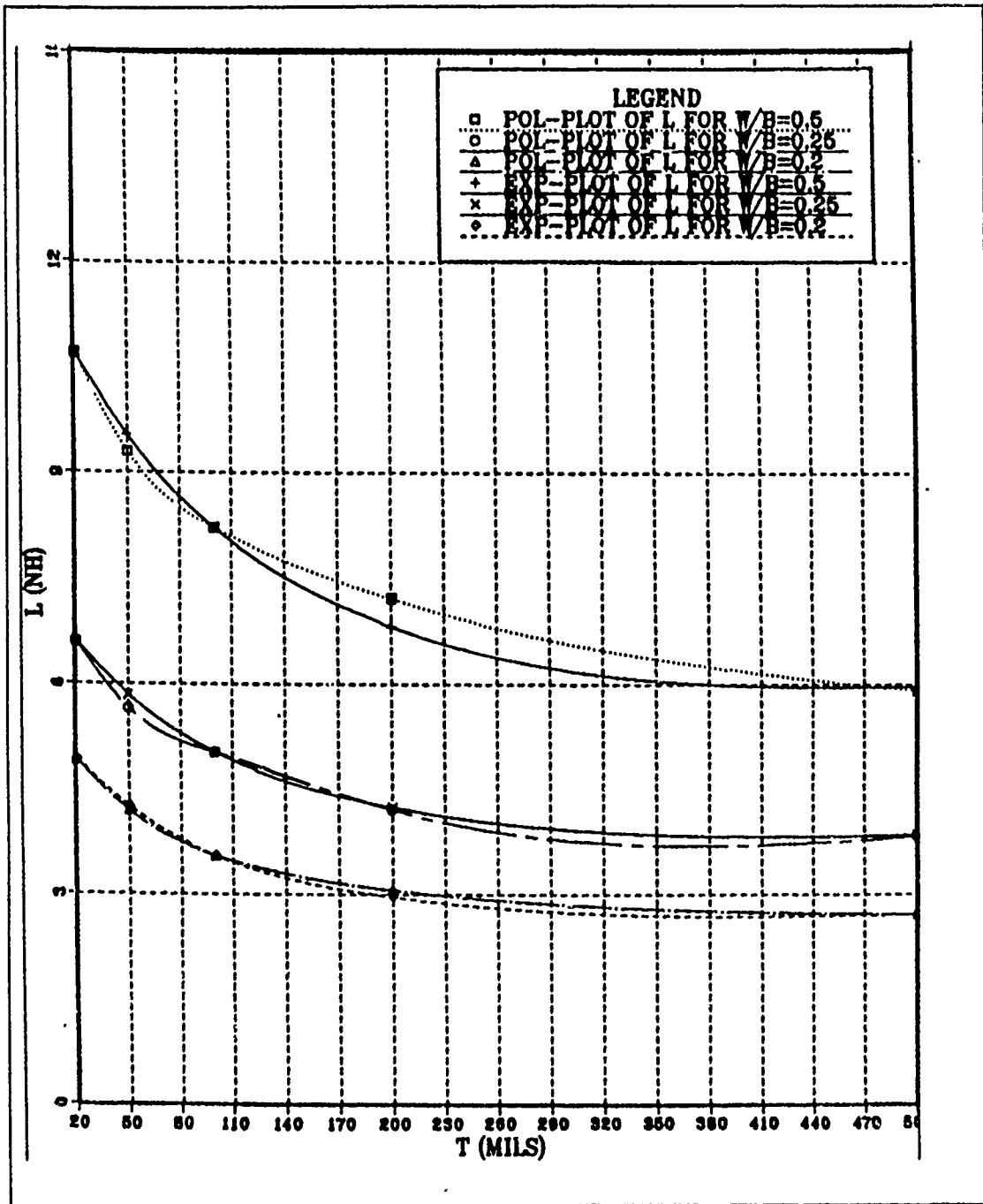


Figure 17. Difference between the exponential and polynomial plots of the model inductance  $L$ , for  $W/b = 0.5, 0.25, 0.2$ .

## IV. CONCLUSIONS AND RECOMMENDATIONS

### A. CONCLUSIONS

This thesis describes a circuit model for an inductive strip in fin-line for the homogeneous case, where  $E_{r2} = 1$  and any value of  $W/b$  in the range  $0 < W/b \leq 1$  is permitted.

The characteristics of integrated fin-line transmission line are reviewed. Fin-line is compatible with batch-processing techniques and superior to microstrip in several respects at millimeter wavelengths. Relative to microstrip, fin-line can provide less stringent tolerances, greater freedom from radiation and higher mode propagation, better compatibility with hybrid devices, and simpler interfaces with waveguide instrumentation [Ref. 1: pp. 1209].

The models discussed here were determined for the 8-12 GHz frequency range using WR(90) waveguide for reasons related to availability of test instrumentation and ease of fabrication. It was in this frequency range that experimental data was available to verify the numerical data generated using Deal's code [Ref. 6]. Numerical data was used to develop the circuit model. X-band was chosen as a starting point to ensure that the model was based on accurate data. Thus the design of a fin-line model was needed for  $b/a = 4/9$ . The values of the cutoff wavelength and the high frequency impedance limit were determined for different values of  $W/b$  ( $W/b = 0.5, 0.25, 0.2, 0.1, 0.05, 0.02, 0.01$ ) using spectral domain data.

The circuit model is elegant in its simplicity, consisting of parallel, below cutoff waveguide sections with lumped inductors at each end. The values of the equivalent dimensions were obtained by using equations (2), which were derived by Prof. Knorr for various values of  $W/b$ .

The model was developed using data for strips with lengths of  $T = 20, 50, 100, 200,$  and  $500$  mils. The value of lumped inductance was determined by varying  $L$  to obtain the best agreement between the value of  $\angle S_{11}$  predicted by the circuit model and the value of  $\angle S_{11}$  computed numerically for strips of various lengths

in WR(90) fin-line. Good agreement was obtained in all cases and the optimum values of inductance were used to determine a function  $L(T)$ .

The good agreement that has been obtained between model data and numerical data suggests that the model may be used to design millimeter filters for communication systems, high-resolution imaging, collision avoidance radars, and environmental monitoring equipment [Ref. 1: pp. 1215].

## B. RECOMMENDATIONS

As a result of the success achieved in the modeling effort reported here, there are several areas which appear fruitful for future investigation.

1. Develop a model for strips centered in finline with  $W/b = 0.1, 0.05, 0.02, 0.01, E_{r2} = 1$ .
2. Investigate the relationship of strip length to the coefficients of the polynomial which describes the function  $L(T)$ .
3. Develop a model for inductive strips which are off-centered with  $W/b < 1, E_{r2} = 1$ .
4. Develop a model for the general case of a strip printed on a dielectric substrate with  $W/b < 1$ .

## APPENDIX A. TABLES

**Table 8. Computed scattering coefficients for WR(90) fin-line for  $W/b=0.25$  and  $T=20, 50, 100, 200,$  and  $500$  mils ( $D=10$  mils).**

FREQUENCY	S11 Mag.	S11 Phase	S12 Mag.	S12 Phase	T OVER D
8.0000	0.9314	155.5734	0.3640	65.5734	2.0000
8.5000	0.9134	152.0578	0.4070	62.0578	2.0000
9.0000	0.8938	149.3438	0.4485	59.3438	2.0000
9.5000	0.8720	146.5172	0.4895	56.5172	2.0000
10.0000	0.8494	143.7188	0.5277	53.7188	2.0000
10.5000	0.8256	140.4563	0.5643	50.4563	2.0000
11.0000	0.7992	138.1219	0.6010	48.1219	2.0000
11.5000	0.7725	134.9719	0.6350	44.9719	2.0000
12.0000	0.7447	132.3562	0.6674	42.3562	2.0000
FREQUENCY	S11 Mag.	S11 Phase	S12 Mag.	S12 Phase	T OVER D
8.0000	0.9591	157.0070	0.2832	67.0070	5.0000
8.5000	0.9476	153.5625	0.3195	63.5625	5.0000
9.0000	0.9347	150.9609	0.3553	60.9609	5.0000
9.5000	0.9202	148.1344	0.3915	58.1344	5.0000
10.0000	0.9035	145.1250	0.4287	55.1250	5.0000
10.5000	0.8855	141.8062	0.4647	51.8062	5.0000
11.0000	0.8648	139.1906	0.5021	49.1906	5.0000
11.5000	0.8423	135.6187	0.5389	45.6187	5.0000
12.0000	0.8174	132.5531	0.5760	42.5531	5.0000
FREQUENCY	S11 Mag.	S11 Phase	S12 Mag.	S12 Phase	T OVER D
8.0000	0.9755	156.6281	0.2198	66.6255	10.0000
8.5000	0.9739	154.5188	0.2270	64.5188	10.0000
9.0000	0.9667	151.8750	0.2561	61.8750	10.0000
9.5000	0.9577	148.9781	0.2877	58.9781	10.0000
10.0000	0.9472	145.8984	0.3207	55.8984	10.0000
10.5000	0.9351	142.3266	0.3544	52.3266	10.0000
11.0000	0.9201	139.4297	0.3917	49.4297	10.0000
11.5000	0.9023	135.4359	0.4311	45.4359	10.0000
12.0000	0.8808	131.6953	0.4736	41.6953	10.0000
FREQUENCY	S11 Mag.	S11 Phase	S12 Mag.	S12 Phase	T OVER D
8.0000	0.9900	157.9996	0.1350	67.9996	20.0000
8.5000	0.9895	154.8844	0.1400	64.8844	20.0000
9.0000	0.9893	152.3250	0.1460	62.3250	20.0000
9.5000	0.9858	149.3719	0.1678	59.3719	20.0000
10.0000	0.9812	146.2078	0.1932	56.2078	20.0000
10.5000	0.9749	142.2984	0.2225	52.2984	20.0000
11.0000	0.9664	138.9937	0.2570	48.9937	20.0000
11.5000	0.9551	134.4516	0.2964	44.4516	20.0000
12.0000	0.9394	129.9516	0.3429	39.9516	20.0000
FREQUENCY	S11 Mag.	S11 Phase	S12 Mag.	S12 Phase	T OVER D
8.0000	0.9999	153.3987	0.0141	63.3987	50.0000
8.5000	0.9998	152.5325	0.0190	62.5325	50.0000
9.0000	0.9996	150.8792	0.0283	60.8792	50.0000
9.5000	0.9994	148.5981	0.0346	58.5981	50.0000
10.0000	0.9988	146.1797	0.0491	56.1797	50.0000
10.5000	0.9980	142.1859	0.0628	52.1859	50.0000
11.0000	0.9966	138.5297	0.0824	48.5297	50.0000
11.5000	0.9941	133.2984	0.1088	43.2984	50.0000
12.0000	0.9889	127.7156	0.1484	37.7156	50.0000

Table 9. Computed scattering coefficients for WR(90) fin-line for  $W/b=0.2$  and  $T=20, 50, 100, 200,$  and  $500$  mils ( $D=10$  mils).

FREQUENCY	S11 Mag.	S11 Phase	S12 Mag.	S12 Phase	T OVER D
8.0000	0.9416	157.4156	0.3367	67.4156	2.0000
8.5000	0.9266	154.4906	0.3761	64.4906	2.0000
9.0000	0.9103	151.7906	0.4140	61.7906	2.0000
9.5000	0.8922	148.5562	0.4516	58.5562	2.0000
10.0000	0.8725	145.8984	0.4886	55.8984	2.0000
10.5000	0.8511	143.3953	0.5250	53.3953	2.0000
11.0000	0.8282	140.8922	0.5605	50.8922	2.0000
11.5000	0.8036	138.1219	0.5951	48.1219	2.0000
12.0000	0.7780	135.0422	0.6283	45.0422	2.0000
FREQUENCY	S11 Mag.	S11 Phase	S12 Mag.	S12 Phase	T OVER D
8.0000	0.9653	158.6531	0.2613	68.6531	5.0000
8.5000	0.9559	155.7984	0.2936	65.7984	5.0000
9.0000	0.9456	153.2109	0.3253	63.2109	5.0000
9.5000	0.9336	150.0188	0.3583	60.0187	5.0000
10.0000	0.9197	147.2203	0.3926	57.2203	5.0000
10.5000	0.9041	144.6187	0.4273	54.6187	5.0000
11.0000	0.8861	141.8766	0.4636	51.8766	5.0000
11.5000	0.8658	138.7969	0.5004	48.7969	5.0000
12.0000	0.8437	135.3375	0.5369	45.3375	5.0000
FREQUENCY	S11 Mag.	S11 Phase	S12 Mag.	S12 Phase	T OVER D
8.0000	0.9793	159.2248	0.2000	69.2248	10.0000
8.5000	0.9770	156.2484	0.2134	66.2484	10.0000
9.0000	0.9725	154.0125	0.2327	64.0125	10.0000
9.5000	0.9656	150.7078	0.2601	60.7078	10.0000
10.0000	0.9565	147.8109	0.2917	57.8109	10.0000
10.5000	0.9463	145.0687	0.3232	55.0687	10.0000
11.0000	0.9333	142.0453	0.3590	52.0453	10.0000
11.5000	0.9179	138.6141	0.3967	48.6141	10.0000
12.0000	0.8991	134.5922	0.4377	44.5922	10.0000
FREQUENCY	S11 Mag.	S11 Phase	S12 Mag.	S12 Phase	T OVER D
8.0000	0.9935	159.1025	0.1138	69.1025	20.0000
8.5000	0.9925	156.9352	0.1222	66.9352	20.0000
9.0000	0.9915	154.6210	0.1301	64.6210	20.0000
9.5000	0.9885	151.0875	0.1513	61.0875	20.0000
10.0000	0.9847	148.0641	0.1743	58.0641	20.0000
10.5000	0.9794	145.0266	0.2018	55.0266	20.0000
11.0000	0.9723	141.7078	0.2339	51.7078	20.0000
11.5000	0.9623	137.7703	0.2719	47.7703	20.0000
12.0000	0.9486	132.9891	0.3165	42.9891	20.0000
FREQUENCY	S11 Mag.	S11 Phase	S12 Mag.	S12 Phase	T OVER D
8.0000	0.9998	152.6000	0.0200	62.6000	50.0000
8.5000	0.9997	151.4000	0.0245	61.4000	50.0000
9.0000	0.9996	150.4500	0.0282	60.4500	50.0000
9.5000	0.9994	148.9000	0.0346	58.9000	50.0000
10.0000	0.9991	147.8000	0.0424	57.8000	50.0000
10.5000	0.9984	144.9141	0.064	54.9141	50.0000
11.0000	0.9973	141.2859	0.0741	51.2859	50.0000
11.5000	0.9951	136.8141	0.0990	46.8141	50.0000
12.0000	0.9906	130.9922	0.1370	40.9922	50.0000

**Table 10.** Touchstone data file containing the computed scattering coefficients of an inductive strip of length  $T=20$  mils centered in WR(90) fin-line,  $W/b=0.5$ .

! SCATTERING PARAMETERS:								
! FREQ	/S11/	<S11	/S21/	<S21	/S12/	<S12	/S22/	<S22
8.0	.8918	150.0188	.4525	60.0188	.4525	60.0188	.8918	150.0188
8.5	.8576	145.6312	.5143	55.6312	.5143	55.6312	.8576	145.6312
9.0	.8217	141.4125	.5700	51.4125	.5700	51.4125	.8217	141.4125
9.5	.7852	137.8969	.6193	47.8969	.6193	47.8969	.7852	137.8969
10.0	.7508	133.8047	.6606	43.8047	.6606	43.8047	.7508	133.8047
10.5	.7140	131.1328	.7001	41.1328	.7001	41.1328	.7140	131.1328
11.0	.6799	127.8141	.7333	37.8141	.7333	37.8141	.6799	127.8141
11.5	.6451	125.9875	.7641	35.9875	.7641	35.9875	.6451	125.9875
12.0	.6150	121.8100	.7940	31.8100	.7940	31.8100	.6150	121.8100

Table 11. Touchstone data file containing the computed scattering coefficients of an inductive strip of length  $T=50$  mils centered in WR(90) fin-line,  $W/b=0.5$ .

! SCATTERING PARAMETERS:								
! FREQ	/S11/	<S11	/S21/	<S21	/S12/	<S12	/S22/	<S22
8.0	.9591	157.0078	.2832	67.0078	.2832	67.0078	.9591	157.0078
8.5	.9476	153.5625	.3195	63.5625	.3195	63.5625	.9476	153.5625
9.0	.9347	150.9609	.3553	60.9609	.3553	60.9609	.9347	150.9609
9.5	.9202	148.1344	.3915	58.1344	.3915	58.1344	.9202	148.1344
10.0	.9035	145.1250	.4287	55.1250	.4287	55.1250	.9035	145.1250
10.5	.8855	141.8062	.4647	51.8062	.4647	51.8062	.8855	141.8062
11.0	.8648	139.1906	.5021	49.1906	.5021	49.1906	.8648	139.1906
11.5	.8423	135.6187	.5389	45.6187	.5389	45.6187	.8423	135.6187
12.0	.8174	132.5531	.5760	42.5531	.5760	42.5531	.8174	132.5531

**Table 12.** Touchstone data file containing the computed scattering coefficients of an inductive strip of length  $T=200$  mils centered in WR(90) fin-line,  $W/b=0.5$ .

! SCATTERING PARAMETERS:								
! FREQ	/S11/	<S11	/S21/	<S21	/S12/	<S12	/S22/	<S22
8.0	.9314	155.5734	.3640	65.5734	.3640	65.5734	.9314	155.5734
8.5	.9134	152.0578	.4070	62.0578	.4070	62.0578	.9134	152.0578
9.0	.8938	149.3438	.4485	59.3438	.4485	59.3438	.8938	149.3438
9.5	.8720	146.5172	.4895	56.5172	.4895	56.5172	.8720	146.5172
10.0	.8494	143.7188	.5277	53.7188	.5277	53.7188	.8494	143.7188
10.5	.8256	140.4563	.5643	50.4563	.5643	50.4563	.8256	140.4563
11.0	.7992	138.1219	.6010	48.1219	.6010	48.1219	.7992	138.1219
11.5	.7725	134.9719	.6350	44.9719	.6350	44.9719	.7725	134.9719
12.0	.7447	132.3562	.6674	42.3562	.6674	42.3562	.7447	132.3562

Table 13. Touchstone data file containing the computed scattering coefficients of an inductive strip of length  $T=500$  mils centered in WR(90) fin-line,  $W/b=0.5$ .

SCATTERING PARAMETERS:								
FREQ	/S11/	<S11	/S21/	<S21	/S12/	<S12	/S22/	<S22
8.0	.9999	150.3000	.0255	60.3000	.0255	60.3000	.9999	150.3000
8.5	.9995	148.4437	.0355	58.4437	.0355	58.4437	.9995	148.4437
9.0	.9989	146.5875	.0464	56.5875	.0464	56.5875	.9989	146.5875
9.5	.9984	142.7625	.0557	52.7625	.0557	52.7625	.9984	142.7625
10.0	.9975	137.5875	.0709	47.5875	.0709	47.5875	.9975	137.5875
10.5	.9960	133.3125	.0895	43.3125	.0895	43.3125	.9960	133.3125
11.0	.9934	127.6172	.1151	37.6172	.1151	37.6172	.9934	127.6172
11.5	.9887	121.6266	.1501	31.6266	.1501	31.6166	.9887	121.6266
12.0	.9802	113.8641	.1980	23.8641	.1980	23.8641	.9802	113.8641

Table 14. Touchstone data file containing the computed scattering coefficients of an inductive strip of length  $T=20$  mils centered in WR(90) fin-line,  $W/b=0.25$ .

SCATTERING PARAMETERS:								
FREQ	/S11/	<S11	/S21/	<S21	/S12/	<S12	/S22/	<S22
8.0	.9314	155.5734	.3640	65.5734	.3640	65.5734	.9314	155.5734
8.5	.9134	152.0578	.4070	62.0578	.4070	62.0578	.9134	152.0578
9.0	.8938	149.3438	.4485	59.3438	.4485	59.3438	.8938	149.3438
9.5	.8720	146.5172	.4895	56.5172	.4895	56.5172	.8720	146.5172
10.0	.8494	143.7188	.5277	53.7188	.5277	53.7188	.8494	143.7188
10.5	.8256	140.4563	.5643	50.4563	.5643	50.4563	.8256	140.4563
11.0	.7992	138.1219	.6010	48.1219	.6010	48.1219	.7992	138.1219
11.5	.7725	134.9719	.6350	44.9719	.6350	44.9719	.7725	134.9719
12.0	.7447	132.3562	.6674	42.3562	.6674	42.3562	.7447	132.3562

**Table 15.** Touchstone data file containing the computed scattering coefficients of an inductive strip of length  $T=50$  mils centered in WR(90) fin-line,  $W/b=0.25$ .

SCATTERING PARAMETERS:								
FREQ	/S11/	<S11	/S21/	<S21	/S12/	<S12	/S22/	<S22
8.0	.9591	157.0078	.2832	67.0078	.2832	67.0078	.9591	157.0078
9.5	.9476	153.5625	.3195	63.5625	.3195	63.5625	.9476	153.5625
9.0	.9347	150.9609	.3553	60.9609	.3553	60.9609	.9347	150.9609
9.5	.9202	148.1344	.3915	58.1344	.3915	58.1344	.9202	148.1344
10.0	.9035	145.1250	.4287	55.1250	.4287	55.1250	.9035	145.1250
10.5	.8855	141.8062	.4647	51.8062	.4647	51.8062	.8855	141.8062
11.0	.8648	139.1906	.5021	49.1906	.5021	49.1906	.8648	139.1906
11.5	.8423	135.6187	.5389	45.6187	.5389	45.6187	.8423	135.6187
12.0	.8174	132.5531	.5760	42.5531	.5760	42.5531	.8174	132.5531

Table 16. Touchstone data file containing the computed scattering coefficients of an inductive strip of length  $T=100$  mils centered in WR(90) fin-line,  $W/b=0.25$ .

SCATTERING PARAMETERS:								
FREQ	/S11/	<S11	/S21/	<S21	/S12/	<S12	/S22/	<S22
8.0	.9755	156.6281	.2198	66.6281	.2198	66.6281	.9755	156.6281
8.3	.9739	154.5189	.2270	64.5189	.2270	64.5189	.9739	154.5189
9.0	.9667	151.8750	.2561	61.8750	.2561	61.8750	.9667	151.8750
9.5	.9577	148.9781	.2877	58.9781	.2877	58.9781	.9577	148.9781
10.0	.9472	145.8984	.3207	55.8984	.3207	55.8984	.9472	145.8984
10.5	.9351	142.3266	.3544	52.3266	.3544	52.3266	.9351	142.3266
11.0	.9201	139.4297	.3917	49.4297	.3917	49.4297	.9201	139.4297
11.5	.9023	135.4359	.4311	45.4359	.4311	45.4359	.9023	135.4359
12.0	.8808	131.6953	.4736	41.6953	.4736	41.6953	.8808	131.6953

Table 17. Touchstone data file containing the computed scattering coefficients of an inductive strip of length  $T=200$  mils centered in WR(90) fin-line,  $W/b = 0.25$ .

SCATTERING PARAMETERS:								
FREQ	/S11/	<S11	/S21/	<S21	/S12/	/S12	/S22/	<S22
8.0	.9900	157.9996	.1350	67.9996	.1350	67.9996	.9900	157.9996
8.5	.9895	154.8844	.1400	64.8844	.1400	64.8844	.9895	154.8844
9.0	.9893	152.3250	.1460	62.3250	.1460	62.3250	.9893	152.3250
9.5	.9858	149.3719	.1678	59.3719	.1678	59.3719	.9858	149.3719
10.0	.9812	146.2078	.1932	56.2078	.1932	56.2078	.9812	146.2078
10.5	.9749	142.2984	.2225	52.2984	.2225	52.2984	.9749	142.2984
11.0	.9664	138.9937	.2570	48.9937	.2570	48.9937	.9664	138.9937
11.5	.9551	134.4516	.2964	44.4516	.2964	44.4516	.9551	134.4516
12.0	.9394	129.9516	.3429	39.9516	.3429	39.9516	.9394	129.9516

Table 18. Touchstone data file containing the computed scattering coefficients of an inductive strip of length  $T=500$  mils centered in WR(90) fin-line,  $W/b=0.25$ .

! SCATTERING PARAMETERS:								
! FREQ	/S11/	<S11	/S21/	<S21	/S12/	<S12	/S22/	<S22
8.0	.9999	153.3987	.0141	63.3987	.0141	63.3987	.9999	153.3987
8.5	.9998	152.5325	.0190	62.5325	.0190	62.5325	.9998	152.5325
9.0	.9996	150.8792	.0283	60.8792	.0283	60.8792	.9996	150.8792
9.5	.9994	148.5981	.0346	58.5981	.0346	58.5981	.9994	148.5981
10.0	.9988	146.1797	.0491	56.1797	.0491	56.1797	.9988	146.1797
10.5	.9980	142.1859	.0628	52.1859	.0628	52.1859	.9980	142.1859
11.0	.9965	138.5297	.0824	48.5297	.0824	48.5297	.9966	138.5297
11.5	.9941	133.2984	.1088	43.2984	.1088	43.2984	.1088	133.2984
12.0	.9889	127.7156	.1484	37.7156	.1484	37.7156	.9889	127.7156

Table 19. Touchstone data file containing the computed scattering coefficients of an inductive strip of length  $T=20$  mils centered in WR(90) fin-line,  $W/b=0.2$ .

SCATTERING PARAMETERS:								
FREQ	/S11/	<S11	/S21/	<S21	/S12/	<S12	/S22/	<S22
8.0	.9416	157.4156	.3367	67.4156	.3367	67.4156	.9416	157.4156
8.5	.9266	154.4906	.3761	64.4906	.3761	64.4906	.9266	154.4906
9.0	.9103	151.7906	.4140	61.7906	.4140	61.7906	.9103	151.7906
9.5	.8922	148.5562	.4516	58.5562	.4516	58.5562	.8922	148.5562
10.0	.8725	145.8984	.4886	55.8984	.4886	55.8984	.8725	145.8984
10.5	.8511	143.3953	.5250	53.3953	.5250	53.3953	.8511	143.3953
11.0	.8282	140.8922	.5605	50.8922	.5605	50.8922	.8282	140.8922
11.5	.8036	138.1219	.5951	48.1219	.5951	48.1219	.8036	138.1219
12.0	.7780	135.0422	.6283	45.0422	.6283	45.0422	.7780	135.0422

Table 20. Touchstone data file containing the computed scattering coefficients of an inductive strip of length  $T=50$  mils centered in WR(90) fin-line,  $W/b=0.2$ .

SCATTERING PARAMETERS:								
FREQ	/S11/	<S11	/S21/	<S21	/S12/	<S12	/S22/	<S22
8.0	.9653	158.6531	.2613	68.6531	.2613	68.6513	.9653	158.6531
8.5	.9559	155.7984	.2936	65.7984	.2936	65.7984	.9559	155.7984
9.0	.9456	153.2109	.3253	63.2109	.3253	63.2109	.9456	153.2109
9.5	.9336	150.0188	.3583	60.0188	.3583	60.0188	.9336	150.0188
10.0	.9197	147.2203	.3926	57.2203	.3926	57.2203	.9197	147.2203
10.5	.9041	144.6187	.4273	54.6187	.4273	54.6187	.9041	144.6187
11.0	.8861	141.8766	.4636	51.8766	.4636	51.8766	.8861	141.8766
11.5	.8658	138.7969	.5004	48.7969	.5004	48.7969	.8658	138.7969
12.0	.8437	135.3375	.5369	45.3375	.5369	45.3375	.8437	135.3375

**Table 21.** Touchstone data file containing the computed scattering coefficients of an inductive strip of length  $T=100$  mils centered in WR(90) fin-line,  $W/b=0.2$ .

SCATTERING PARAMETERS:								
FREQ	/S11/	<S11	/S21/	<S21	/S12/	<S12	/S22/	<S22
8.0	.9793	159.2248	.2000	69.2248	.2000	69.2248	.9793	159.2248
8.5	.9770	156.2484	.2134	66.2484	.2134	66.2484	.9770	156.2484
9.0	.9725	154.0125	.2327	64.0125	.2327	64.0125	.9725	154.0125
9.5	.9656	150.7078	.2601	60.7078	.2601	60.7078	.9656	150.7078
10.0	.9565	147.8109	.2917	57.8109	.2917	57.8109	.9565	147.8109
10.5	.9463	145.0687	.3232	55.0687	.3232	55.0687	.9463	145.0687
11.0	.9333	142.0453	.3590	52.0453	.3590	52.0453	.9333	142.0453
11.5	.9179	138.6141	.3967	48.6141	.3967	48.6141	.9179	138.6141
12.0	.8991	134.5922	.4377	44.5922	.4377	44.5922	.8991	134.5922

Table 22. Touchstone data file containing the computed scattering coefficients of an inductive strip of length  $T=200$  mils centered in WR(90) fin-line,  $W/b=0.2$ .

SCATTERING PARAMETERS:								
FREQ	/S11/	<S11	/S21/	<S21	/S12/	<S12	/S22/	<S22
8.0	.9935	159.1025	.1138	69.1025	.1138	69.1025	.9935	159.1025
8.5	.9925	156.9352	.1222	66.9352	.1222	66.9352	.9925	156.9352
9.0	.9915	154.6210	.1301	64.6210	.1301	64.6210	.9915	154.6210
9.5	.9885	151.0875	.1513	61.0875	.1513	61.0875	.9885	151.0875
10.0	.9847	148.0641	.1743	58.0641	.1743	58.0641	.9847	148.0641
10.5	.9794	145.0266	.2018	55.0266	.2018	55.0266	.9794	145.0266
11.0	.9723	141.7078	.2339	51.7078	.2339	51.7078	.9723	141.7078
11.5	.9623	137.7703	.2719	47.7703	.2719	47.7703	.9623	137.7703
12.0	.9486	132.9891	.3165	42.9891	.3165	42.9891	.9486	132.9891

Table 23. Touchstone data file containing the computed scattering coefficients of an inductive strip of length  $T=500$  mils centered in WR(90) fin-line,  $W/b=0.2$ .

SCATTERING PARAMETERS:								
FREQ	/S11/	<S11	/S21/	<S21	/S12/	<S12	/S22/	<S22
8.0	.9998	152.6000	.0200	62.6000	.0200	62.6000	.9998	152.6000
8.5	.9997	151.4000	.0245	61.4000	.0245	61.4000	.9997	151.4000
9.0	.9996	150.4500	.0282	60.4500	.0282	60.4500	.9996	150.4500
9.5	.9994	148.9000	.0346	58.9000	.0346	58.9000	.9994	148.9000
10.0	.9991	147.8000	.0424	57.8000	.0424	57.8000	.9991	147.8000
10.5	.9984	144.9141	.0564	54.9141	.0564	54.9141	.9984	144.9141
11.0	.9973	141.2859	.0741	51.2859	.0741	51.2859	.9973	141.2859
11.5	.9951	136.8141	.0990	46.8141	.0990	46.8141	.9951	136.8141
12.0	.9906	130.9922	.1370	40.9922	.1370	40.9922	.9906	130.9922

## APPENDIX B. SUPPORTIVE FIGURES

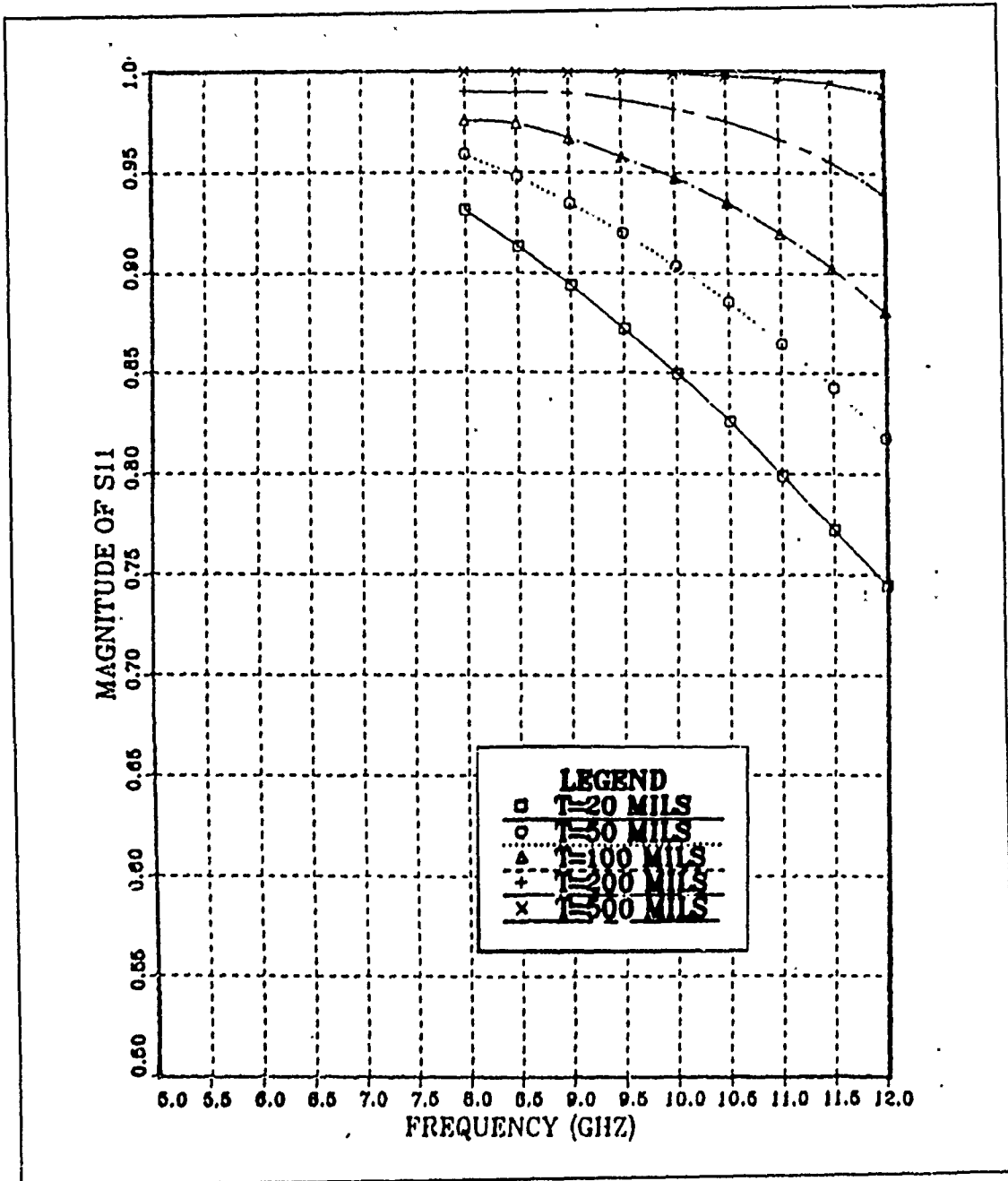


Figure 18.  $|S_{11}|$  vs. frequency for inductive strips centered in WR(90) fin-line.  
 $W/b = 0.25, E_2 = 1.$

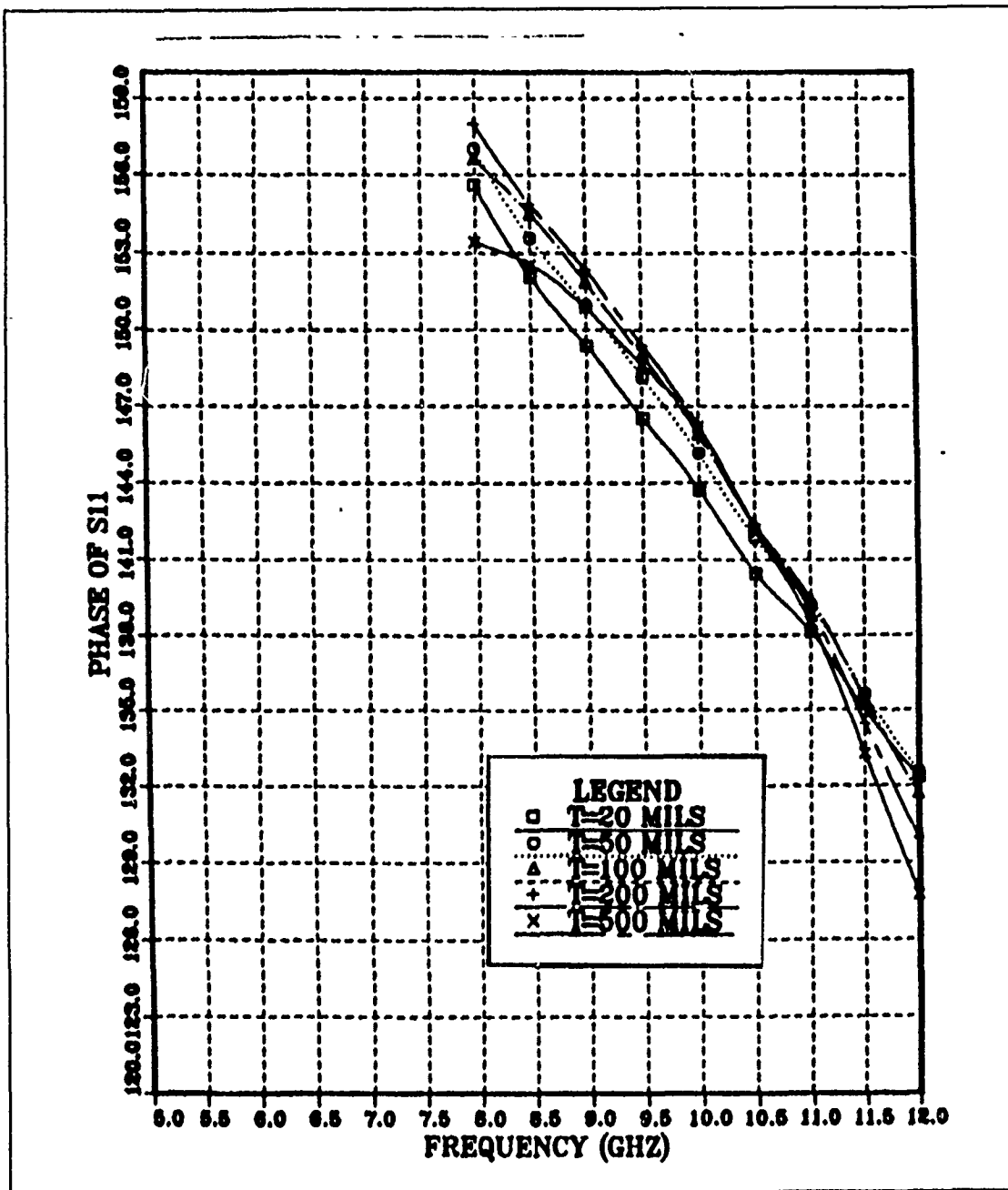


Figure 19.  $\theta_{11}$  vs. frequency for inductive strips centered in WR(90) fin-line.  
 $W/b = 0.25$ ,  $E_r = 1$ .

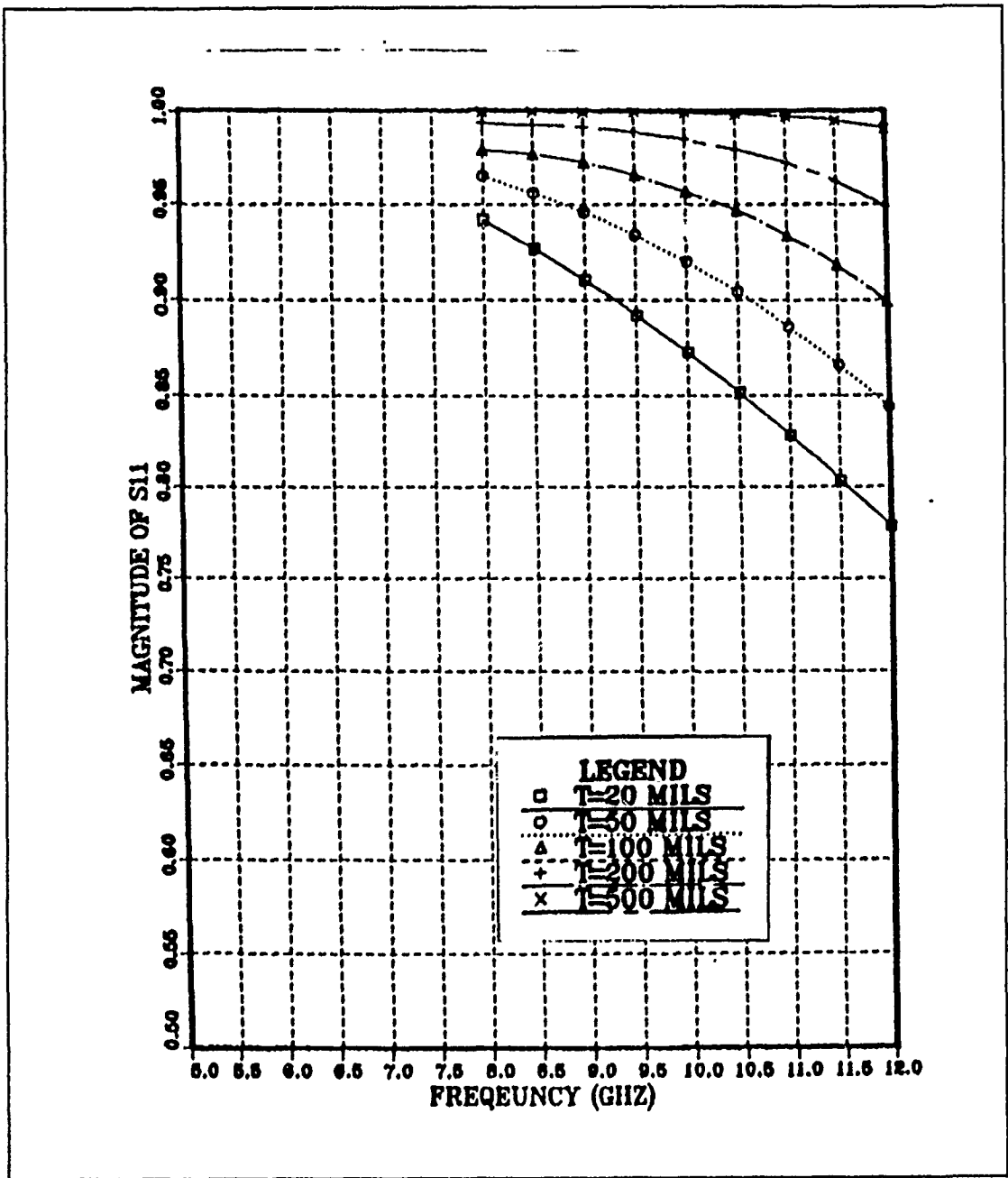


Figure 20.  $|S_{11}|$  vs. frequency for inductive strips centered in  $W_1(90)$  fin-line.  
 $W/b=0.2, E_r=1$ .

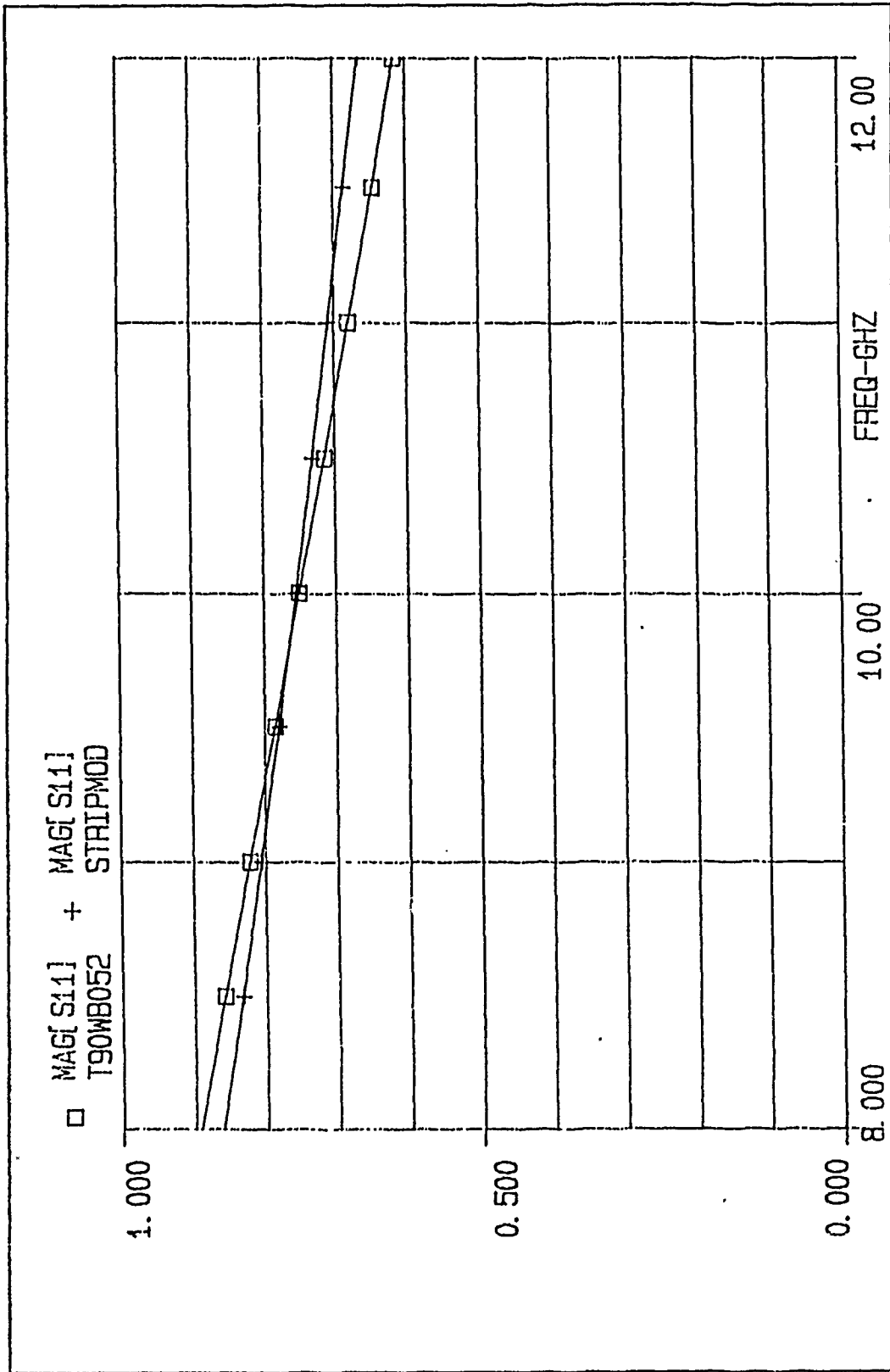


Figure 22. Computed and predicted values of  $|S_{11}|$  vs. frequency for a  $T = 20$  mils inductive strip centered in WR(90) finline,  $W/b = 0.5$ ,  $E_2 = 1$ . Model inductance  $L = 10.7$  nH.

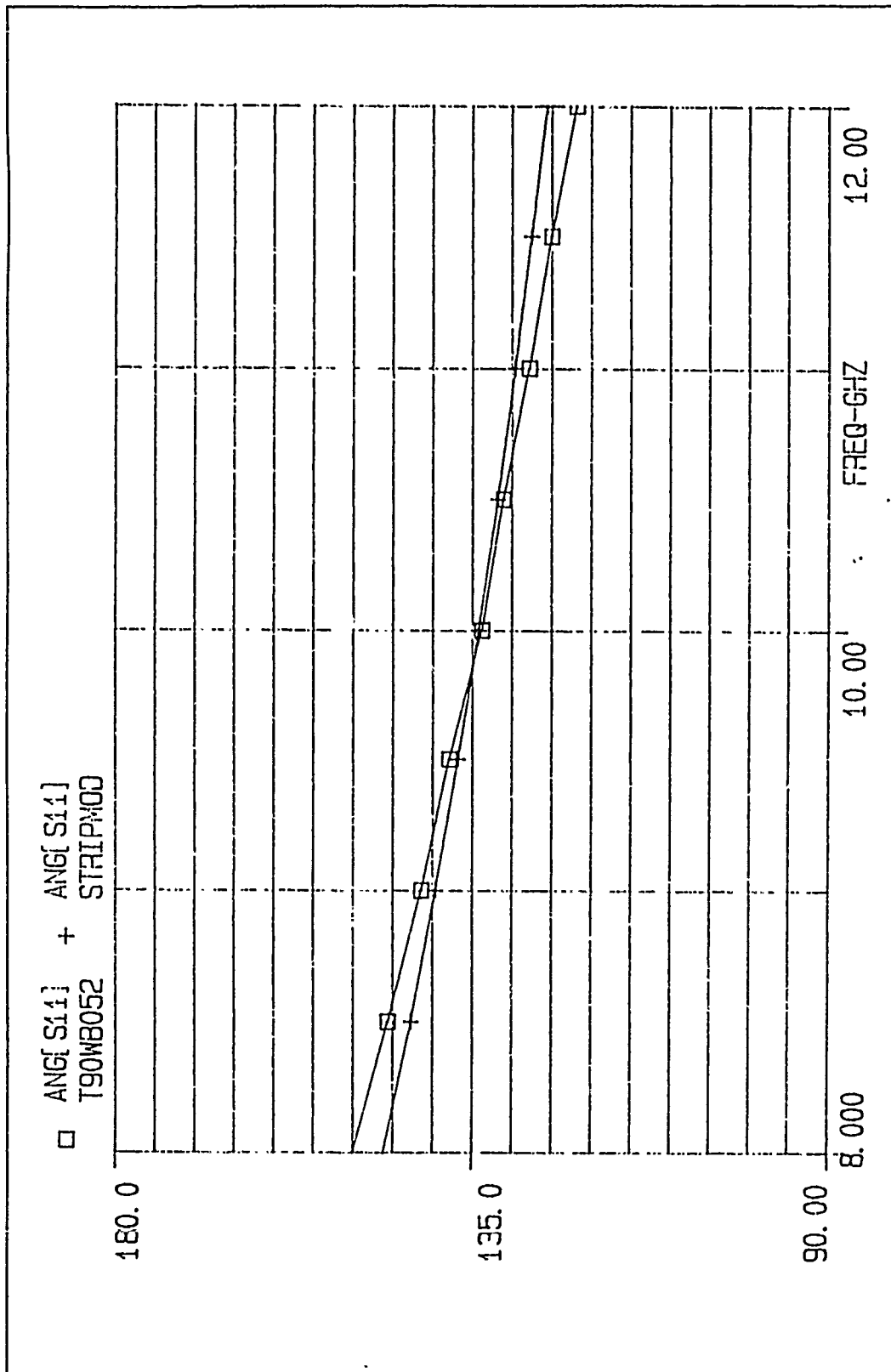


Figure 23. Computed and predicted values of  $\theta_{11}$  vs. frequency for a  $T = 20$  mils inductive strip centered in YR(90) fin-line,  $W/b = 0.5$ ,  $E_2 = 1$ . Model inductance  $L = 10.7$  nH.

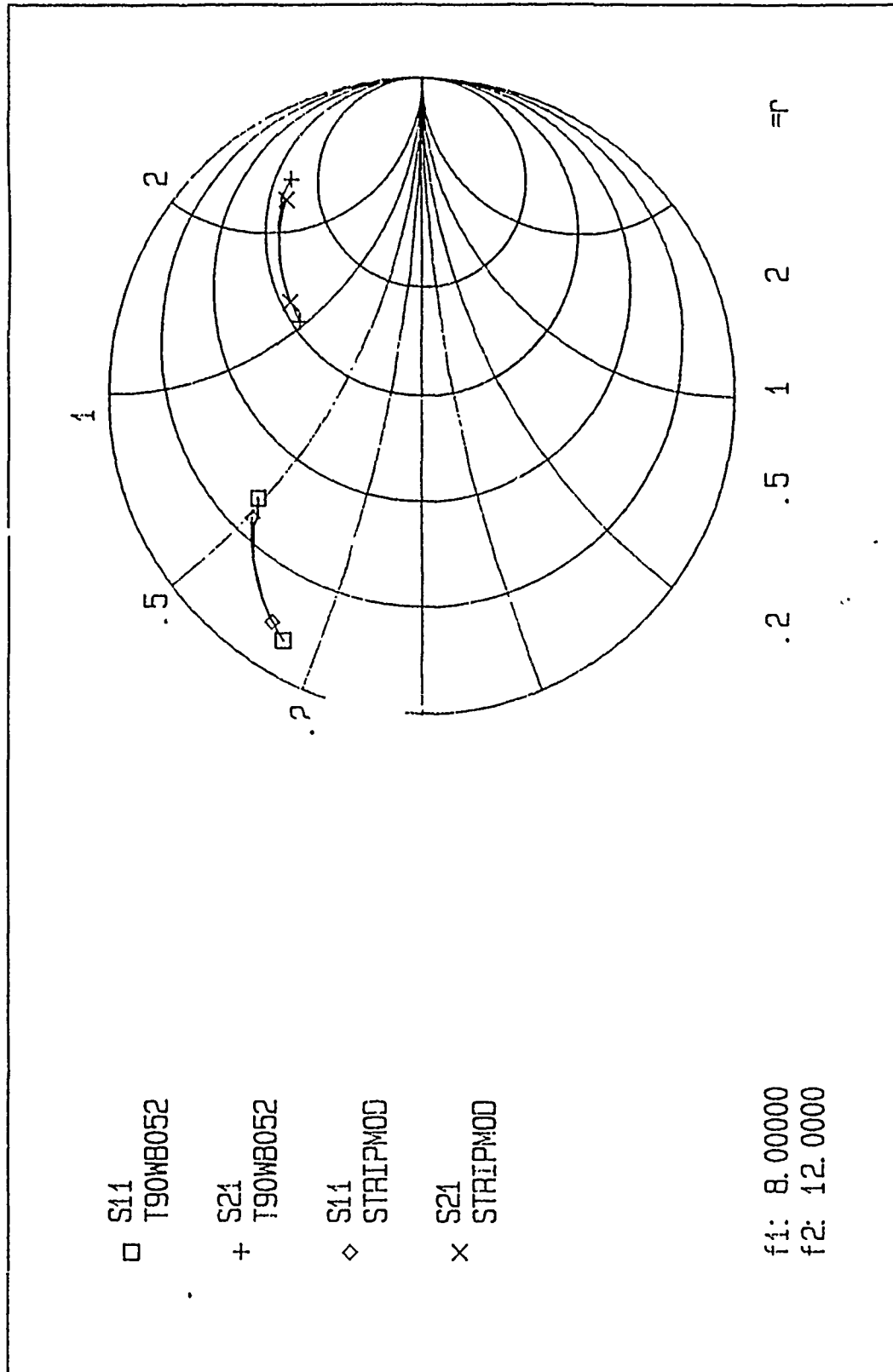


Figure 24. Smith chart plot of computed and predicted values of  $S_{11}$  and  $S_{21}$  for a  $T = 20$  mils inductive strip centered in WR(90) fin-line,  $W/b = 0.5$ ,  $E_2 = 1$ . Model inductance  $L = 10.7$  nH.

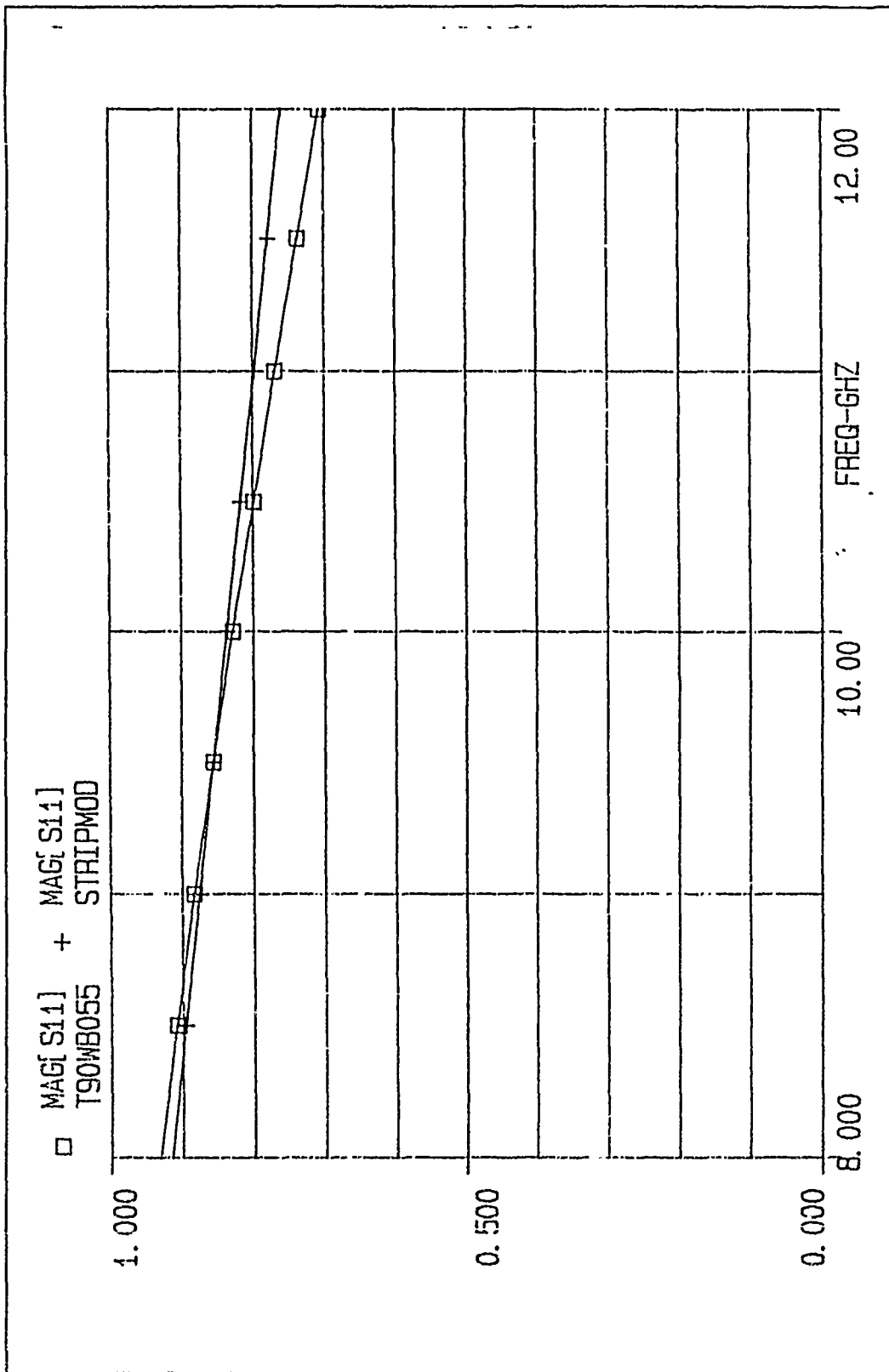


Figure 25. Computed and predicted values of  $|S_{11}|$  vs. frequency for a  $T = 50$  mils inductive strip centered in WR(90) in-line,  $W/b = 0.5$ ,  $E_r = 1$ . Model inductance  $L = 9.35$  nH.

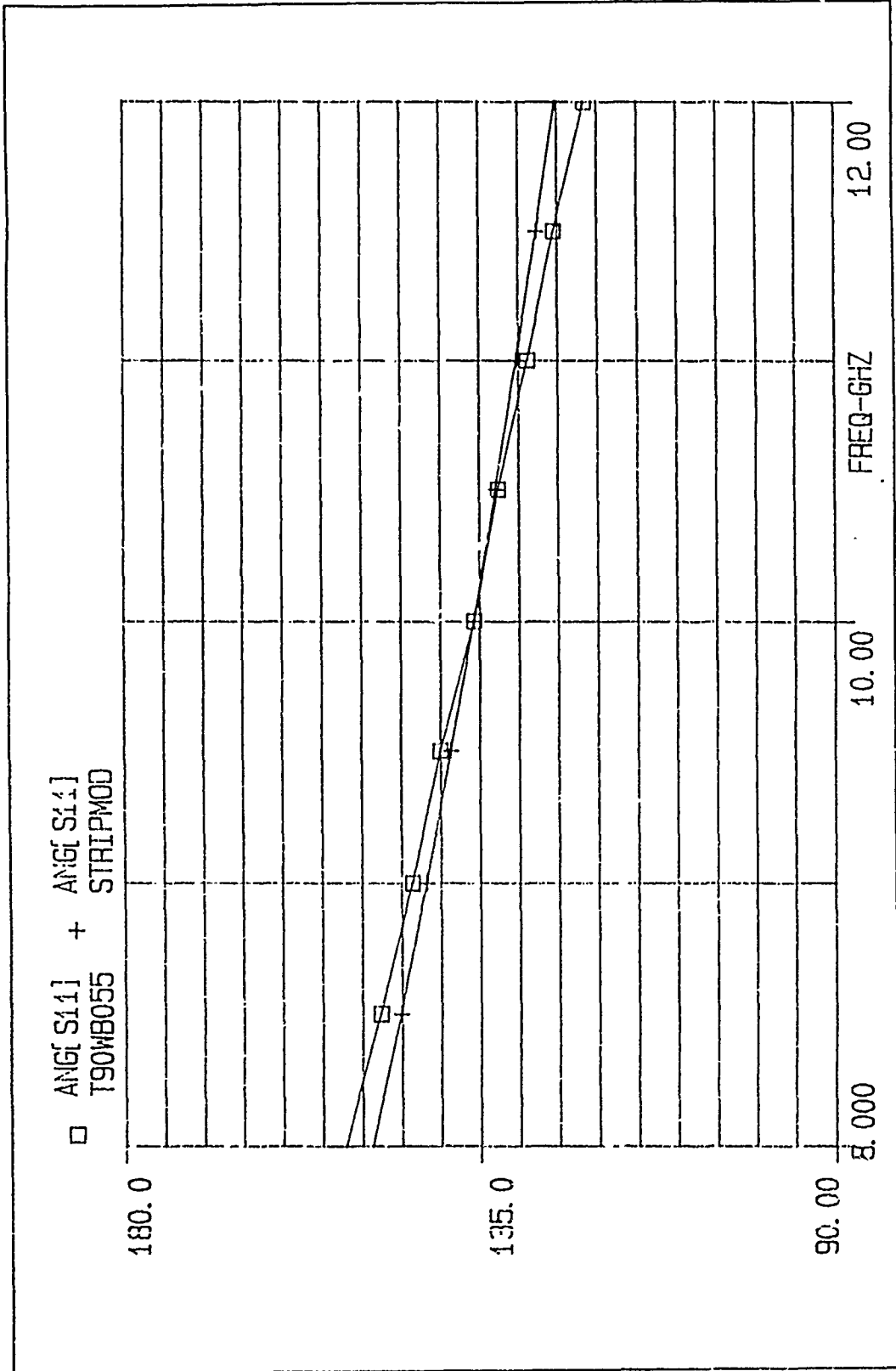


Figure 26. Computed and predicted values of  $\theta_{11}$  vs. frequency for a  $T = 50$  rails inductive strip centered in WR(90) fin-line,  $W/b = 0.5$ ,  $E_2 = 1$ . Model inductance  $L = 9.35$  nH.

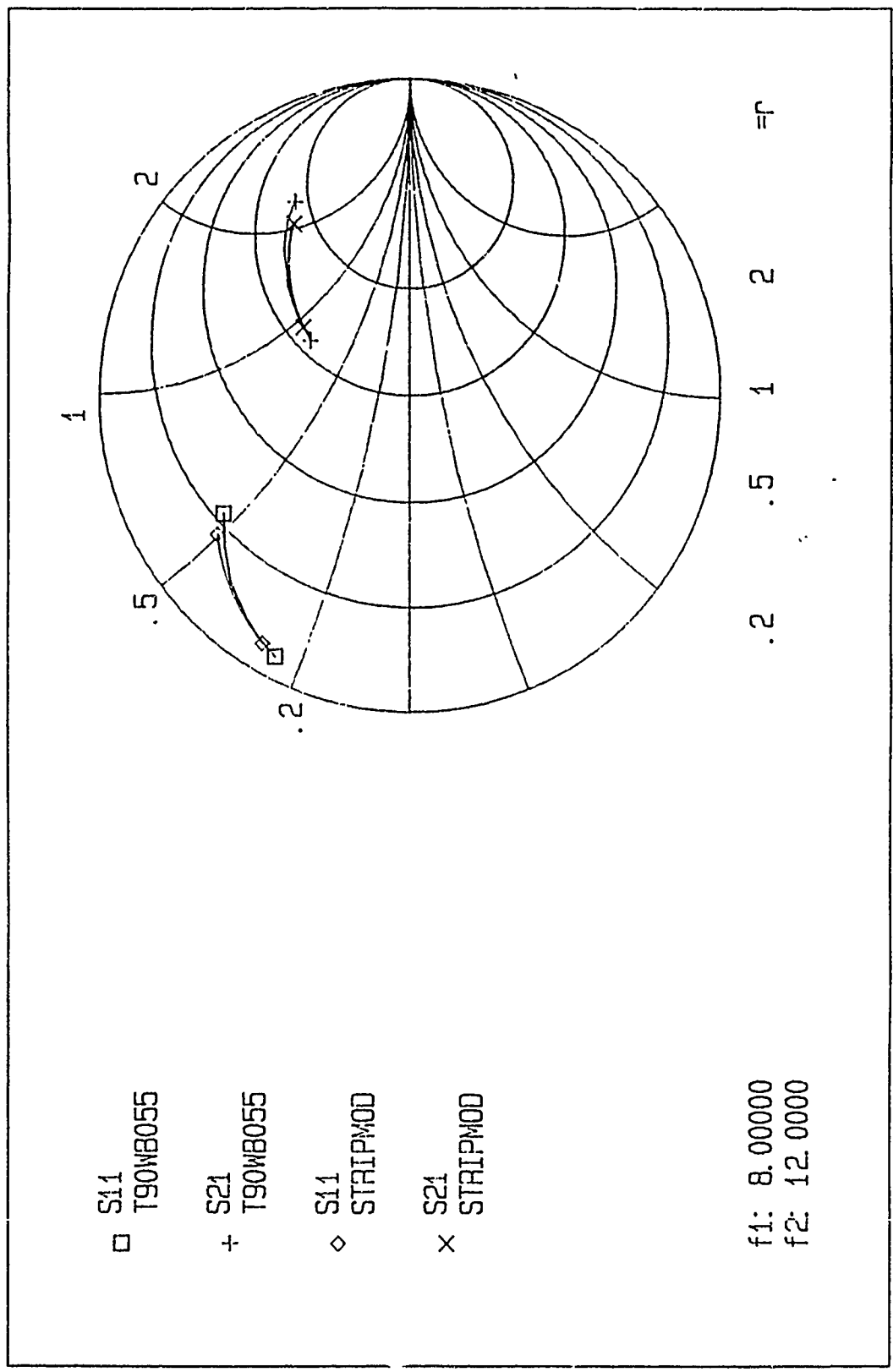


Figure 27. Smith chart plot of computed and predicted values of  $S_{11}$  and  $S_{21}$  for a  $T = 50$  mils inductive strip centered in  $WR(90)$  fin-line,  $W/b = 0.5$ ,  $E_z = 1$ . Model inductance  $L = 9.35$  nH.

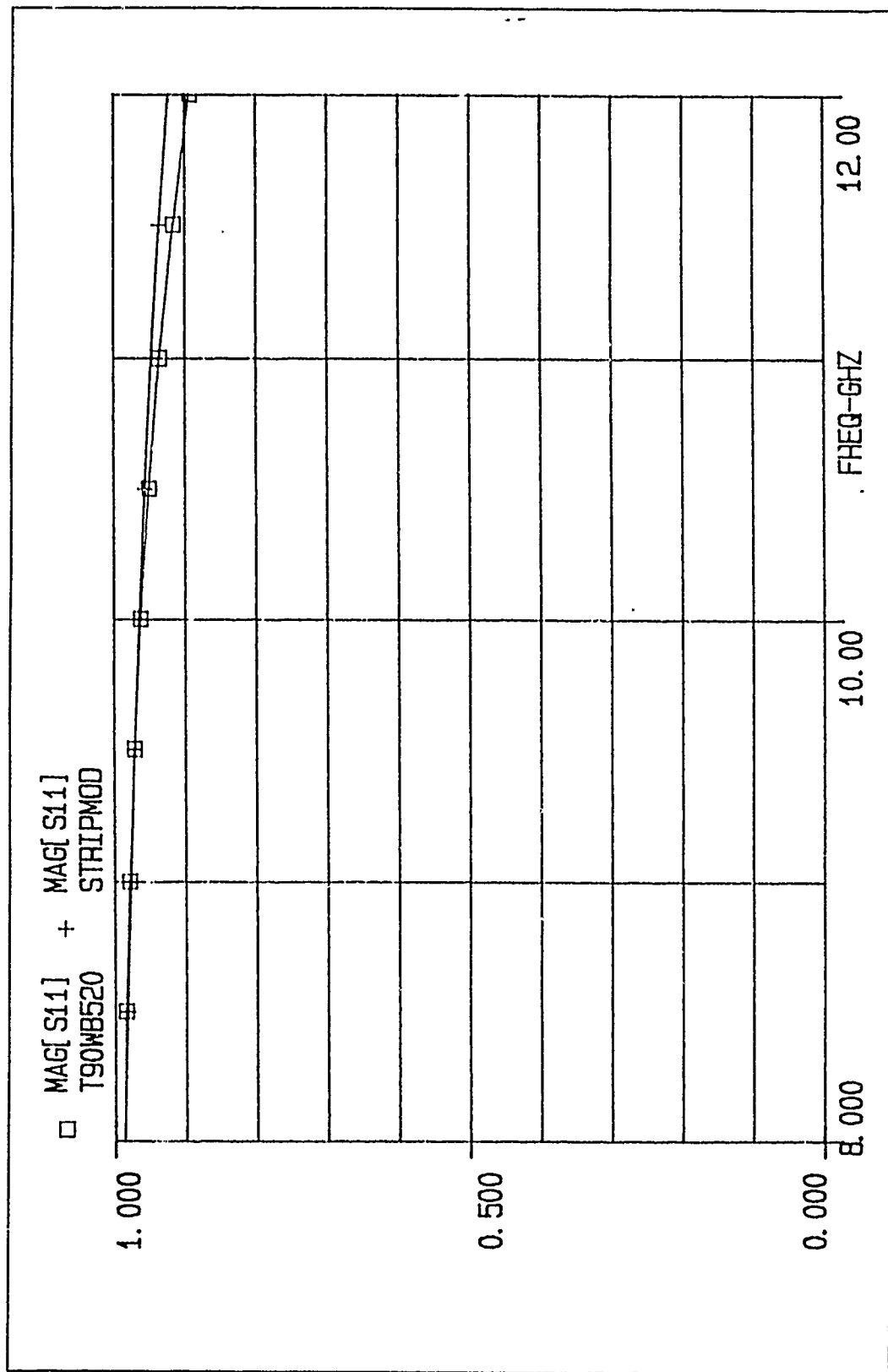


Figure 28. Computed and predicted values of  $|S_{11}|$  vs. frequency for a  $T = 200$  mils inductive strip centered in WR(90) fin-line,  $W/b = 0.5$ ,  $E_2 = 1$ . Model inductance  $L = 7.10$  nH.

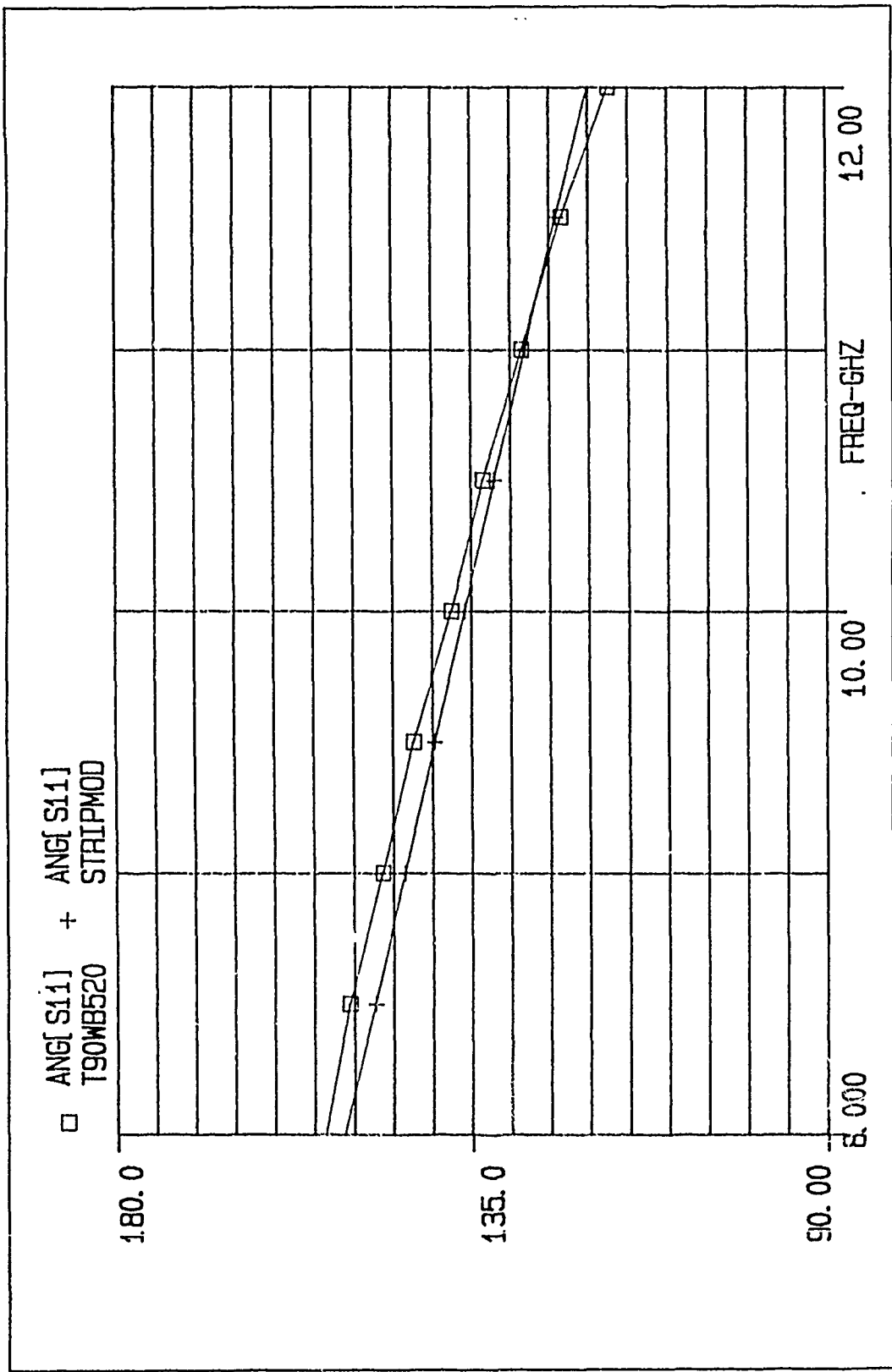


Figure 29. Computed and predicted values of  $\theta_{11}$  vs. frequency for a  $T = 200$  mils inductive strip centered in WR(90) finline,  $W/b = 0.5$ ,  $E_2 = 1$ . Model inductance  $L = 7.10$  nH.

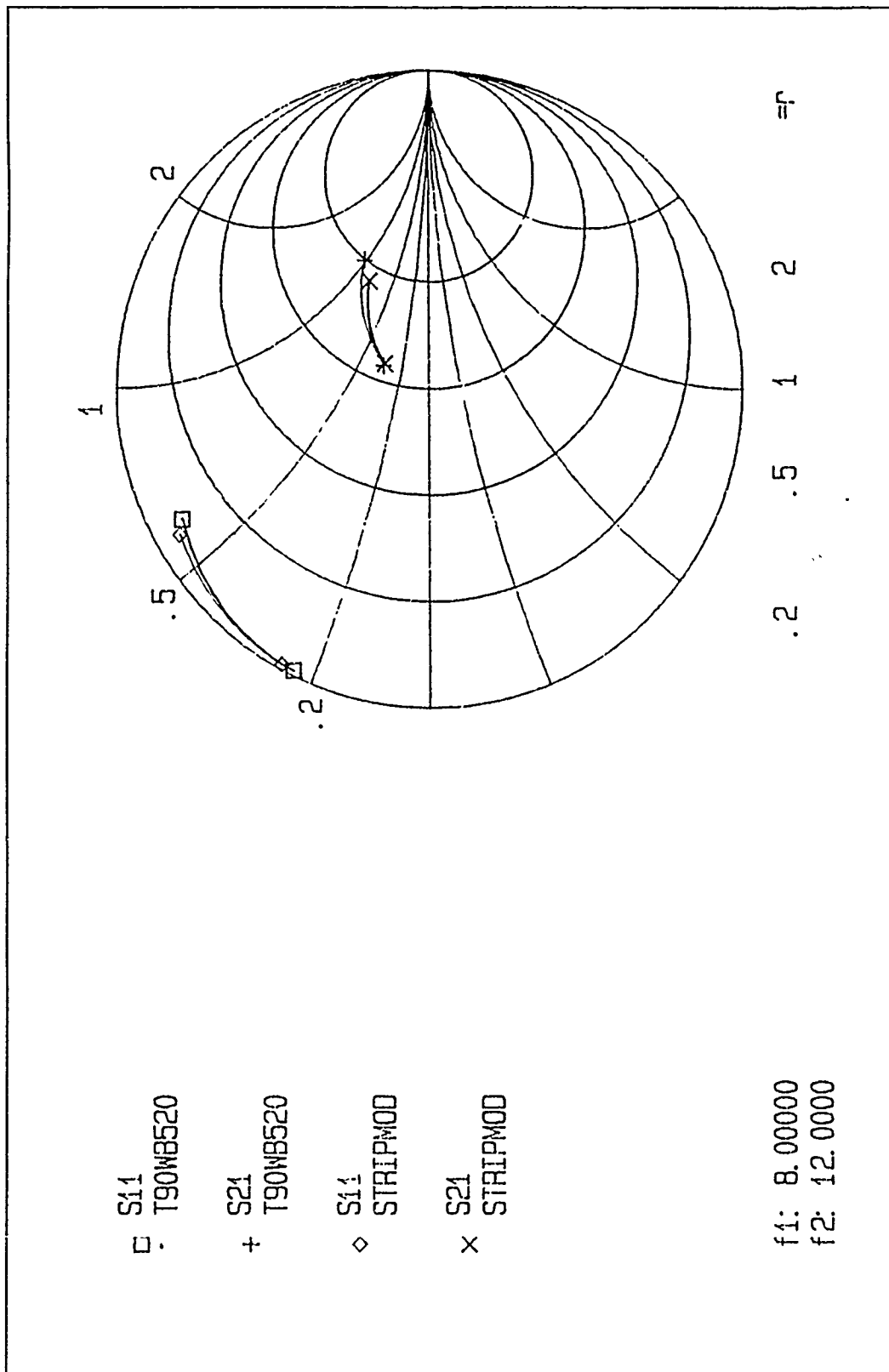


Figure 30. Smith chart plot of computed and predicted values of  $S_{11}$  and  $S_{21}$  for a  $T = 200$  mils inductive strip centered in WR(90) fin-line,  $W/b = 0.5$ ,  $E_z = 1$ . Model inductance  $L = 8.20$  nH.

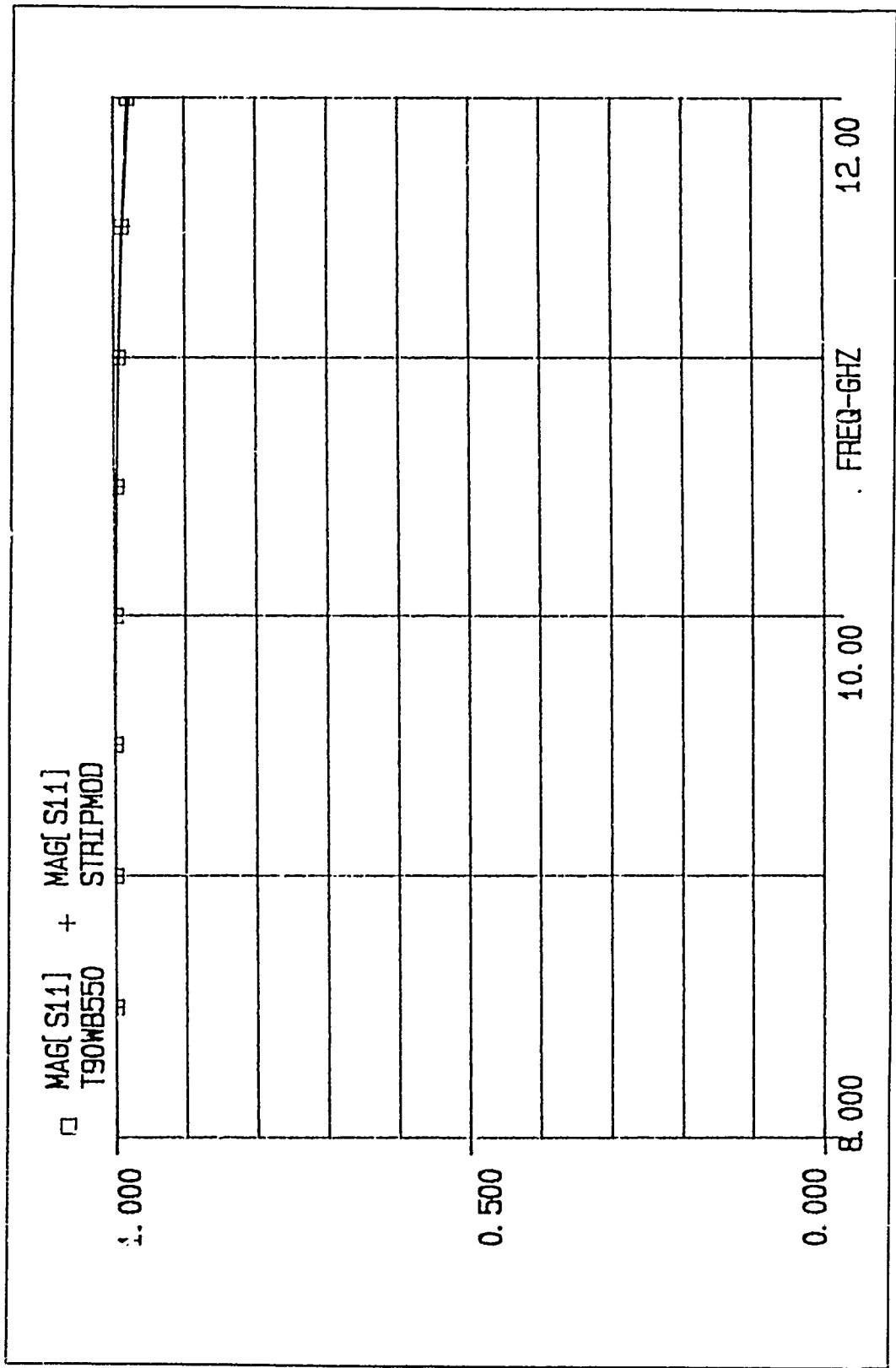


Figure 31. Computed and predicted values of  $|S_{11}|$  vs. frequency for a T = 500 mils inductive strip centered in WR(90) fin-line,  $W/b = 0.5$ ,  $E_r = 1$ . Model inductance  $L = 5.90$  nH.

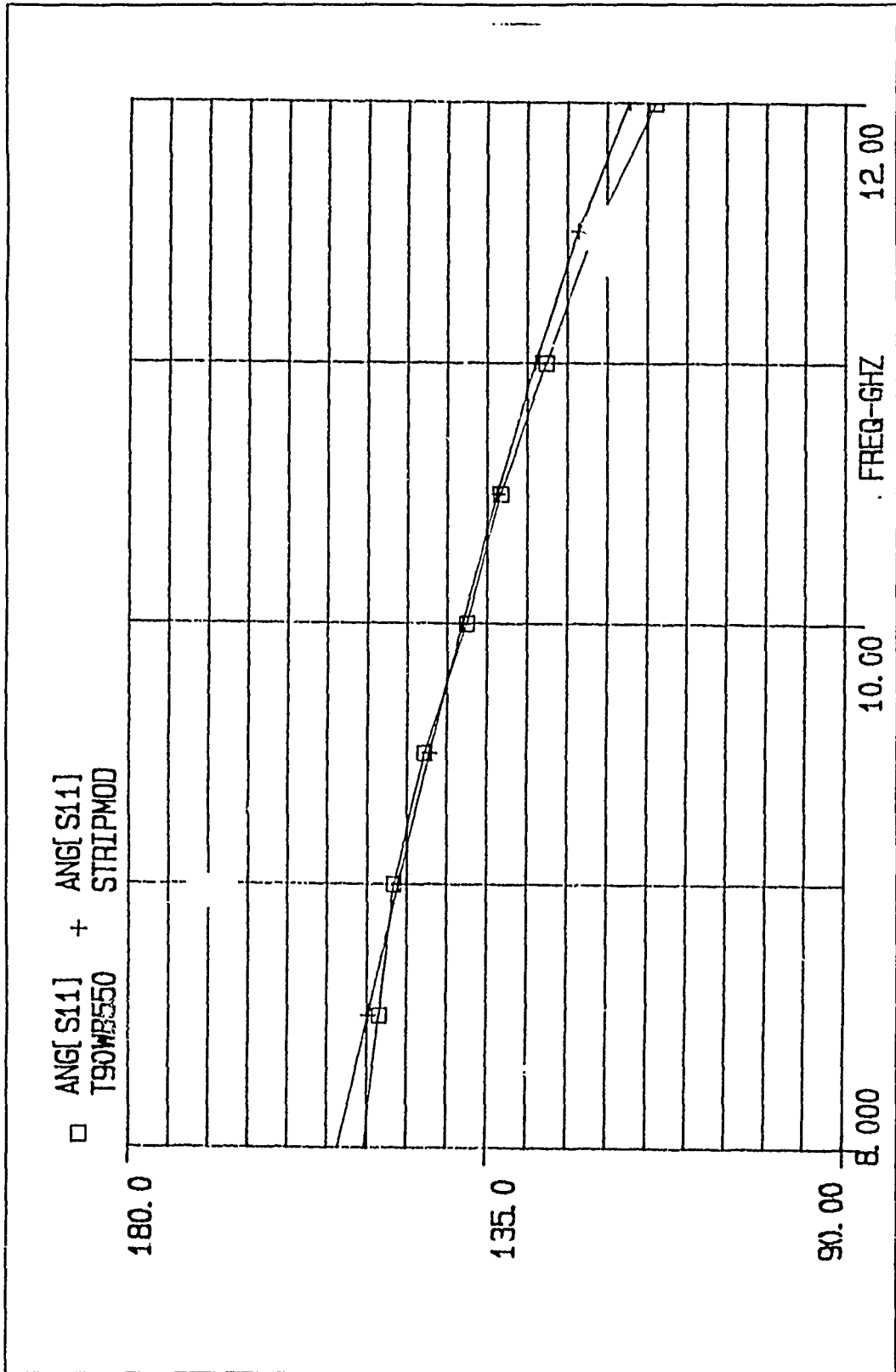


Figure 32. Computed and predicted values of  $\angle S_{11}$  vs. frequency for a  $T = 500$  mils inductive strip centered in WR(90) fin-line,  $W/b = 0.5$ ,  $E_2 = 1$ . Model inductance  $L = 5.90$  nH.

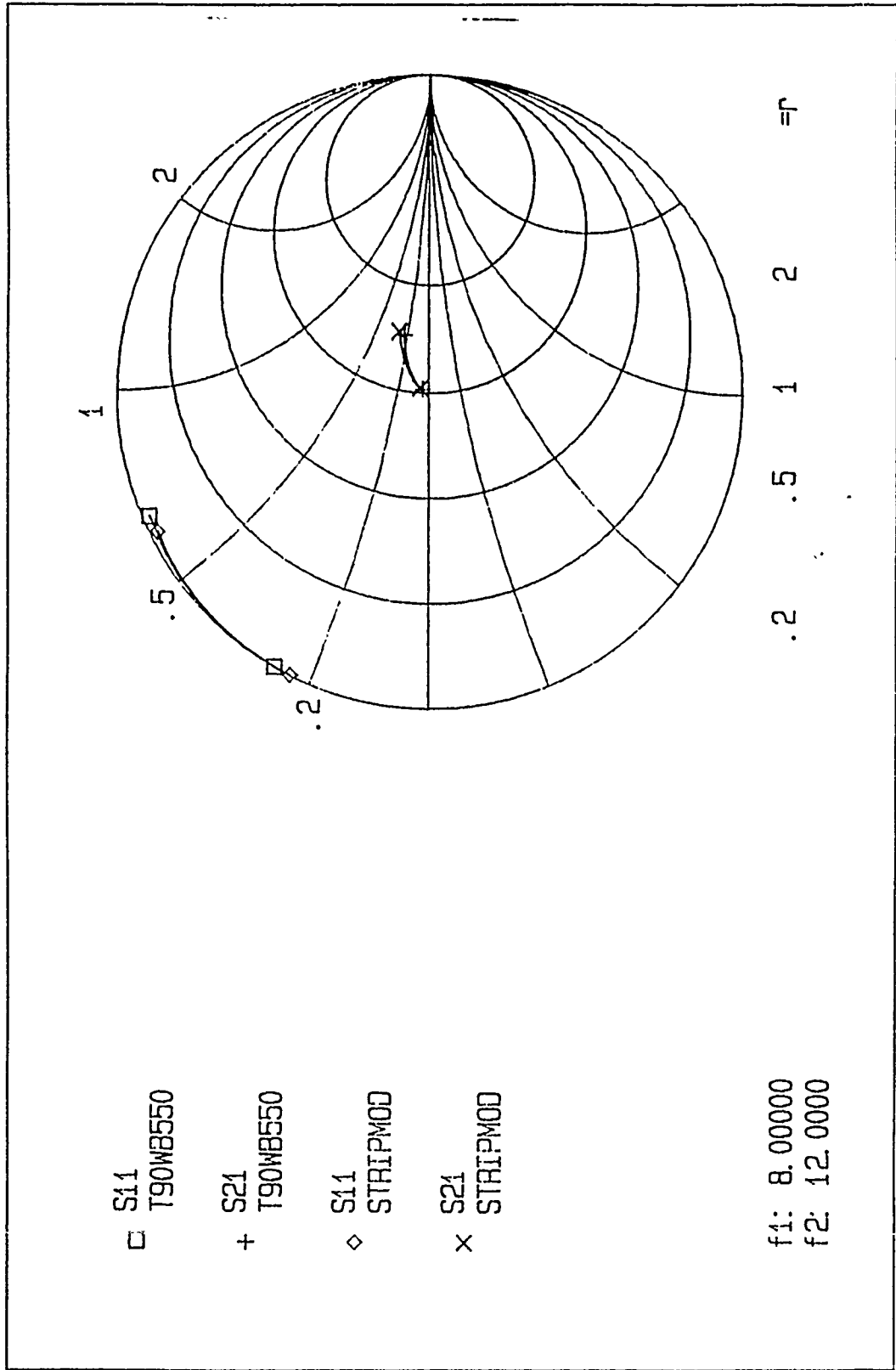


Figure 33. Smith chart plot of computed and predicted values of  $S_{11}$  and  $S_{21}$  for a  $T=500$  mils inductive strip centered in WR(90) fin-line,  $W/b=0.5$ ,  $E_r=1$ . Model inductance  $L=5.90$  nH.

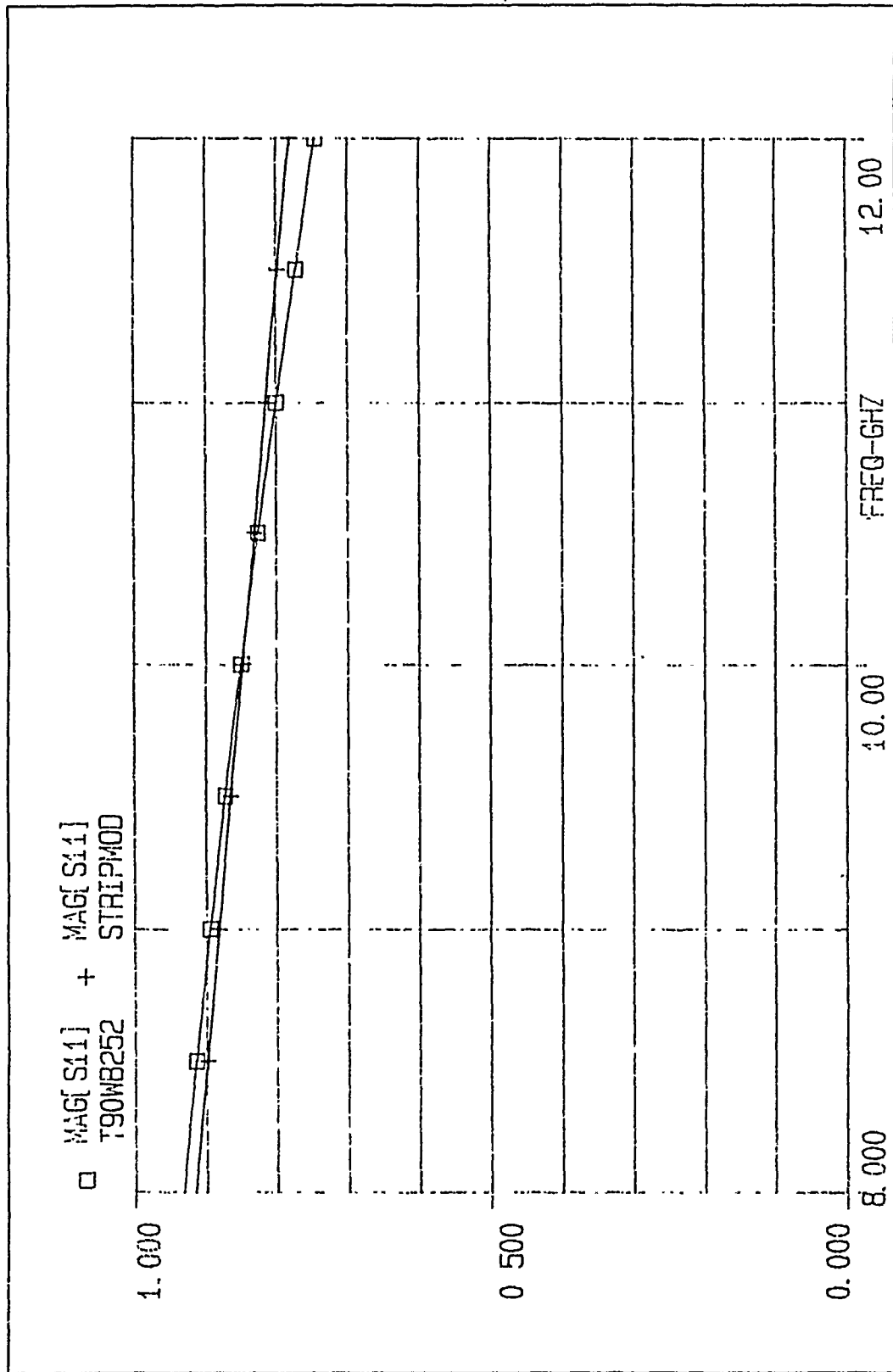


Figure 34. Computed and predicted values of  $|S_{11}|$  vs. frequency for a  $T = 20$  mils inductive strip centered in WR(90) line,  $W/b = 0.25$ ,  $E_r = 1$ . Model inductance  $L = 6.60$  nH.

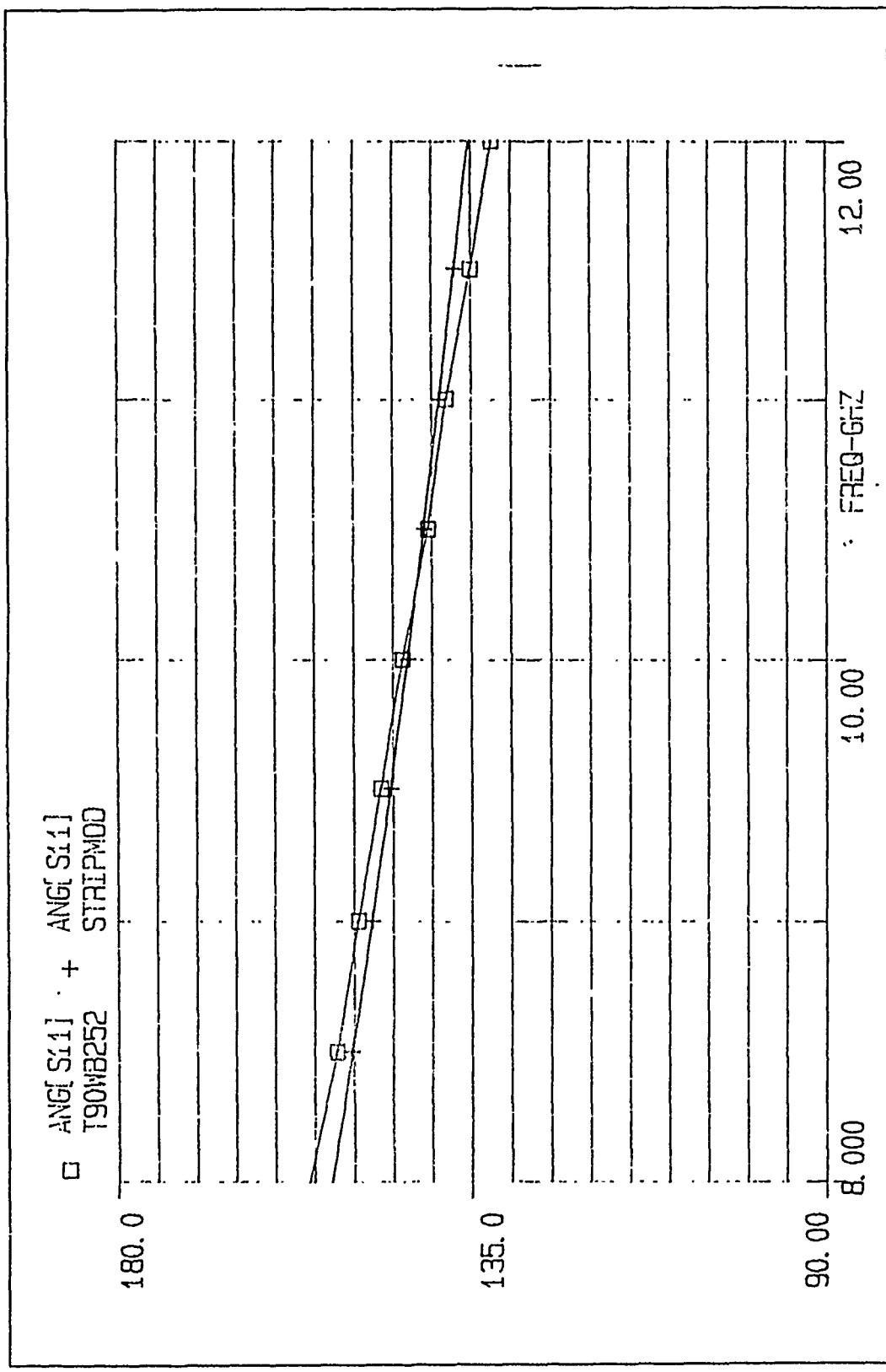


Figure 35. Computed and predicted values of  $\theta_{11}$  vs. frequency for a  $T = 20$  mils inductive strip centered in WR(90) fin-line,  $W/b = 0.25$ ,  $E_2 = 1$ . Model inductance  $L = 6.60$  nH.

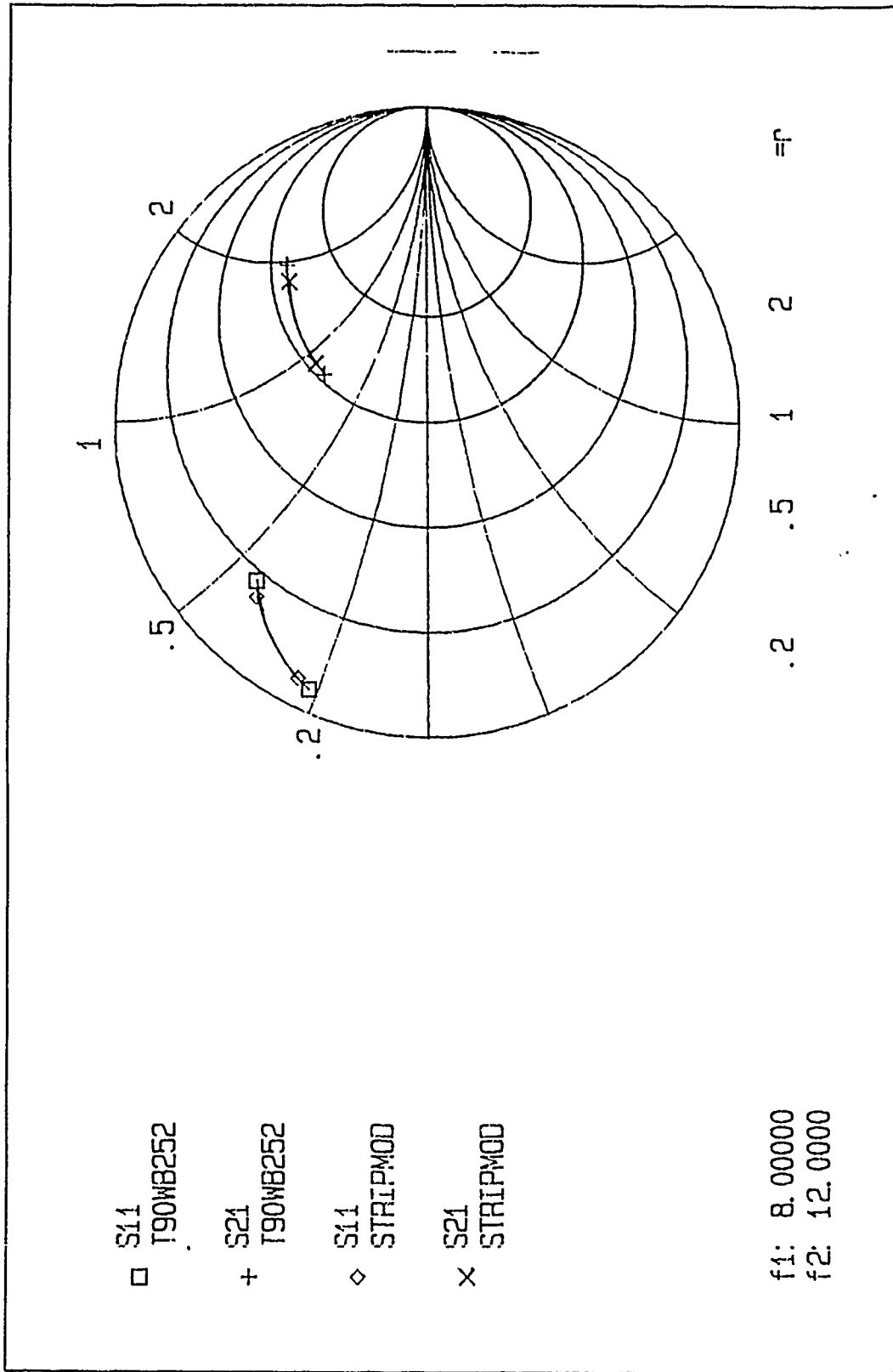


Figure 36. Smith chart plot of computed and predicted values of  $S_{11}$  and  $S_{21}$  for a  $T = 20$  mils inductive strip centered in WR(90) fin-line,  $W/b = 0.25$ ,  $E_2 = 1$ . Model inductance  $L = 6.60$  nH.

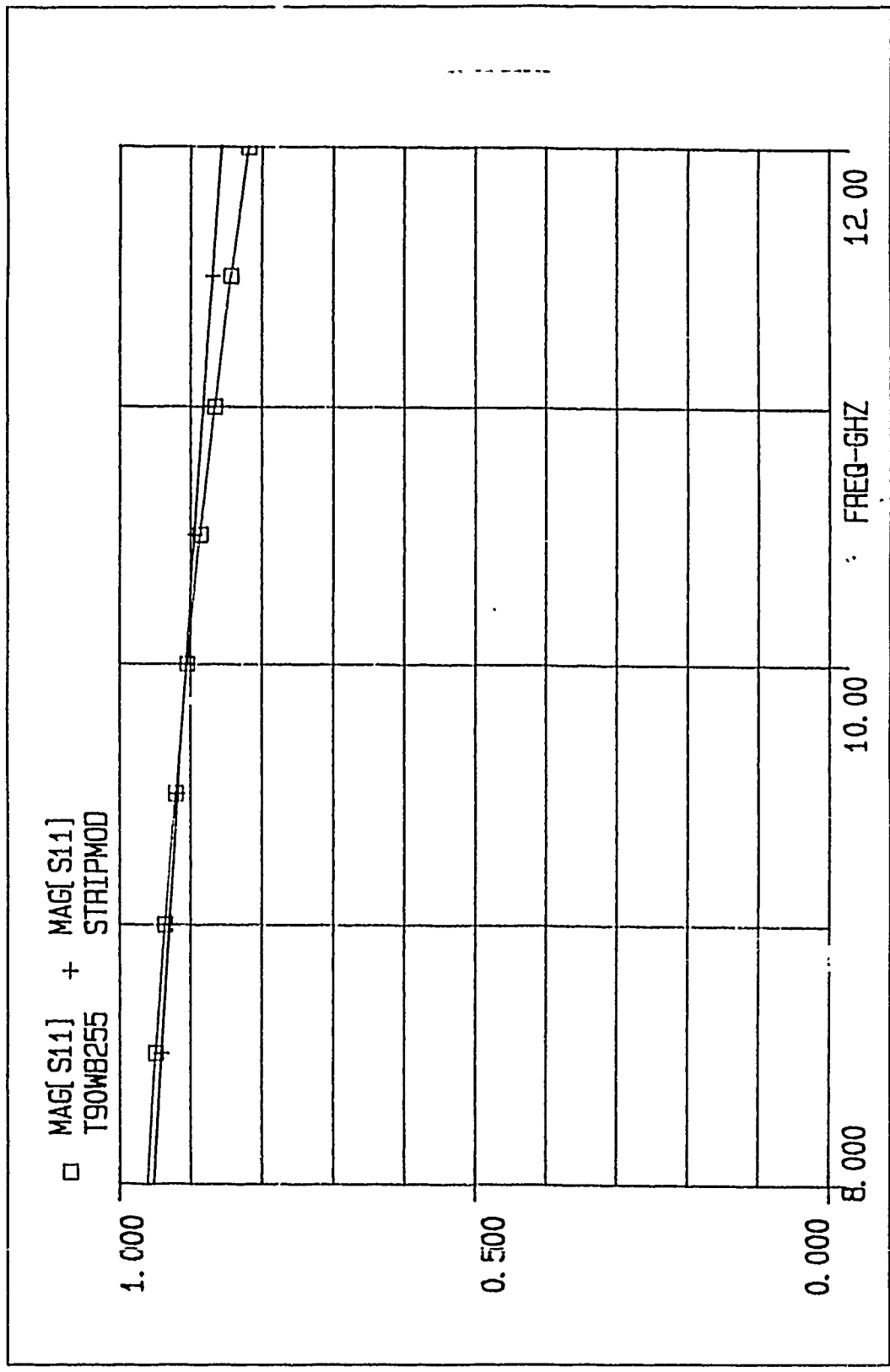


Figure 37. Computed and predicted values of  $|S_{11}|$  vs. frequency for a  $T = 50$  mils inductive strip centered in WR(90) finline,  $W/b = 0.25$ ,  $E_2 = 1$ . Model inductance  $L = 5.65$  nH.

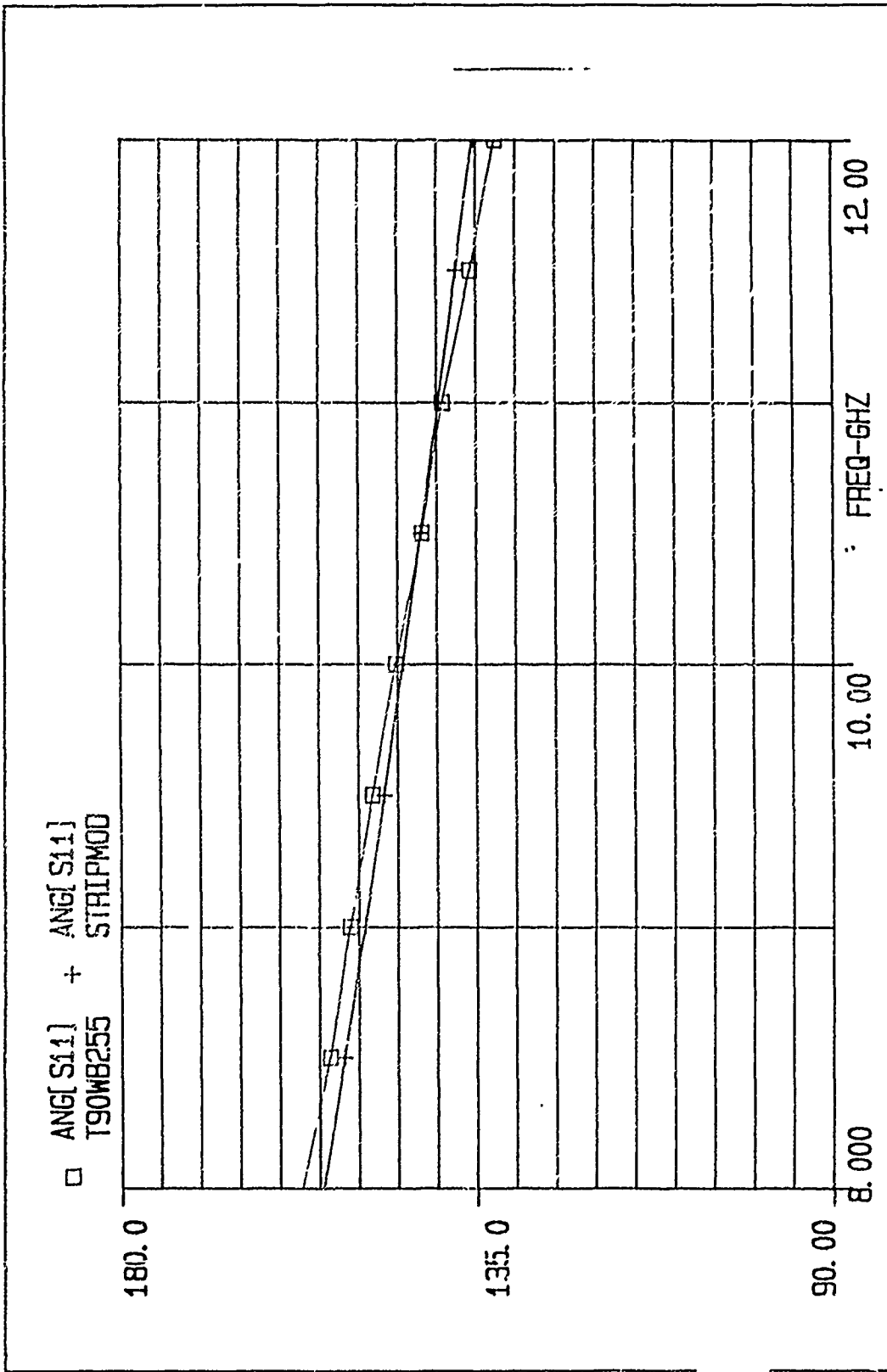


Figure 58. Computed and predicted values of  $\theta_{11}$  vs. frequency for a  $T = 50$  mills inductive strip centered in WR(90) fin-line,  $W/b = 0.25$ ,  $E_r = 1$ . Model inductance  $L = 5.65$  nH.

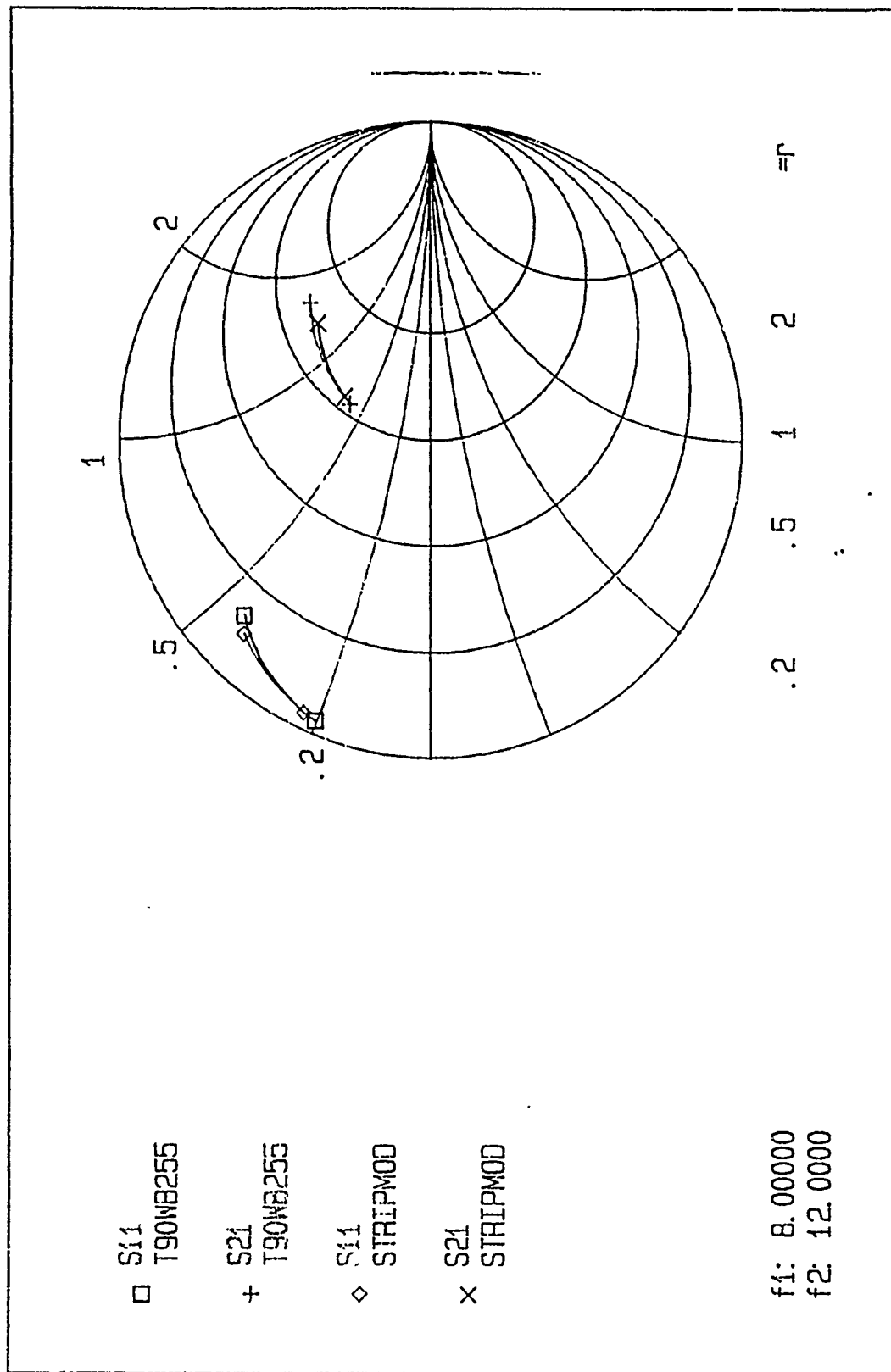


Figure 39. Smith chart plot of computed and predicted values of  $S_{11}$  and  $S_{21}$  for a  $T = 50$  mils inductive strip centered in WR(90) fin-line,  $W/b = 0.25$ ,  $E_2 = 1$ . Model inductance  $L = 5.65$  nH.

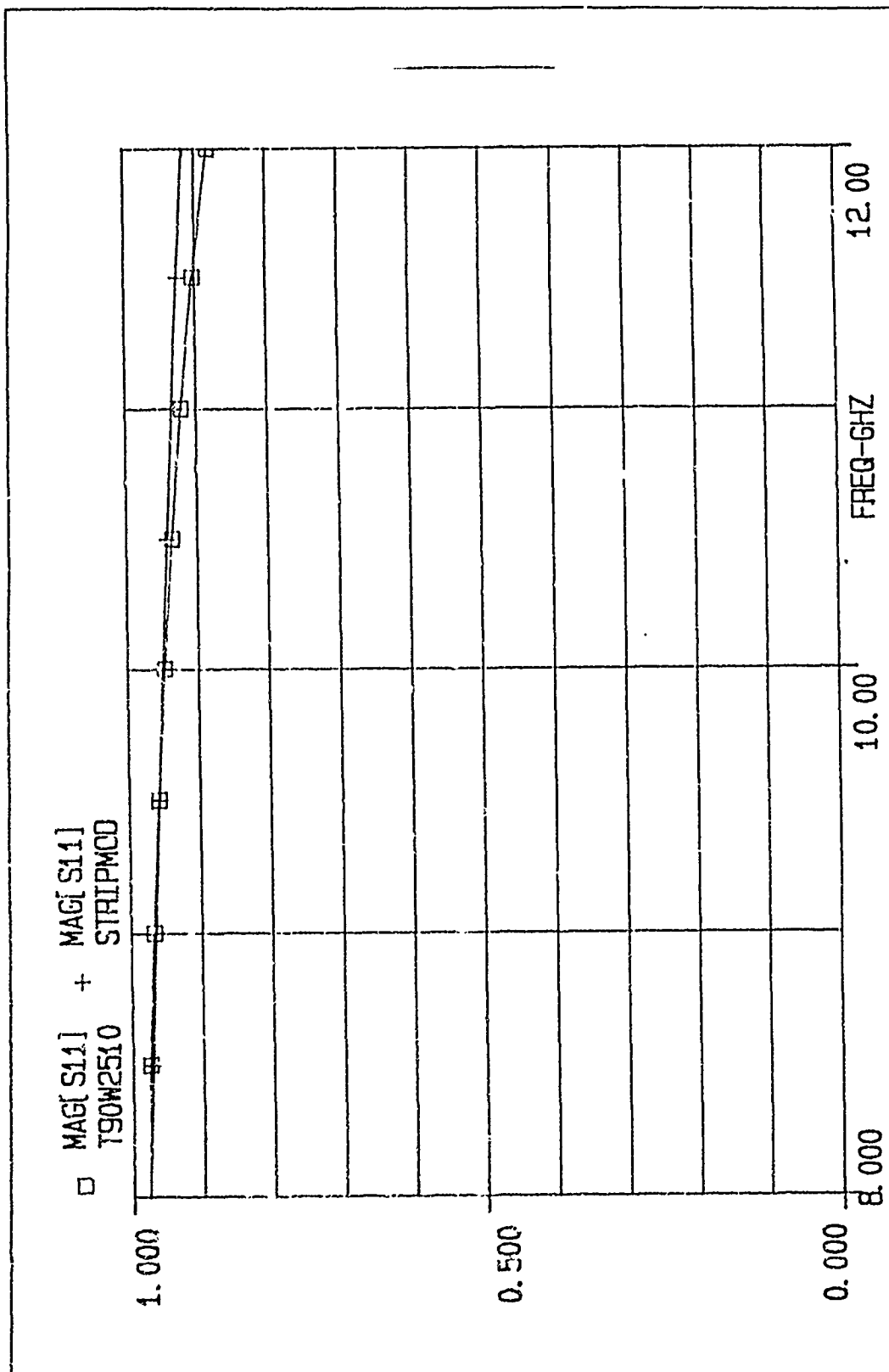


Figure 40. Computed and predicted values of  $|S_{11}|$  vs. frequency for a  $T = 100$  mils inductive strip centered in  $WR(90)$  fin-line,  $W/b = 0.25$ ,  $E_r = 1$ . Model inductance  $L = 5.005$  nH.

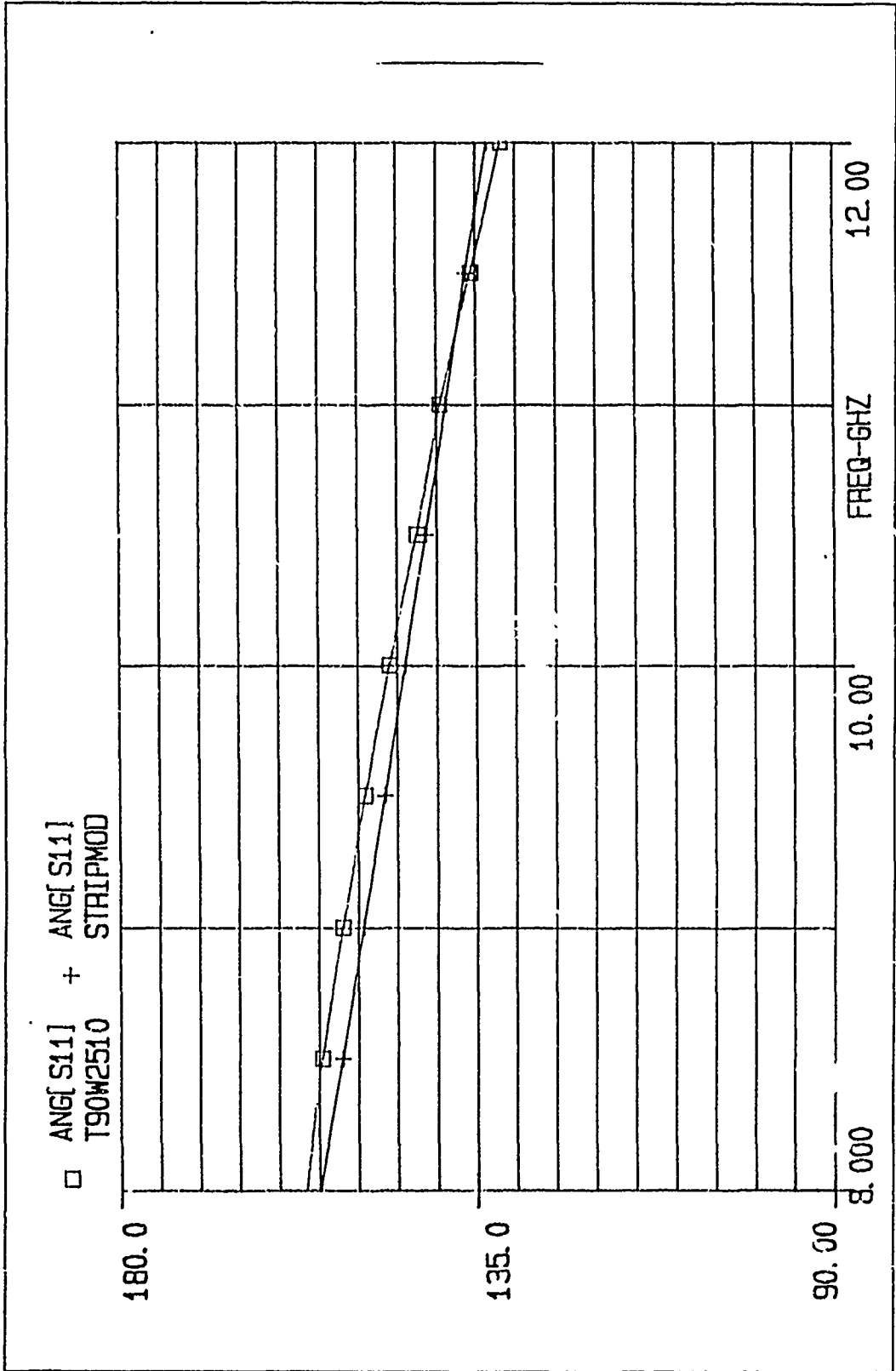


Figure 41. Computed and predicted values of  $\theta_{11}$  vs. frequency for a  $T = 100$  mils inductive strip centered in WVR(90) fin-line,  $W/b = 0.25$ ,  $E_{r2} = 1$ . Model inductance  $L = 5.005$  nH.

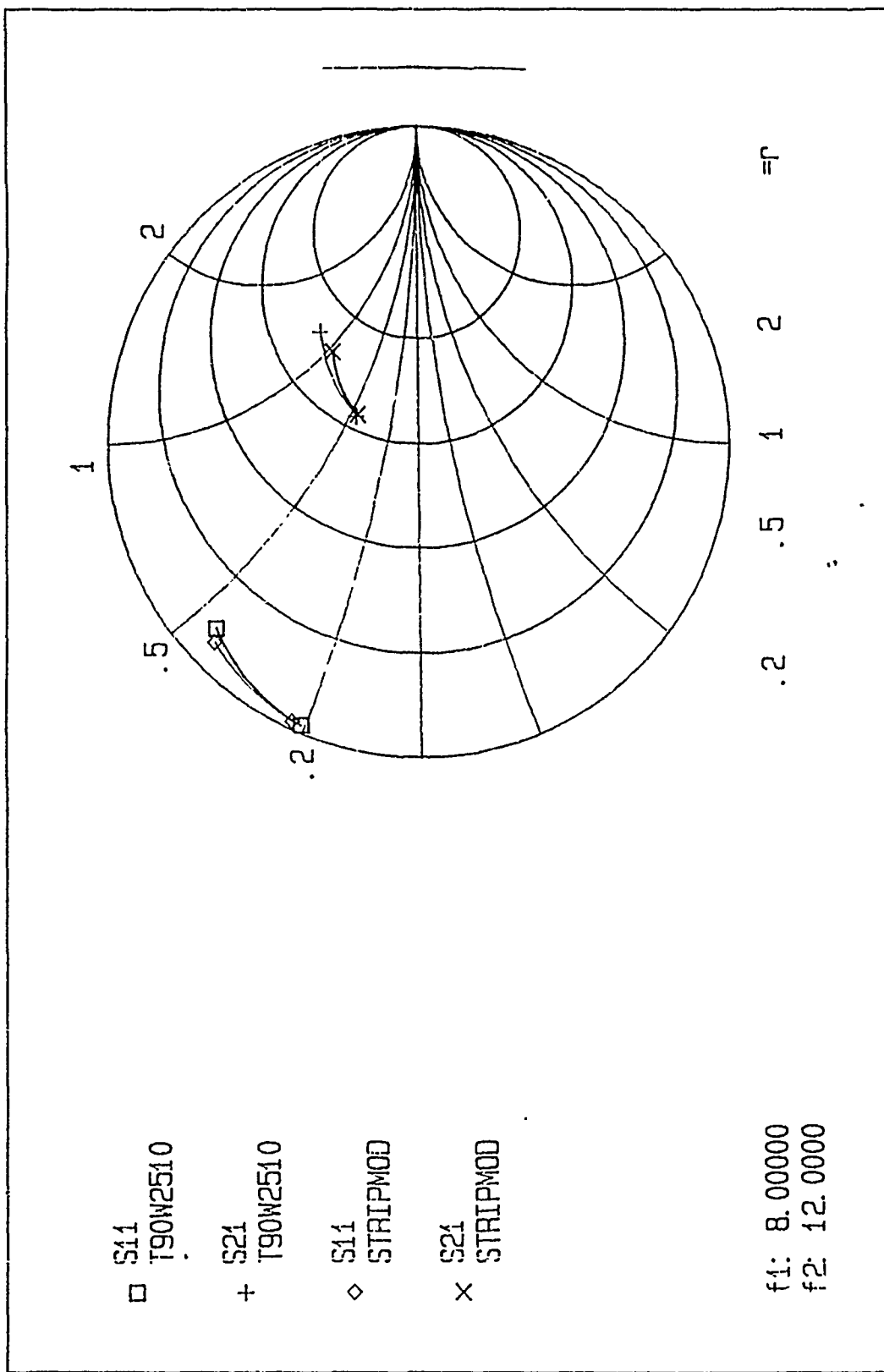


Figure 42. Smith chart plot of computed and predicted values of  $S_{11}$  and  $S_{21}$  for a  $T = 100$  mils inductive strip centered in  $WR(90)$  fin-line,  $W/b = 0.25$ ,  $E_2 = 1$ . Model inductance  $L = 5.005$  nH.

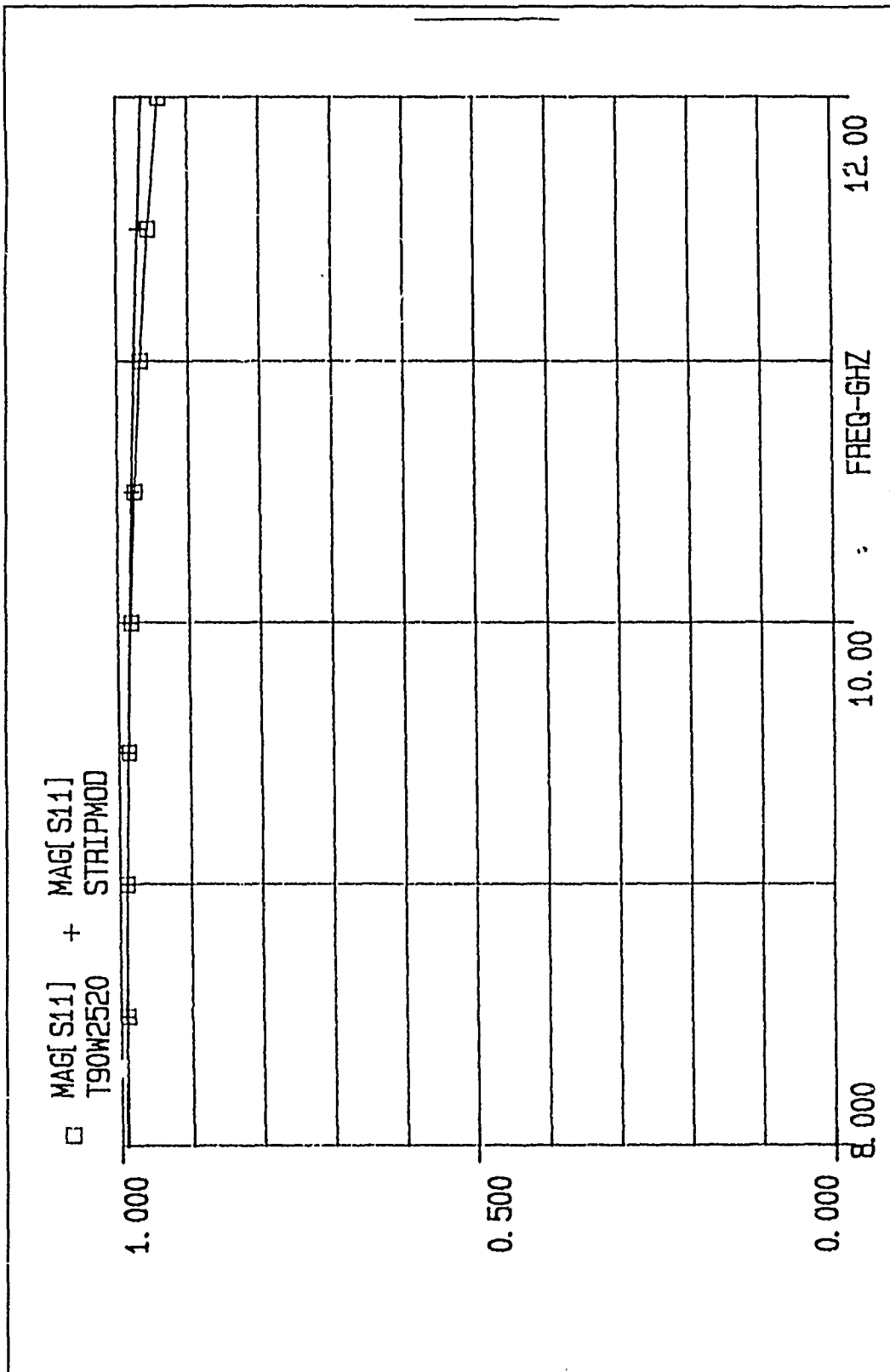


Figure 43. Computed and predicted values of  $|S_{11}|$  vs. frequency for a  $T = 200$  mils inductive strip centered in WR(90) fin-line,  $W/b = 0.25$ ,  $E_{r2} = 1$ . Model inductance  $L = 4.20$  nH.

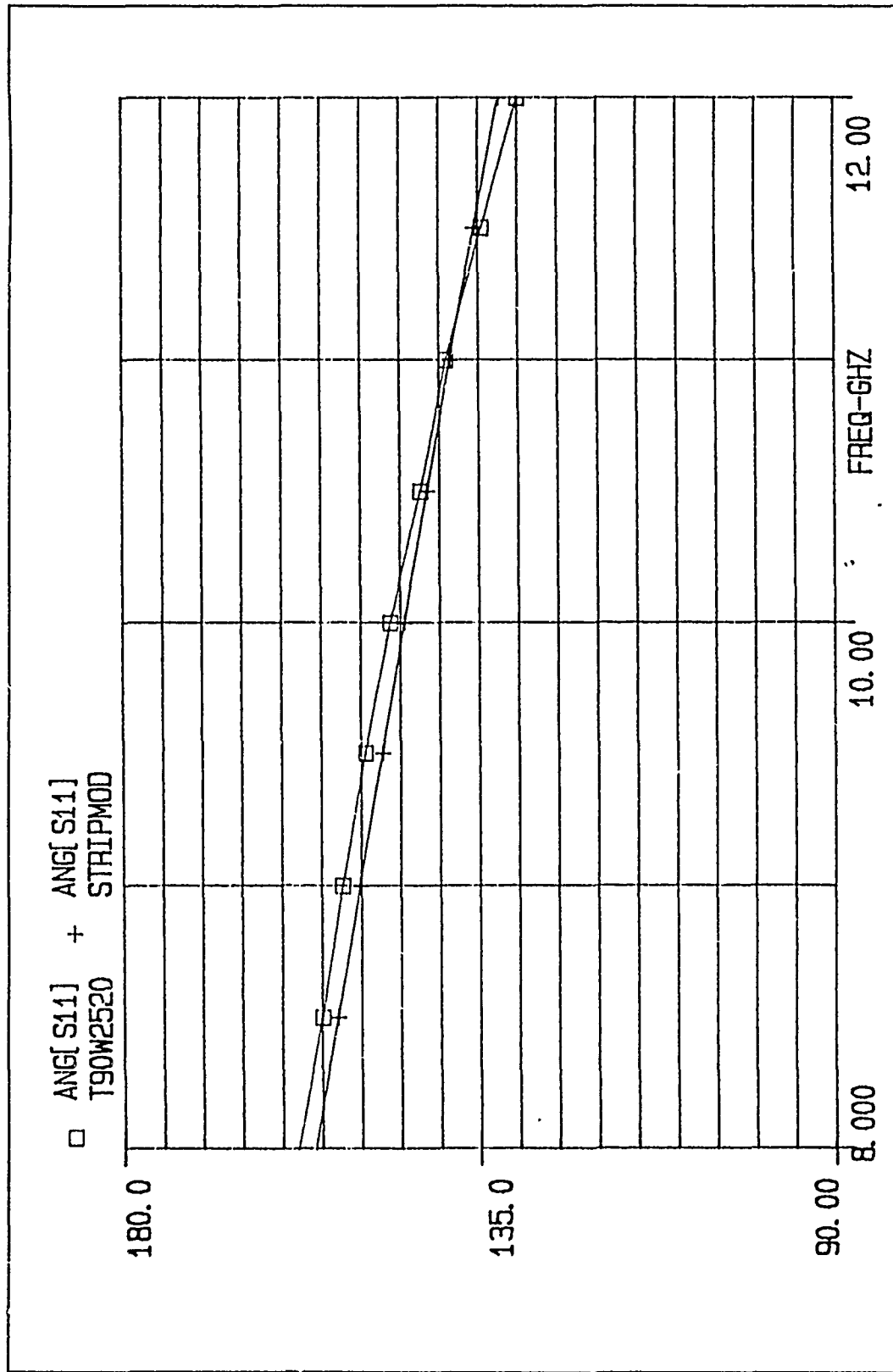


Figure 44. Computed and predicted values of  $\theta_{11}$  vs. frequency for a  $T = 200$  mils inductive strip centered in WR(90) line,  $W/b = 0.25$ ,  $E_2 = 1$ . Model inductance  $L = 4.20$  nH.

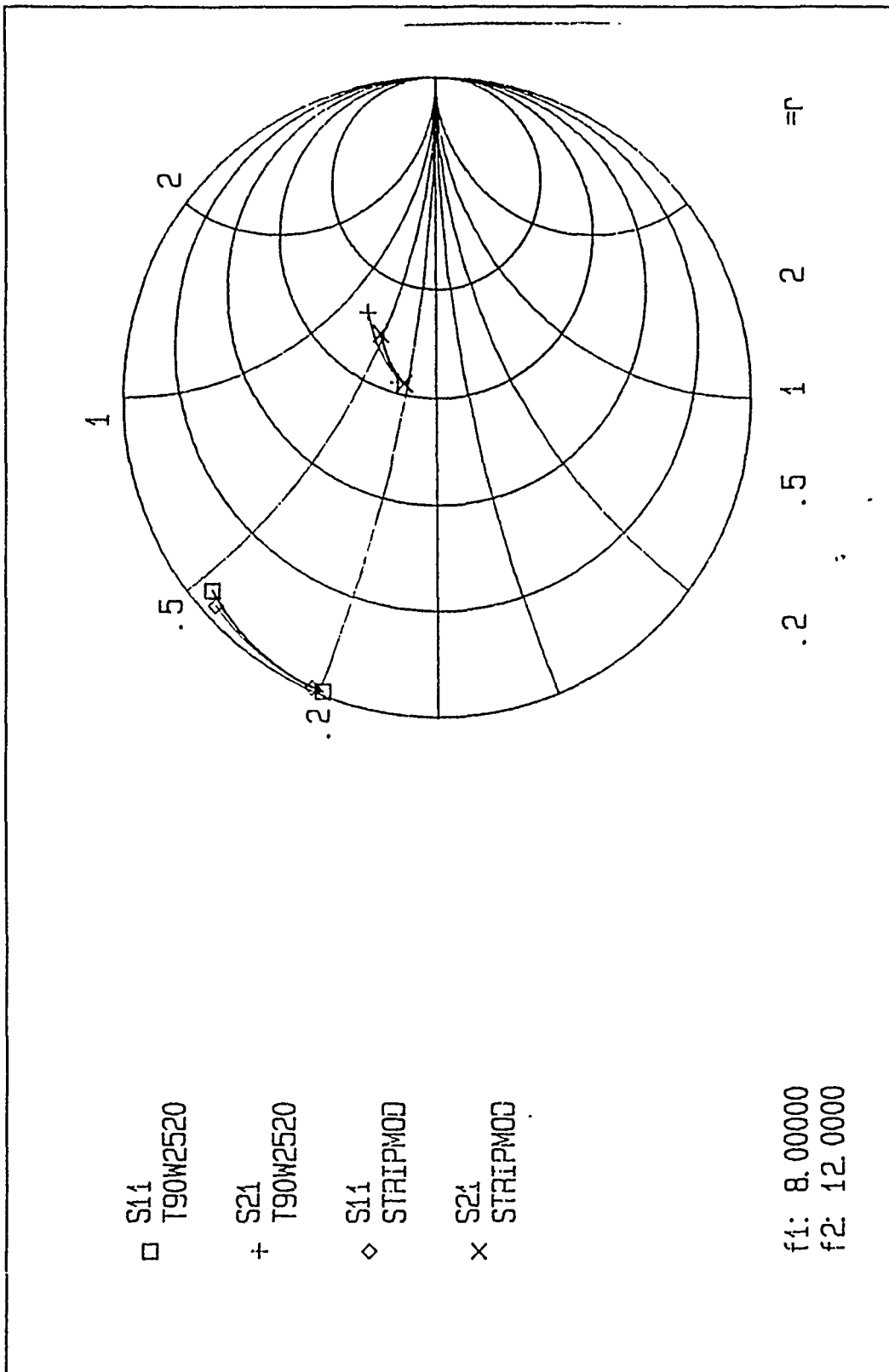


Figure 45. Smith chart plot of computed and predicted values of  $S_{11}$  and  $S_{21}$  for a  $T = 200$  mils inductive strip centered in WR(90) fin-line,  $W/b = 0.25$ ,  $E_2 = 1$ . Model inductance  $L = 4.20$  nH.

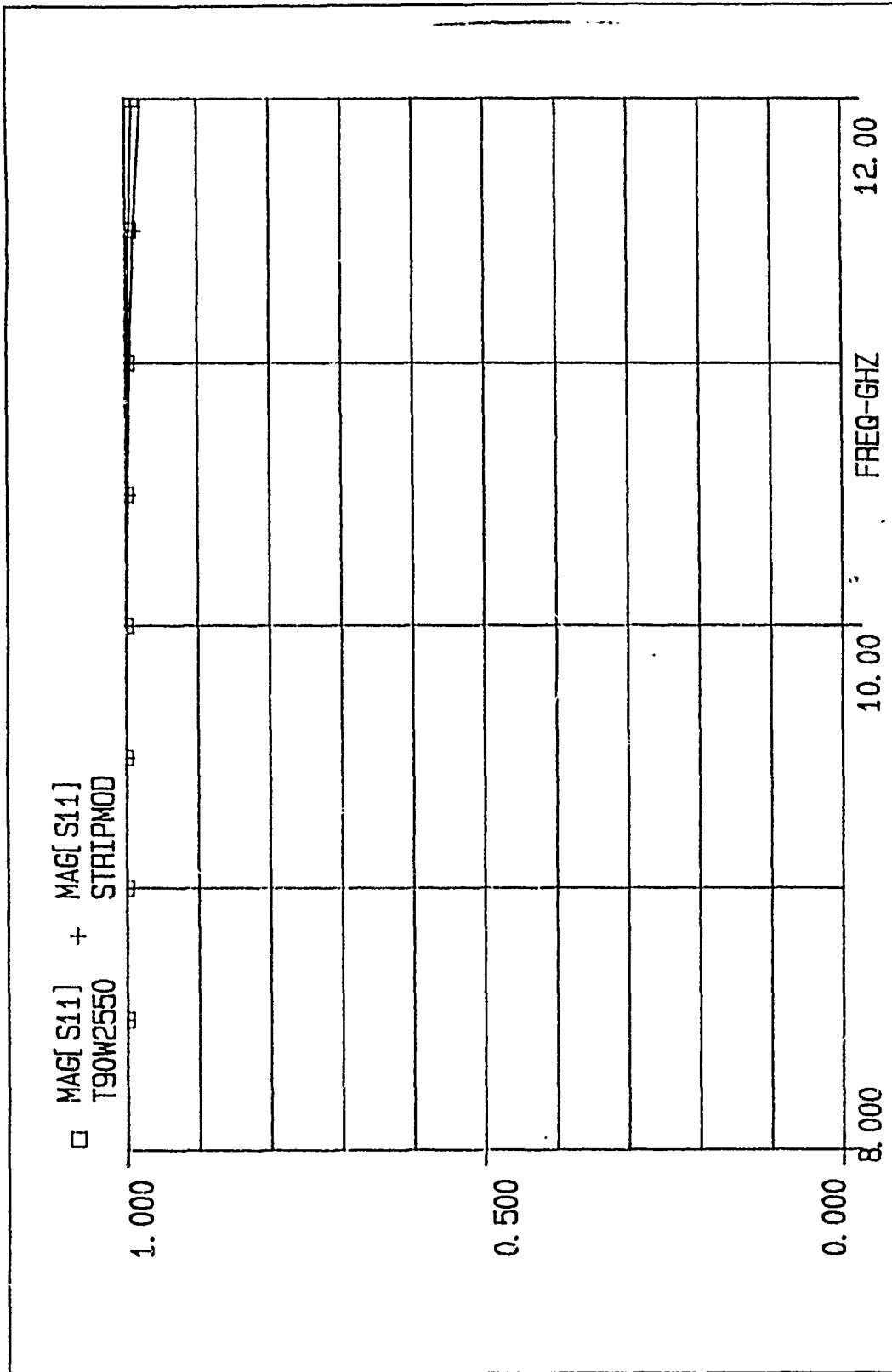


Figure 46. Computed and predicted values of  $|S_{11}|$  vs. frequency for a  $T = 500$  mils inductive strip centered in  $WR(90)$  fin-line,  $W/b = 0.25$ ,  $\epsilon_2 = 1$ . Model inductance  $L = 3.82$  nH.

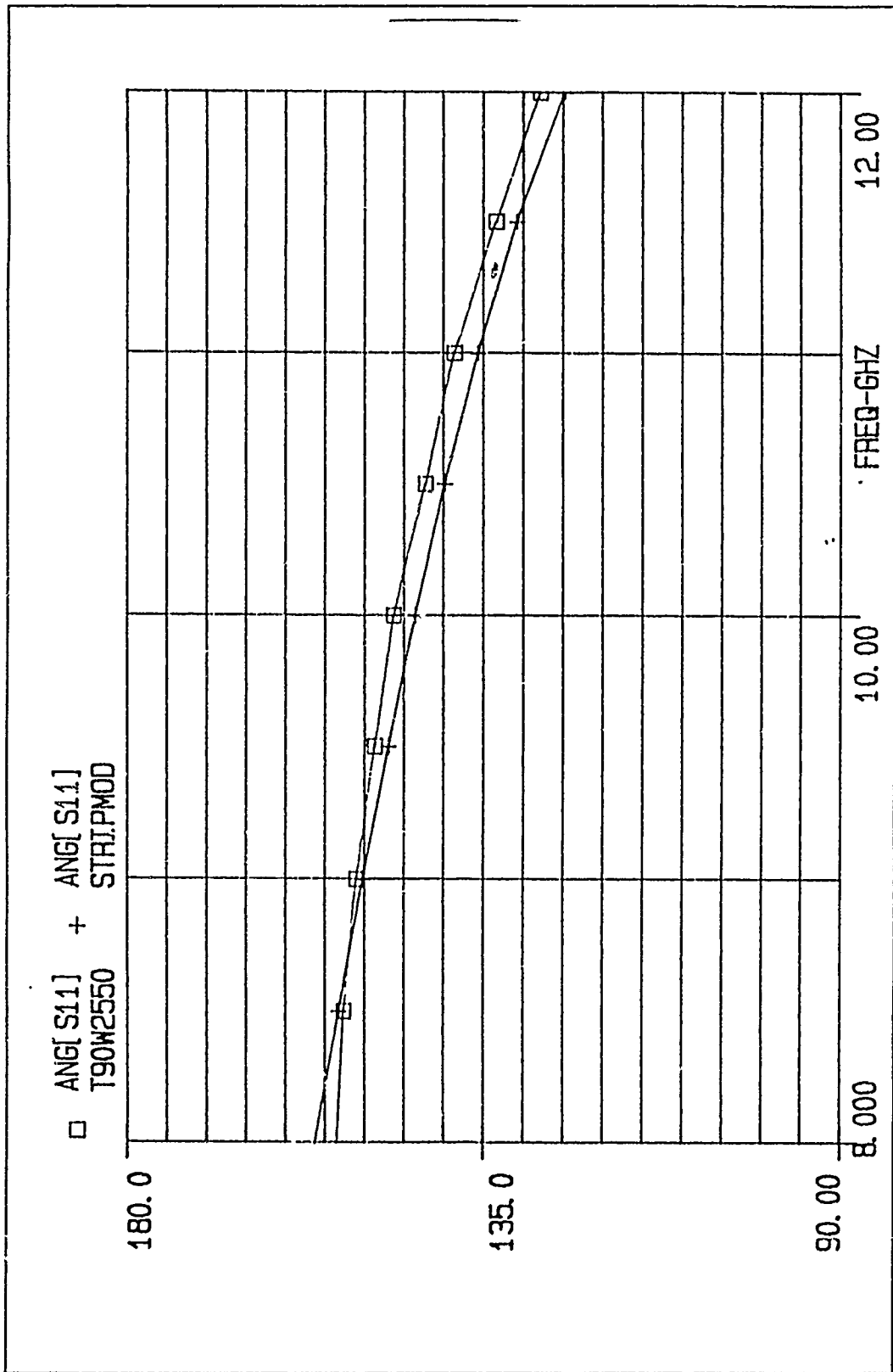


Figure 47. Computed and predicted values of  $\theta_{11}$  vs. frequency for a  $T = 500$  mils inductive strip centered in VWR(90) finline,  $W/b = 0.25$ ,  $E_2 = 1$  Model inductance  $L = 3.82$  nH.

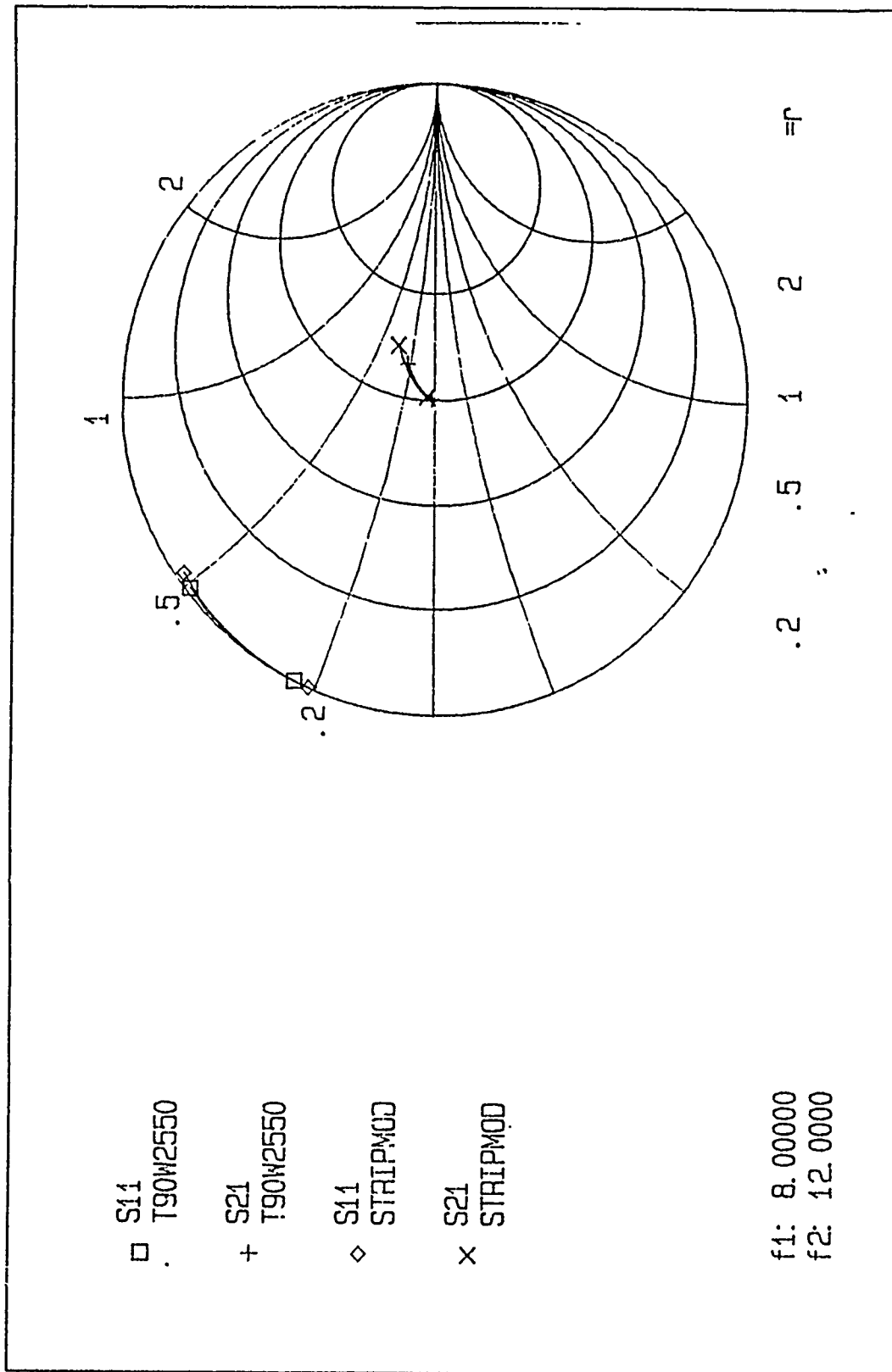


Figure 48. Smith chart plot of computed and predicted values of  $S_{11}$  and  $S_{21}$  for a  $T = 500$  mils inductive strip centered in WR(90) fin-line,  $W/b = 0.25$ ,  $E_r = 1$  Model inductance  $L = 3.82$  nH.

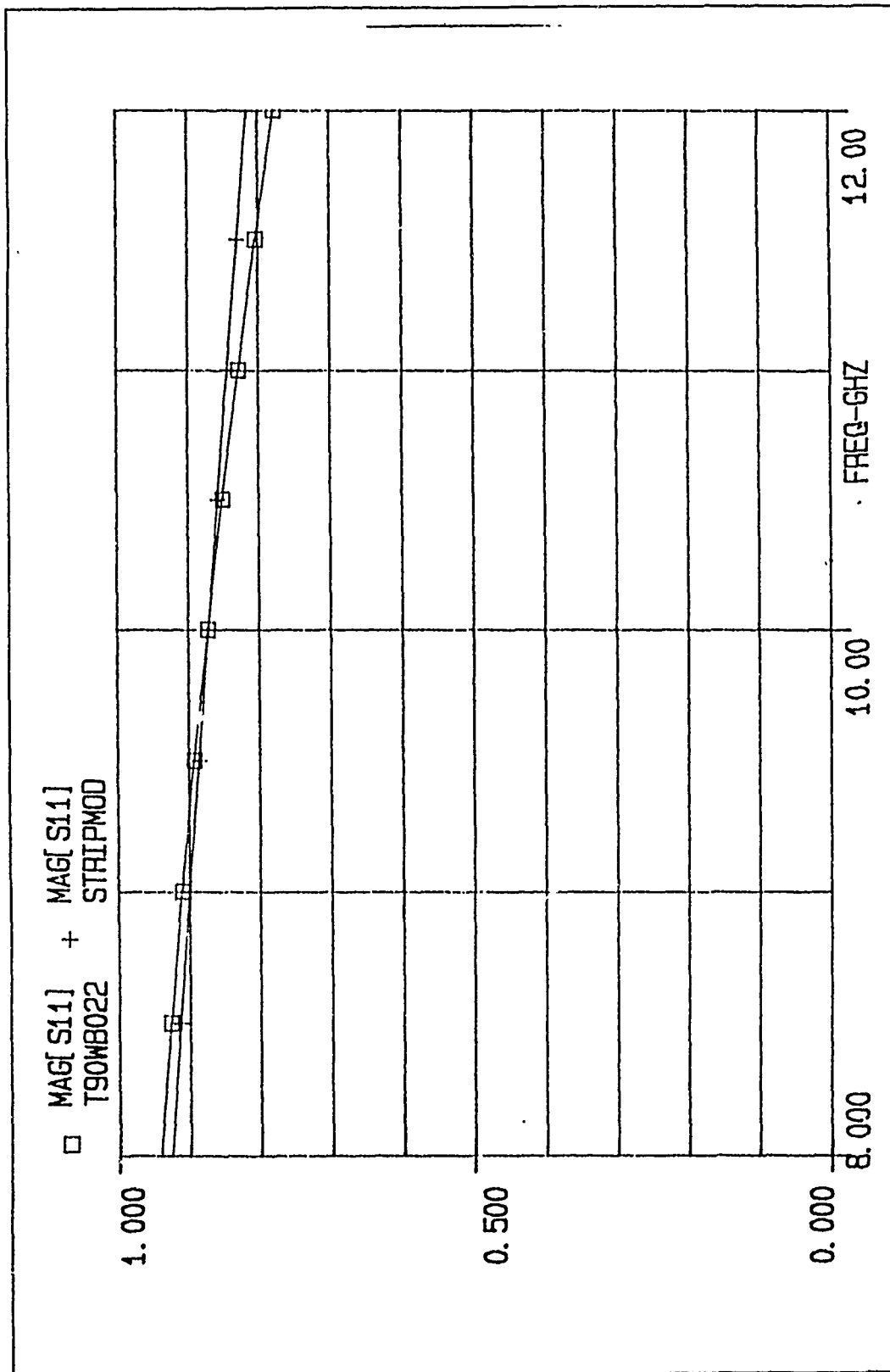


Figure 49. Computed and predicted values of  $|S_{11}|$  vs. frequency for a  $T = 20$  mils inductive strip centered in WR(90) finline,  $W/b = 0.2$ ,  $E_z = 1$ . Model inductance  $L = 4.89$  nH.

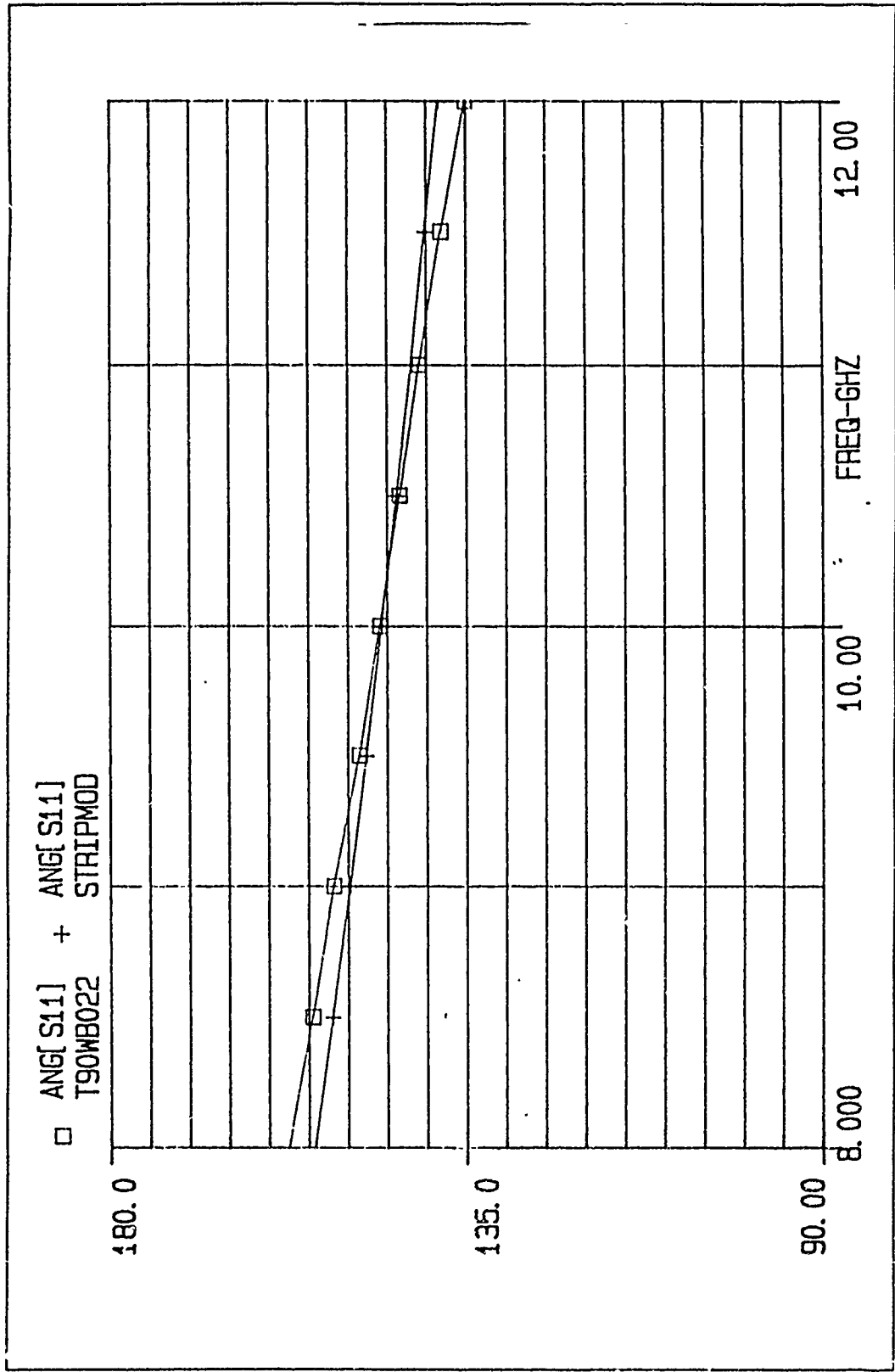


Figure 50. Computed and predicted values of  $\theta_{11}$  vs. frequency for a  $T = 20$  mils inductive strip centered in WR(90) air-line,  $W/b = 0.2$ ,  $E_2 = 1$ . Model inductance  $L = 4.89$  nH.



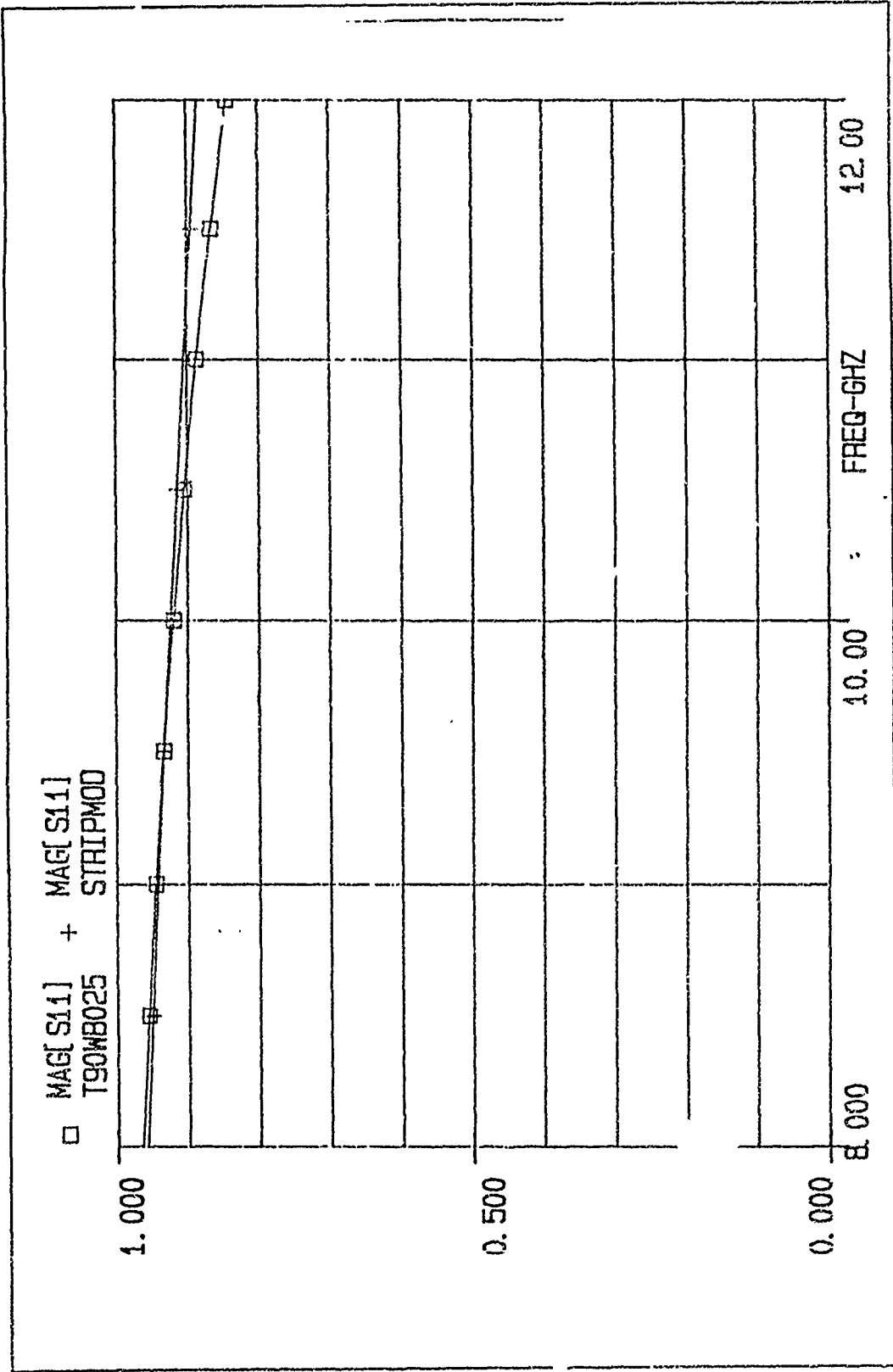


Figure 52. Computed and predicted values of  $|S_{11}|$  vs. frequency for a  $T = 50$  mils inductive strip centered in WR(90) line,  $W/b = 0.2$ ,  $\epsilon_r = 1$ . Model inductance  $L = 4.18$  nH.

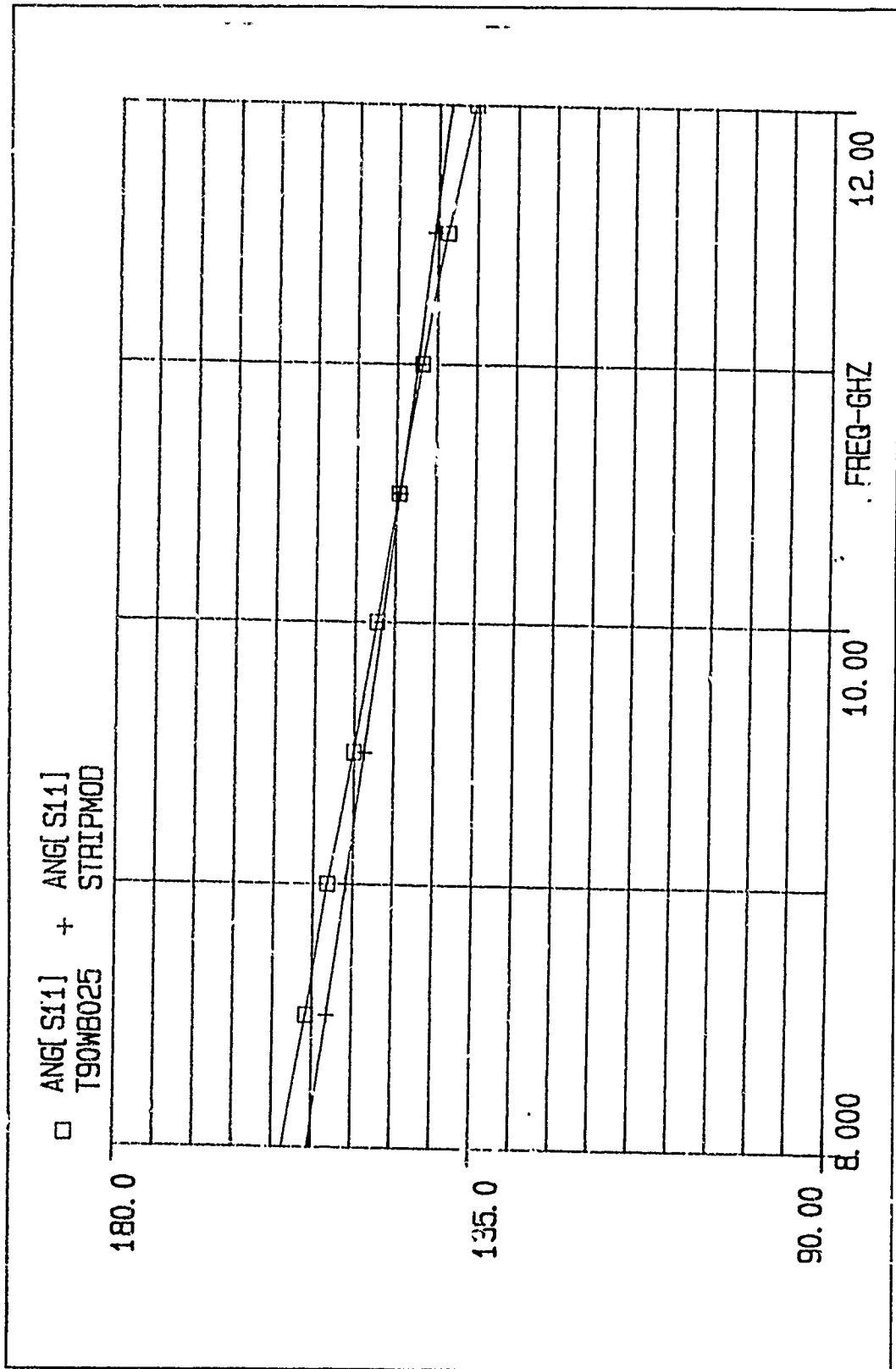


Figure 53. Computed and predicted values of  $\theta_{11}$  vs. frequency for a  $T = 50$  mils inductive strip centered in VWR(90) fin-line,  $W/b = 0.2$ ,  $E_2 = 1$ . Model inductance  $L = 4.18$  nH.

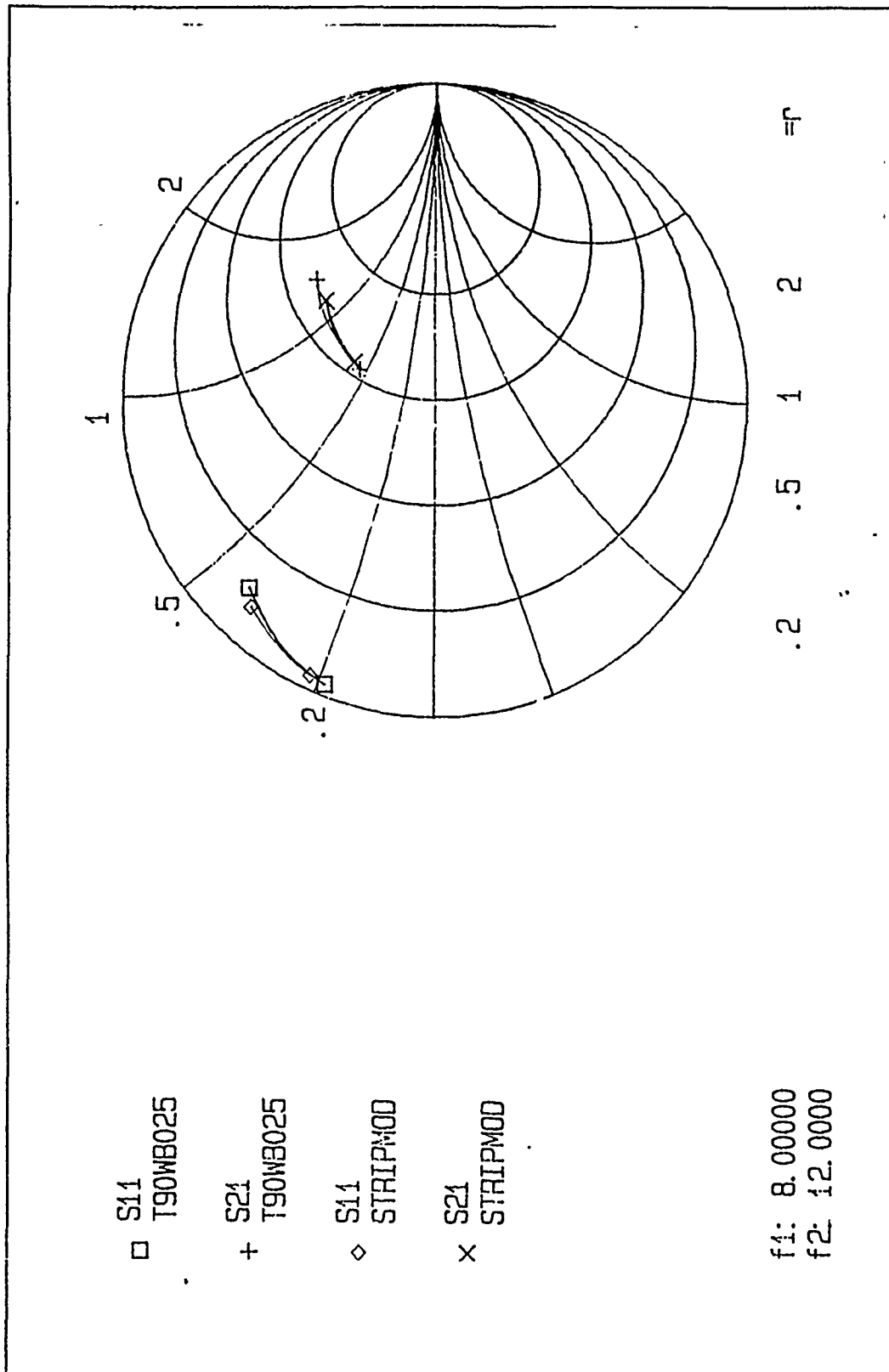


Figure 54. Smith chart plot of computed and predicted values of  $S_{11}$  and  $S_{21}$  for a  $T = 50$  mils inductive strip centered in WR(90) fin-line,  $W/b = 0.2$ ,  $E_2 = 1$ . Model inductance  $L = 4.18$  nH.

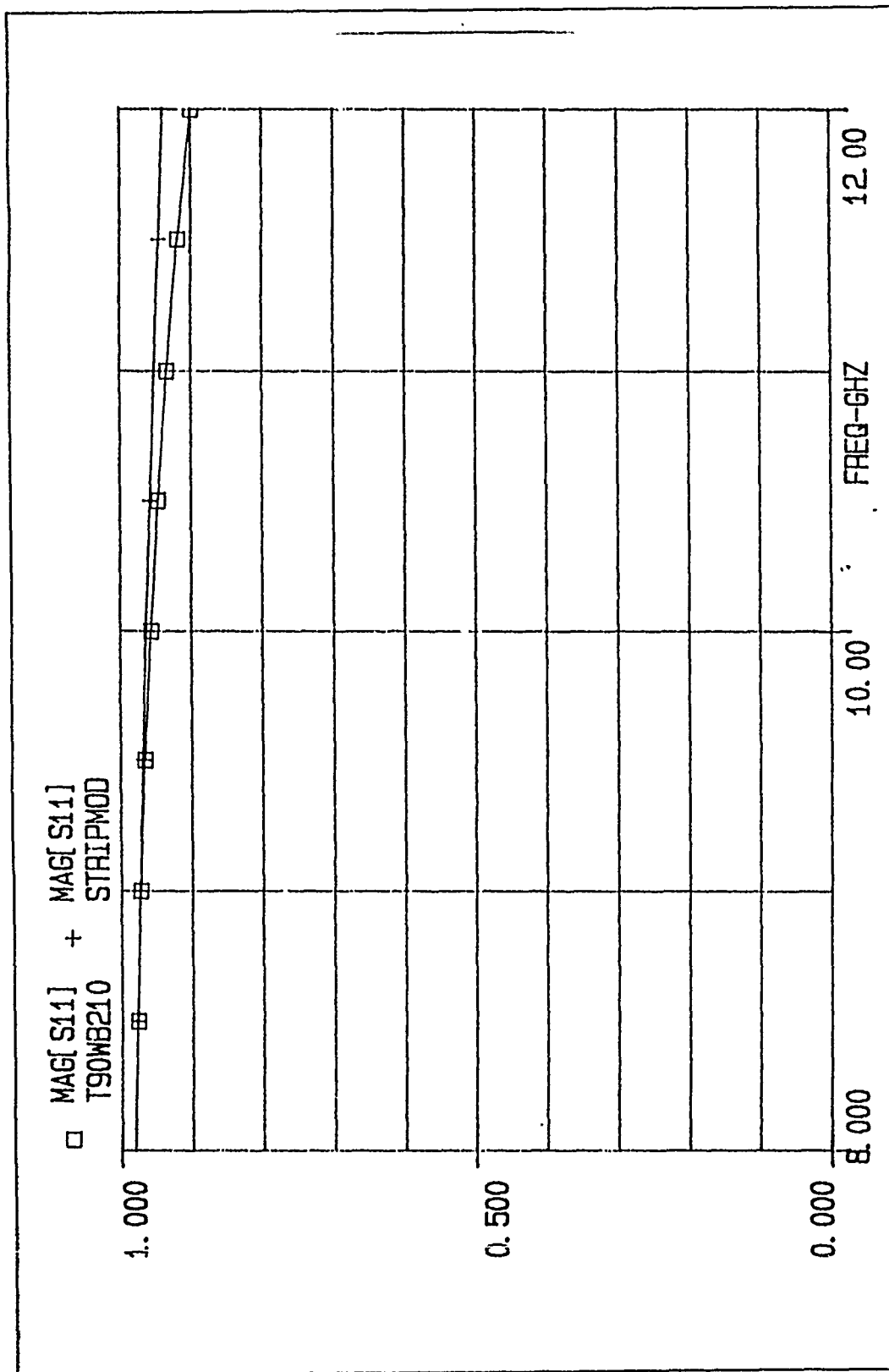


Figure 55. Computed and predicted values of  $|S_{11}|$  vs. frequency for a  $T = 160$  mils inductive strip centered in WR(90) fin-line,  $W/b = 0.2$ ,  $E_2 = 1$ . Model inductance  $L = 3.55$  nH.

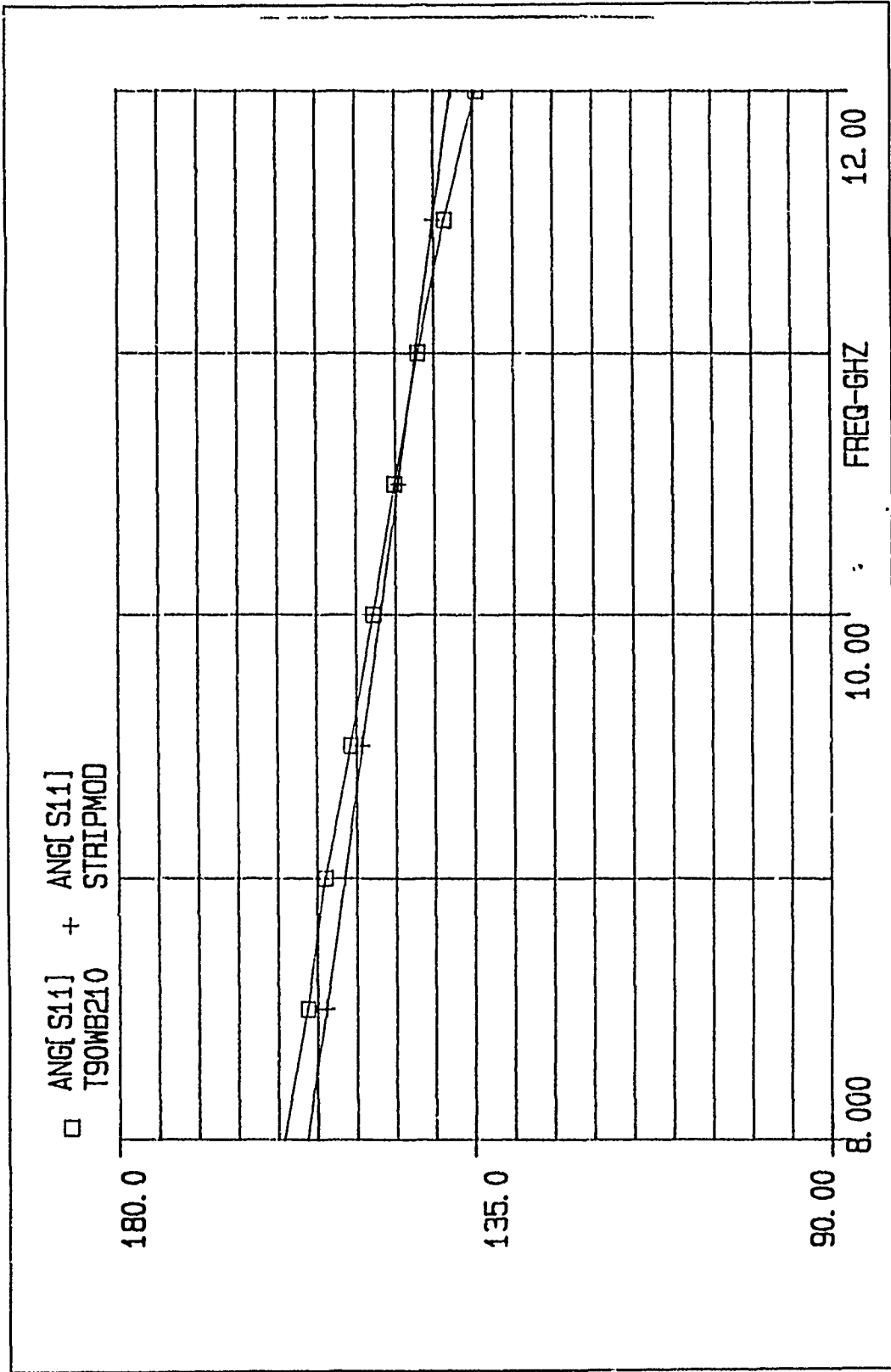


Figure 56. Computed and predicted values of  $\theta_{11}$  vs. frequency for a  $T = 100$  mils inductive strip centered in WR(90) finline,  $W/b = 0.2$ ,  $E_2 = 1$ . Model inductance  $L = 3.55$  nH.

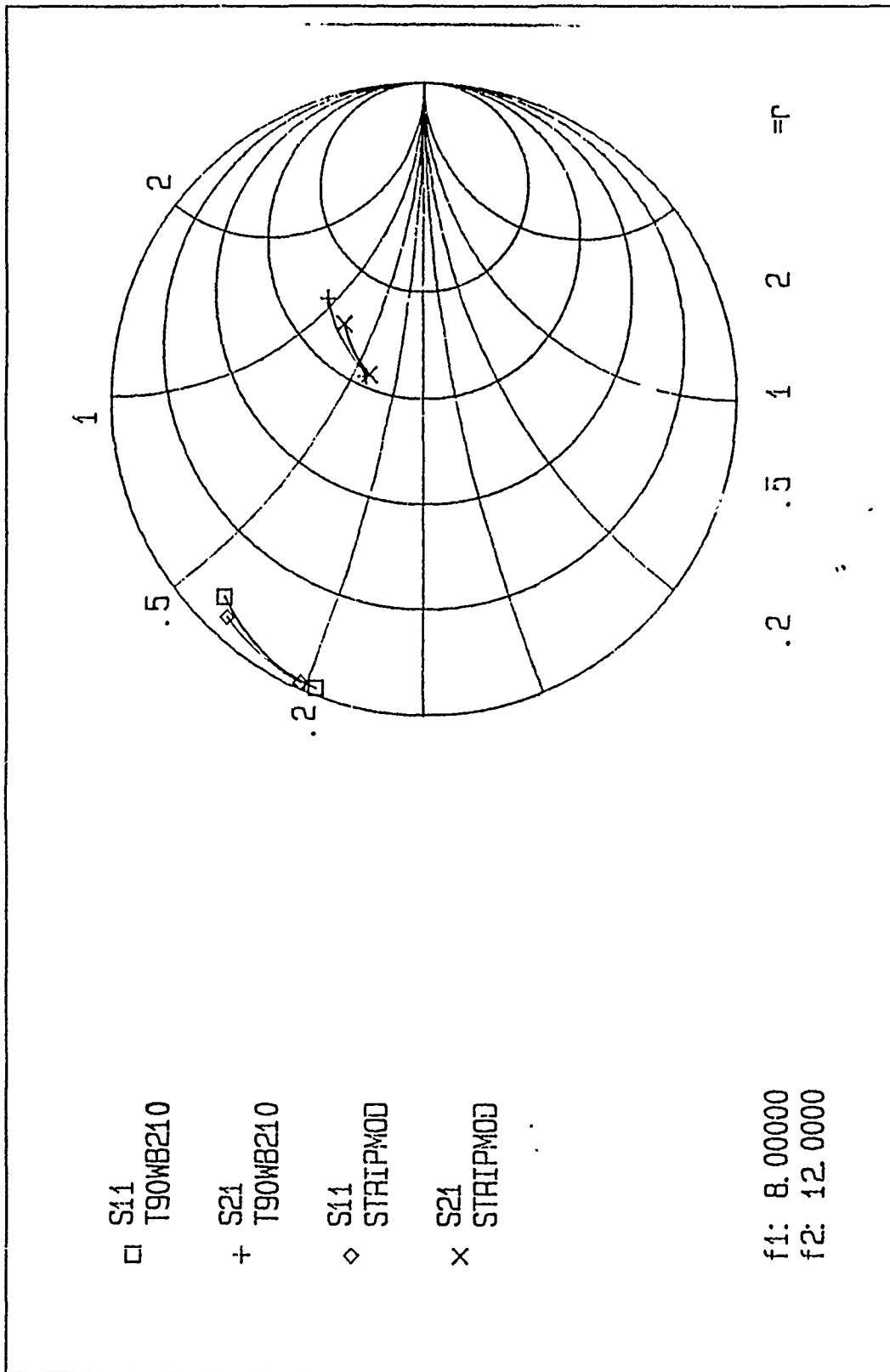


Figure 57. Smith chart plot of computed and predicted values of  $S_{11}$  and  $S_{21}$  for a  $T = 100$  mils inductive strip centered in WR(90) fin-line,  $W/b = 0.2$ ,  $E_2 = 1$ . Model inductance  $L = 3.55$  nH.

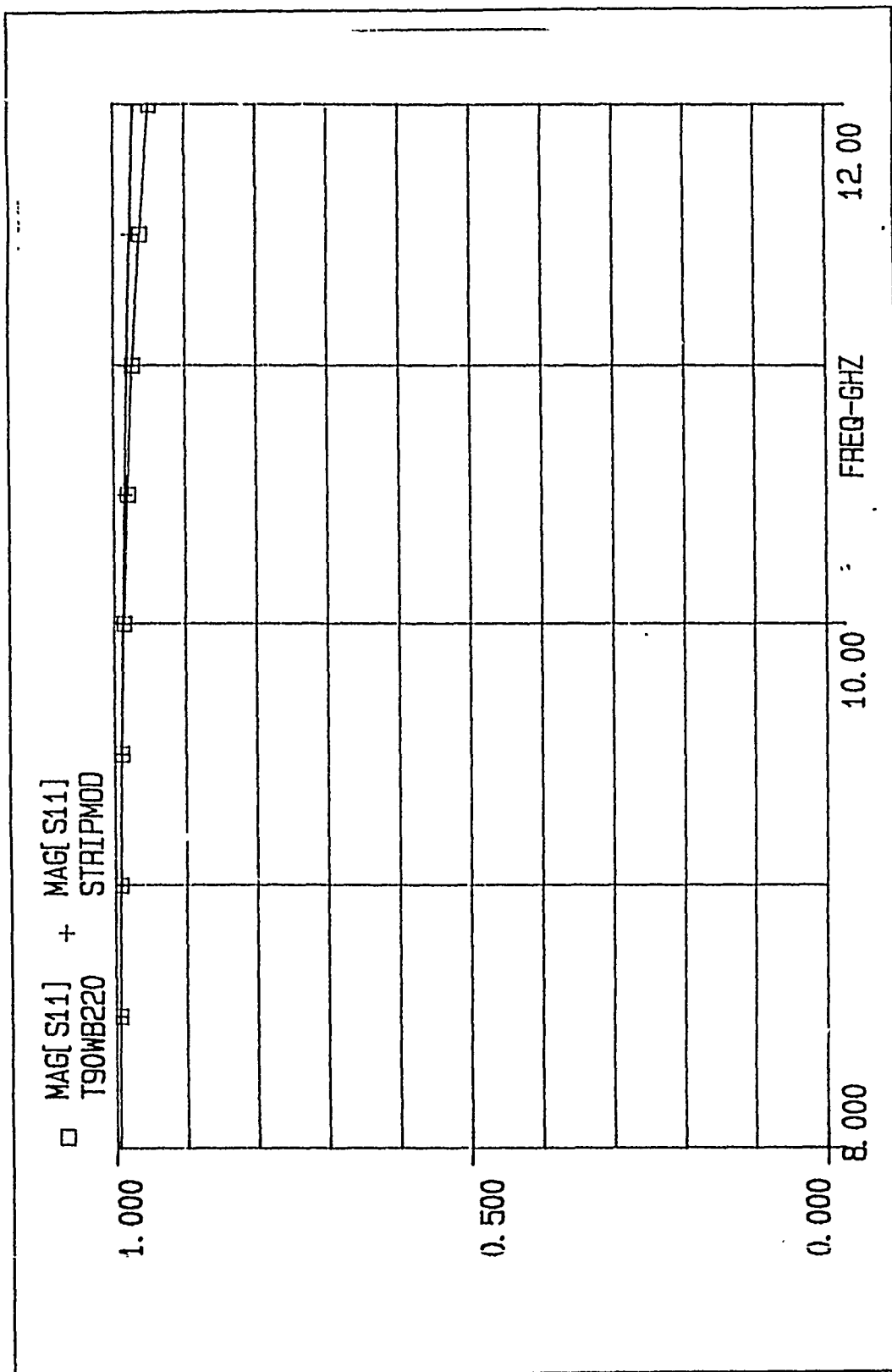


Figure 58. Computed and predicted values of  $|S_{11}|$  vs. frequency for a  $T=200$  mils inductive strip centered in WR(90) fin-line,  $W/b=0.2$ ,  $E_2=1$ . Model inductance  $L=3.06$  nH.

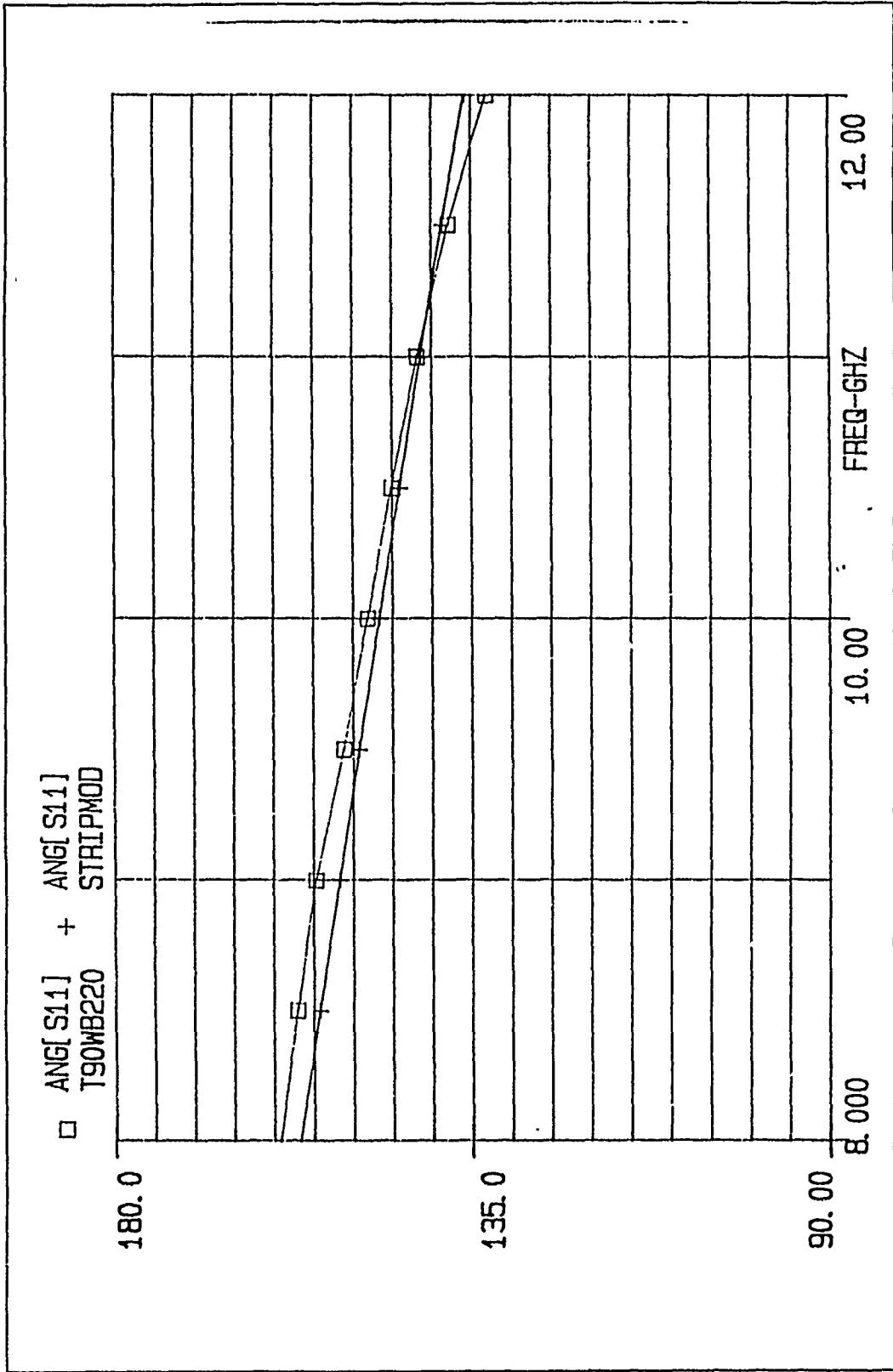


Figure 59. Computed and predicted values of  $\theta_{11}$  vs. frequency for a  $T = 200$  mils inductive strip centered in  $W1_{(90)}$  fin-line,  $W/b = 0.2$ ,  $E_2 = 1$ . Model inductance  $L = 3.06$  nH.

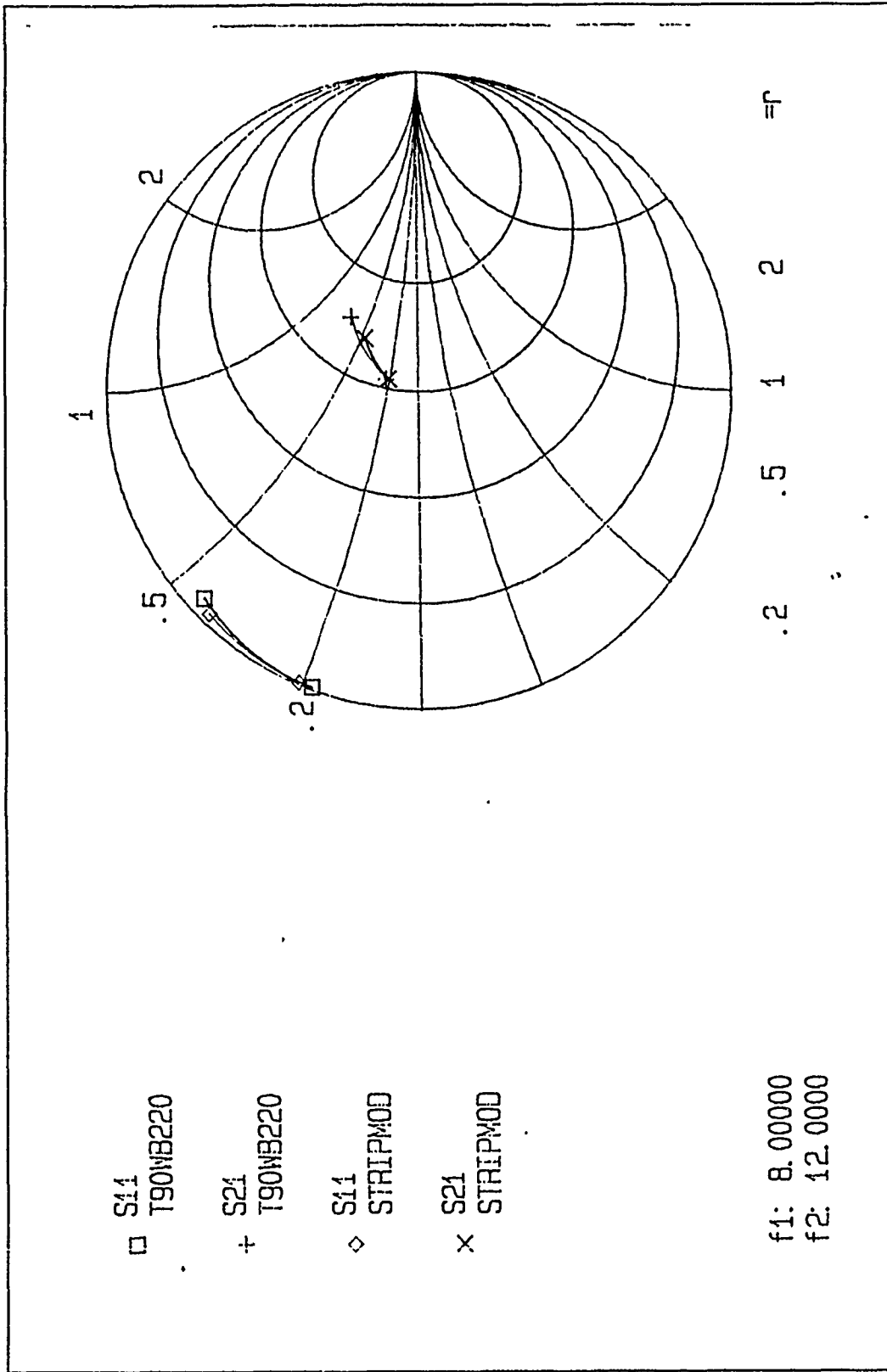


Figure 60. Smith chart plot of computed and predicted values of  $S_{11}$  and  $S_{21}$  for a  $T = 200$  mils inductive strip centered in WR(90) fin-line,  $W/b = 0.2$ ,  $E_2 = 1$ . Model inductance  $L = 3.06$  nH.

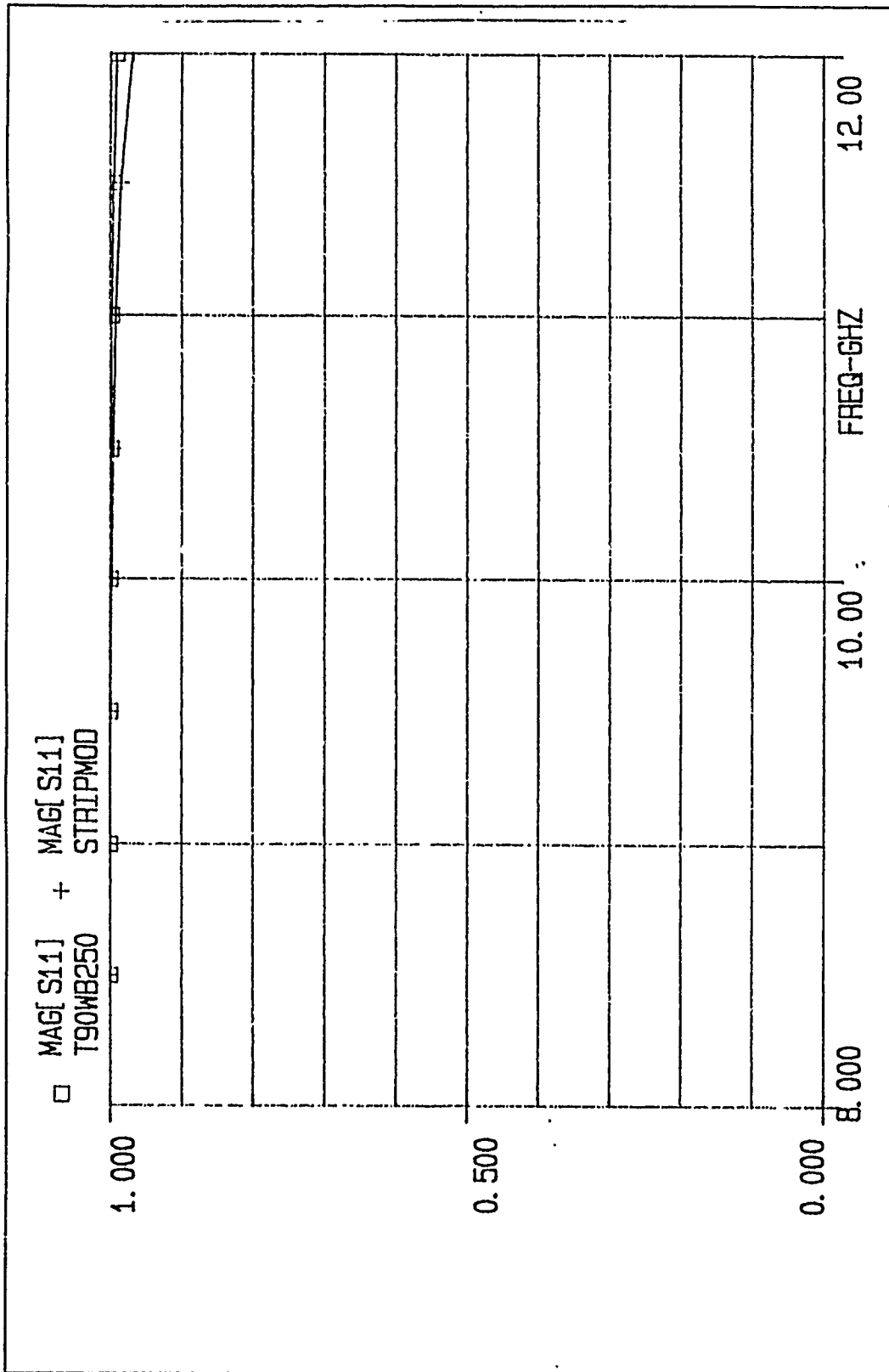


Figure 61. Computed and predicted values of  $|S_{11}|$  vs. frequency for a  $T = 500$  mils inductive strip centered in WR(90) fin-line,  $W/b = 0.2$ ,  $E_r = 1$ . Model inductance  $L = 2.70$  nH.

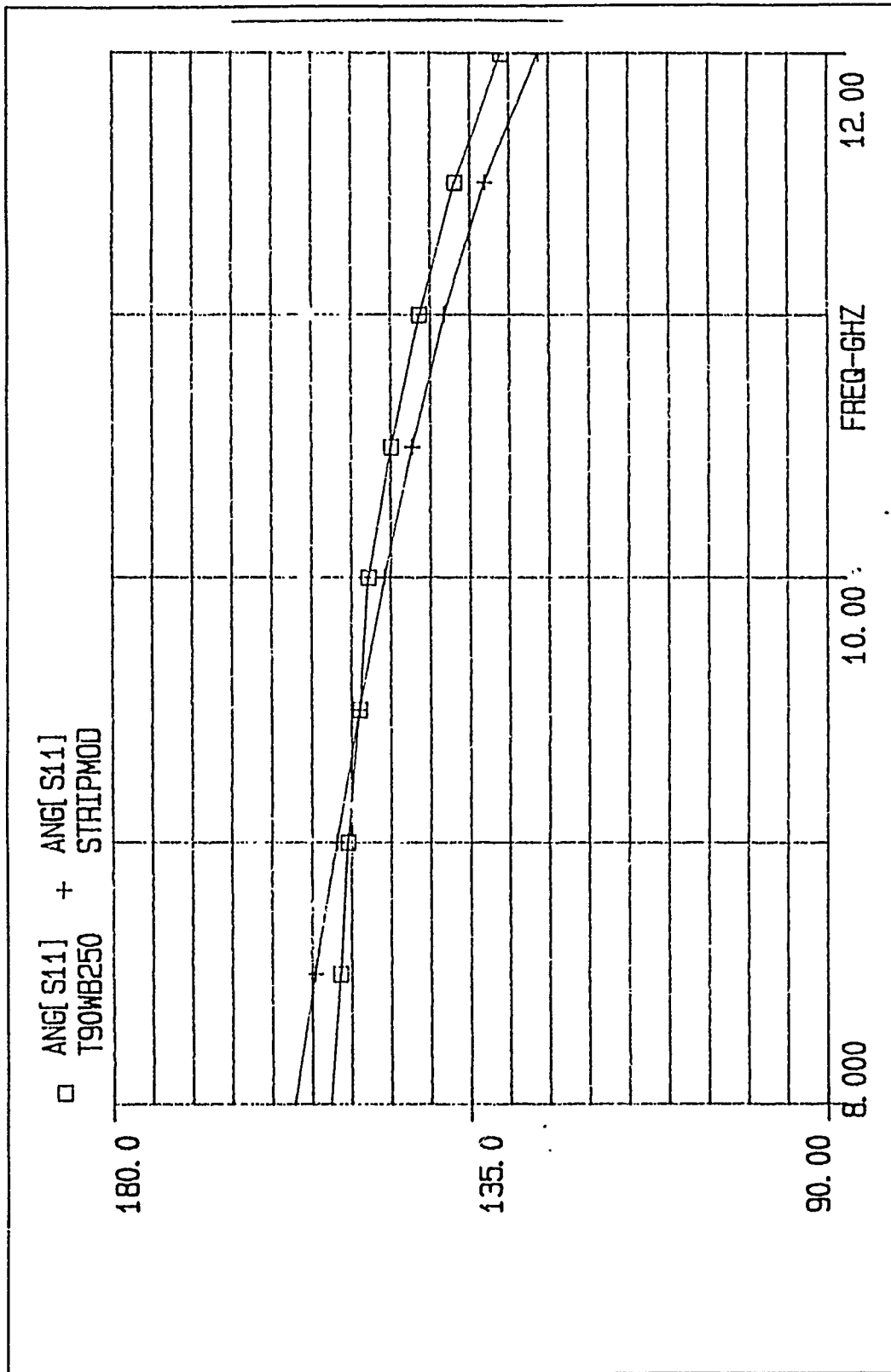


Figure 62. Computed and predicted values of  $\theta_{11}$  vs. frequency for a  $T = 500$  mils inductive strip centered in WVR(90) fineline,  $W/b = 0.2$ ,  $E_2 = 1$ . Model inductance  $L = 2.70$  nH.

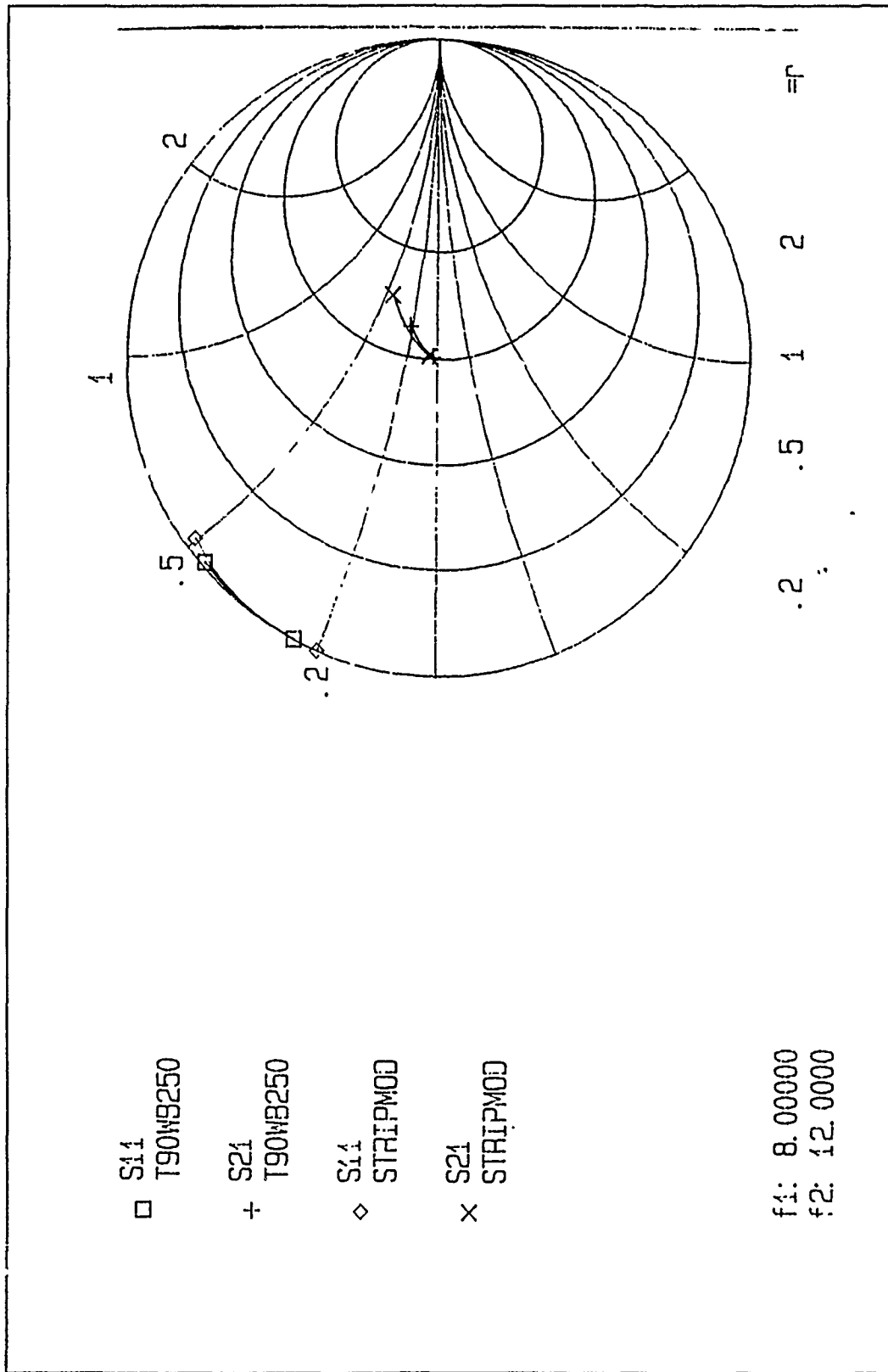


Figure 63. Smith chart plot of Computed and predicted values of  $S_{11}$  and  $S_{21}$  for a  $T = 500$  mils inductive strip centered in WR(90) fin-line,  $W/b = 0.2$ ,  $E_2 = 1$ . Model inductance  $L = 2.70$  nH.

## LIST OF REFERENCES

1. Meier, P. J., *Integrated Fin-line Millimeter Components*, IEEE Trans. Microwave Theory and Tech., vol. MTT-22, pp. 1209-1216, Dec. 1974.
2. Knorr, J. B. and Shayda, P. M., *Millimeter-Wave fin-line Characteristics*, IEEE Trans. Microwave Theory and Tech., vol. MTT-28, pp. 737-743, July 1980.
3. Knorr, J. B., *Equivalent Reactance of a Shorting Septum in a Fin-line*, IEEE Trans. Microwave Theory and Tech., vol. MTT-29, pp. 1196-1202, Nov. 1981
4. Rizzi, A.P., *Microwave Engineering: Passive Circuits*. Prentice Hall, Englewood Cliffs, N.J. 1988.
5. Knorr, J. B, and Deal, J. C., *Scattering Coefficients of an Intuctive Strip in Fin-line*, IEEE Trans. Microwave Theory and Tech., vol. MTT-33, pp. 1011-1017, Oct. 1980.
6. Deal, J. C., *Numerical Computation of the Scattering Coefficients of an Intuctive Strip in a Fin-line*, M. S. Thesis, Naval Postgraduate School, Monterey, CA, March 1984.
7. Knorr, J. B., *A CAD Model for the Inductive Strip in Fin-line*, Technical Report, NPS 62-88-013, Naval Postgraduate School, Monterey, CA, March 1988.

## INITIAL DISTRIBUTION LIST

	No. Copies
1. Defense Technical Information Center Cameron Station Alexandria, VA 22304-6145	2
2. Library, Code 0142 Naval Postgraduate School Monterey, CA 93943-5002	2
3. Chairman, Code 62 Department of Electrical and Computer Engineering Naval Postgraduate School Monterey, CA 93943-5000	1
4. Professor Jeffrey Knorr, Code 62Kvo Department of Electrical and Computer Engineering Naval Postgraduate School Monterey, CA 93943-5000	3
5. Professor R. Janaswamy, Code 62Ja Department of Electrical and Computer Engineering Naval Postgraduate School Monterey, CA 93943-5000	1
6. Georgios Karaminas Dimosthenous 37-39 Kallithea 17671 Athens / GREECE	2
7. Hellenic Navy General Staff 2nd Branch, Education Department Stratopedon Papagou, Holargos Athens 155.61, GREECE	4